THERMAL AND CHARGE TRANSPORT IN CORRELATED ELECTRON SYSTEMS

BY INDRANIL PAUL

A dissertation submitted to the
Graduate School—New Brunswick
Rutgers, The State University of New Jersey
in partial fulfillment of the requirements
for the degree of
Doctor of Philosophy
Graduate Program in Physics and Astronomy
Written under the direction of
Professor Gabriel Kotliar
and approved by

New Brunswick, New Jersey
October, 2003

ABSTRACT OF THE DISSERTATION

Thermal and Charge Transport in Correlated Electron Systems

by Indranil Paul

Dissertation Director: Professor Gabriel Kotliar

In this thesis we investigate two topics. First, in chapter 2 we study the basis dependence of dynamical mean field theory. For the purpose of using this theory as a numerical tool for predicting properties of materials, the choice of a suitably localized basis is important. We propose and test a criterion for making this choice of basis. In the rest of the thesis we study thermal and charge transport in systems in which correlation effects are important. In chapter 3 we clarify some aspects in the calculation of the thermal transport coefficients. For a tight-binding Hamiltonian we discuss the approximate nature of the charge and the thermal current obtained by Peierls substitution. Using equation of motion we derive the thermal current for a generalized Hubbard model with density interaction. We identify a part which is the contribution to the thermal current from the long-range interactions. For the Hubbard model we derive expressions for the transport coefficients which are exact in the limit of large dimensions. In chapter 4 we study the form of the charge current operator in a downfolding scheme. By treating the down-folding procedure to lowest order in perturbation we derive expressions for the charge current in the low- energy sector. In chapter 5 we

study the thermoelectric behaviour of a heavy-fermion compound when it is close to an antiferromagnetic quantum critical point. When the low-energy spin fluctuations are quasi two-dimensional with a three-dimensional Fermi surface, the "hot" regions on the Fermi surface have a finite area. We argue that there is an intermediate energy scale where the qualitative aspects of the renormalized hot electrons are captured by a weak-coupling perturbative calculation. Due to enhanced scattering with the nearly critical spin fluctuations, the quasiparticle mass in the hot region is strongly renormalized. This accounts for the anomalous logarithmic temperature dependence of specific heat observed in these materials. We show that the same mechanism produces logarithmic temperature dependence in thermopower. This has been observed in $CeCu_{6-x}Au_x$. We expect to see the same behaviour from future experiments on $YbRh_2Si_2$.

Acknowledgements

During the last six years my advisor helped me whenever he had the time. For this I thank him.

It is my special pleasure to thank Prof. Piers Coleman for being a mentor during a crucial period of the Ph.D.

I thank Achim Rosch, Catherine Pépin and Prof. D. Vanderbilt for insightful discussions.

I do not know how I can thank Torun (Masud). With him, I discussed not just physics and politics, but I shared every joy and misery of the last few years. He is among the most important people in my life.

I thank my friends Sergey Pankov and Edouard Boulat with pleasure. Discussing physics with them was educational and exhilarating. The time I spent with them will evoke warm memories.

Thanks to my office-mates Pankaj Mehta and Jerome Rech for a wonderful time in room 281. And I also thank my office-neighbour Craig Fennie for his friendship.

The years of Ph.D. were trying at times. But I will remember the time spent at Rutgers with fondness only because of a wonderful group of friends. Few of them I have already mentioned. Among others, I mention specially David Brookes, Fatiha Benmokhtar, Bruno El-Bennich, Sahana Murthy, Marcello Civelli, Maxime Dion, and William Ratcliffe.

I thank my parents, my sister and my brother for their love and care that transcended distance.

Finally, I acknowledge the sacrifice of millions of taxpayers of India whose money paid for my undergraduate education.

Dedication

To Ma and Baba

Table of Contents

At	strac	t	ii			
Acknowledgements						
De	Dedication					
Li	st of I	Figures	viii			
1.	Intr	oduction	1			
	1.1.	Overview of Quantum Phase transition	2			
	1.2.	Magnetic Quantum Criticality in Heavy-Fermion Systems	4			
	1.3.	Landau Ginzburg Description of Magnetic QCP : Spin Fluctuation				
		Theory	7			
	1.4.	Application of Spin Fluctuation Theory to Heavy-Fermion Quantum				
		Criticality	11			
	1.5.	Brief Introduction to Dynamical Mean Field Theory	13			
2.	Basi	s Dependence and Choice of Basis for DMFT	15			
	2.1.	Basis Dependence of Local Approximations	15			
	2.2.	Choice of a Localized Basis for DMFT	16			
	2.3.	Maximization of Local Interaction Functional by Unitary Transforma-				
		tions	19			
	2.4.	Example: Lattice with Two Sites and Two Orbitals	22			
	2.5.	Attempt to Include Non-Unitary Transformations	28			
3.	The	rmal and Charge Transport for Many Body Tight-Binding Models	34			

	3.1.	Introduction	34			
	3.2.	Charge Current	36			
	3.3.	Thermal Current	43			
	3.4.	Transport Coefficients	45			
	3.5.	Conclusion	50			
4.	The	Charge Current Operator in Down-folding Scheme	51			
	4.1.	Introduction	51			
	4.2.	Charge Current Operator in Low-Energy Sector	54			
	4.3.	Downfolding in the Presence of a Vector Potential	57			
	4.4.	Example: Non-Interacting Anderson Lattice Model	60			
	4.5.	Conclusion	62			
5.	The	rmoelectric Behaviour of Heavy-Fermion Systems Near Magnetic Quar	n-			
tu	m Cri	tical Point	63			
	5.1.	Introduction	63			
	5.2.	Model	67			
	5.3.	Spin-Fermion Vertex and Electron Self-Energy	70			
	5.4.	Thermopower	74			
	5.5.	Conclusion	76			
АĮ	pend	ix A. DMFT Equations for the Hubbard Model	81			
Appendix B. Mathematical Preliminary						
АĮ	Appendix C. Few Calculations for Non-Unitary Transformation					
АĮ	pend	ix D. Two Dimensional Spin-Fermion Model	90			
Re	References					
Vi	ta		00			

List of Figures

1.1.	Two possible phase diagrams with quantum critical points. In (a) a	
	line of classical continuous phase transitions end at a quantum critical	
	point. The region within the dashed lines is the critical regime. In	
	(b) only the ground state energy is non-analytic. At finite temperature	
	thermodynamic free energy is analytic	3
1.2.	The competition between the Kondo effect and the RKKY interaction	
	give rise to magnetic quantum phase transitions in heavy-fermion sys-	
	tems	6
3.1.	Diagrams in configuration space for thermoelectric power. \mathcal{H}_I is the	
	interaction term. In (a) and (b) the thermal current is a two-point vertex,	
	while in (c) and (d) it is a four-point vertex. In the limit of infinite \boldsymbol{d}	
	contribution from (b) and (d) can be neglected	46
5.1.	Two possible scenarios for heavy-fermion quantum criticality. T^* is the	
	temperature below which heavy Fermi liquid forms. Local moments	
	exist above this temperature. In (a) T^* is zero at the critical point x_c .	
	Local moments exist down to the lowest temperature. In (b) T^{\ast} is	
	finite at the critical point. The phase transition is by spin density wave	
	instability of the Fermi liquid.	65
5.2.	Logarithmic temperature dependence of thermopower over tempear-	
	ture for ${\rm CeCu}_{5.9}{\rm Au}_{0.1}.$ Data courtesy of C. Pfleiderer and A. Rosch. $$.	66
5.3.	Lowest order (a) electron self-energy and (b) spin-fermion vertex cor-	
	rection. For the vertex external frequency has been set to zero	70

5.4.	Magnetization (M) vs external magnetic field (H) at different tempera-	
	tures: a) T=0.15K, b) T=0.3K and c) T=0.8K. The discrete points are	
	experimental. The solid lines are fits using equation (10)	77
5.5.	Entropy (S) per Ce atom vs temperature (T) at different magnetic fields	
	: a) H=0T, b) H=1.5T and c) H=3T. The discrete points are experimen-	
	tal, obtained by numerically integrating data from specific heat mea-	
	surement. The solid lines are fits using equation (10)	78
D.1.	Two-dimensional Fermi surface with hot spots. Pairs of hot spots are	
	connected by magnetic ordering wave-vector Q. The connected hot	
	spots are not nested	90

Chapter 1

Introduction

Understanding the various quantum states of matter such as metals, insulators, super-conductors, superfluids and magnets, and the description of phase transitions from one state to another are among the basic goals of condensed matter physics [1]. In the last two decades the discovery of heavy-fermion materials [2] and high temperature superconductors have posed a formidable challenge to this field. In these materials the electron-electron interaction is comparable to the kinetic energy of the electrons. The correlation effects arising from the strong interaction between the electrons play a crucial role in these materials.

Theorists try to understand these strongly correlated electron systems by studying microscopic model Hamiltonians such as the Hubbard model and the Kondo lattice model. In spatial dimensions greater than one there are no known exact solutions of these models and so one has to resort to various approximations. The main difficulty with strongly correlated systems is the non-perturbative nature of these systems. This means the physical properties of these systems cannot be understood by expanding various quantities in powers of the interaction. On the other hand, there are very few known non-perturbative approximations which are controlled in the sense that these approximations are exact in certain limits. In problems involving spins, examples of controlled non-perturbative approximations include the large-S technique, where the size of the spin is assumed to be large, and the large-N technique, which assumes the spin degeneracy N to be large [3].

1.1 Overview of Quantum Phase transition

A quantum phase transition [4,5] is a zero temperature phenomenon in which the nature of the ground state of a material undergoes profound change by the tuning of a microscopic parameter. The energies of the ground state and the excited states are functions of the microscopic parameters of the Hamiltonian. As one of them, say g, is changed, the transition can occur either by a level-crossing in which an excited state becomes the ground state, or by the limiting case of an avoided level-crossing. Mathematically, a quantum phase transition is a point of non-analyticity in the ground state energy $E_g(g)$ at some $g=g_c$. This transition is typically from an ordered ground state (broken symmetry state) to one without order (symmetry restored). The transition is said to be driven by quantum fluctuations. When the transition is continuous, second order, the phase transition point is called a quantum critical point (QCP). It is associated with diverging length and time scales. This is to be contrasted with a classical phase transition which occurs by tuning the temperature (T). In this case it is the thermal fluctuations that drive the transition. Mathematically, a classical phase transition is associated with non-analyticity in the thermodynamic free energy.

A second order phase transition, both quantum and classical, is associated with the divergence of a characteristic length scale ξ (correlation length). Physically, this length scale is the average spatial size of the fluctuations of a relevant quantity about the mean value. More precisely, it is the length scale that determines the exponential decay of correlation functions. The divergence of the correlation function is expressed as

$$\left(\frac{\xi}{a}\right)^{-1} \sim |g - g_c|^{\nu} \,. \tag{1.1}$$

Here ν is a critical exponent, and a is a microscopic length scale (lattice spacing, or resolution in a coarse-grained description). For a quantum phase transition there is also an energy scale Ω that goes to zero at the QCP. For a gapped system this energy scale is the gap between the ground state and the excitations. For a gapless system this is the characteristic scale of the excitation spectrum. The vanishing of Ω is expressed as

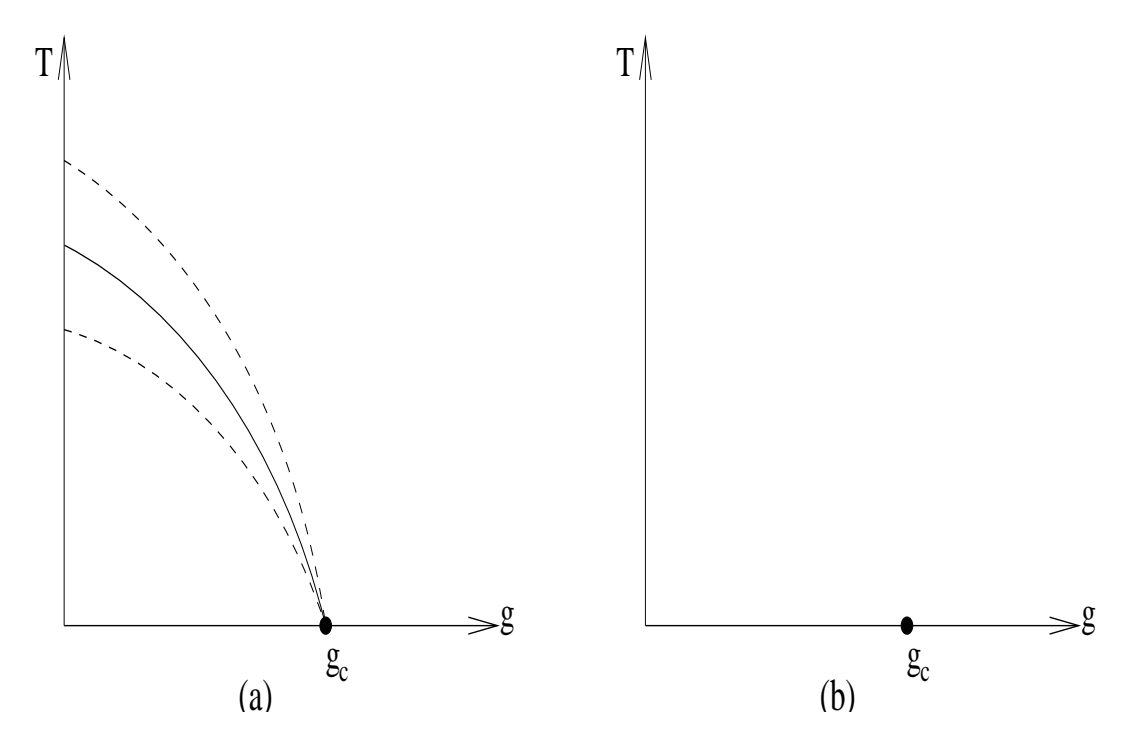


Figure 1.1: Two possible phase diagrams with quantum critical points. In (a) a line of classical continuous phase transitions end at a quantum critical point. The region within the dashed lines is the critical regime. In (b) only the ground state energy is non-analytic. At finite temperature thermodynamic free energy is analytic.

$$\left(\frac{\Omega}{J}\right) \sim |g - g_c|^{z\nu} \sim \left(\frac{\xi}{a}\right)^{-z}.$$
 (1.2)

The exponent z is the called the dynamical exponent. Here J is a microscopic energy scale. The disappearance of the energy scale is associated with the divergence of a time scale τ_{ϕ} , called the phase coherence time. Physically, this is the time scale over which a many-body wavefunction retains phase memory. One can write

$$\tau_{\phi} \sim \hbar \left(\frac{\xi}{a}\right)^{z}.$$
(1.3)

The dynamical critical exponent gives the scaling of time compared to the scaling of space.

There are three generic possibilities for the T-g phase diagram of a system in the presence of a QCP at T=0 and $g=g_c$. First, a line of continuous phase transitions at T>0 can end at a QCP. The line is defined by the non-analyticity of the free energy. This is illustrated in Fig. 1.1(a). The region within the dashed lines is the

critical regime where $k_BT\gg\hbar\omega_{\rm typ}$. Here $\omega_{\rm typ}$ is the frequency scale of the long range fluctuations of the system close to criticality. In this regime it is possible to think of the dynamics of the long range fluctuating modes as frozen in time. Then the phase transition can be described in terms of classical statistical mechanics, a subject which is well studied [6]. Close to the QCP this region shrinks and there is a wide regime in the phase diagram where both quantum fluctuations and thermal fluctuations come into play. We will study this scenario in greater detail in a later chapter of this thesis in the context of magnetic QCPs in heavy-fermion systems. A second possibility is illustrated in Fig. 1.1(b). In this situation only the ground state energy is non-analytic as a function of g. At T>0 the free energy is analytic and there is no finite temperature phase transition. A third possibility is when a line of discontinuous first order transitions at T>0 end at a QCP. For all these cases, studying the system close to the QCP reveals information that is important to understand the nature of the system at low temperatures.

1.2 Magnetic Quantum Criticality in Heavy-Fermion Systems

Heavy-fermion systems are compounds and alloys which contain rare earth metals such as Ce, Yb, U and Np as one of their constituents. Typical heavy-fermion systems are CeCu_2Si_2 , CeCu_6 , UPt_3 , UBe_{13} , NpBe_{13} . The presence of 4f and 5f electrons in these materials has dramatic influences on their properties [7,8,9]. Below a certain characteristic temperature T^* , these materials behave as Landau Fermi liquids characterized by linear temperature dependence of specific heat $C \propto T$, quadratic temperature dependence of resistivity $\rho(T) \propto T^2$, and temperature independent Pauli paramagnetic susceptibility χ . But the effective mass m^* of the quasiparticles is typically several hundred times the mass of a free electron. As a consequence, the specific heat coefficient $\gamma = C/T$ is very large. For example, in heavy-fermions typically $\gamma \sim 1 \text{ J mol}^{-1}$ K^2 , while in an ordinary metal such as Na, $\gamma \sim 1 \text{ mJ mol}^{-1}$ K^2 . Similarly, below

 T^* the Pauli paramagnetic susceptibility is rather large. As the temperature is raised above T^* , the quasiparticles lose their heavy mass and the specific heat levels off. The susceptibility changes from being Pauli-like to Curie-like. The Ce and U ions start behaving like ions with localized magnetic moments.

The f-electrons are localized and so their interaction energy is very high compared to those between s, p and d orbitals. Consequently the low-energy excitations involving f-electrons are predominantly the spin degrees of freedom, while the high-energy excitations are the charge degrees of freedom. The model Hamiltonian for studying the microscopics of heavy-fermion systems is the "Kondo Lattice Model" (when charge fluctuations of the f-electrons are important one has to study the more basic "Periodic Anderson model"). It has the form

$$\mathcal{H} = \sum_{\mathbf{k},\alpha} \epsilon_{\mathbf{k}} c_{\mathbf{k},\alpha}^{\dagger} c_{\mathbf{k},\alpha} + J \sum_{i,\alpha,\beta} \bar{S}_{i} \cdot \psi_{\alpha}^{\dagger}(i) \bar{\sigma}_{\alpha\beta} \psi_{\beta}(i). \tag{1.4}$$

It describes a band of conduction electrons, whose creation and annihilation operators are $c_{\mathbf{k},\alpha}^{\dagger}$ and $c_{\mathbf{k},\alpha}$ respectively, interacting with localized SU(2) spin degrees of freedom at each lattice site i. $\psi_{\alpha}(i)$ is the Fourier transform of $c_{\mathbf{k},\alpha}$. Here α , β are spin indices, and $\bar{\sigma}$ are the Pauli matrices. $\epsilon_{\mathbf{k}}$ is the spectrum of the non-interacting conduction electrons. J is the energy scale of the Kondo coupling. The localized spins are formed at each unit cell by unpaired f-electrons of the rare earth ions. Charge fluctuation of the f-electrons is suppressed due to high repulsion energy.

In the last decade several heavy-fermion materials have been discovered which exhibit antiferromagnetic quantum critical behaviour [10]. Examples include $CePd_2Si_2$ [11], $CeIn_3$ [11], $CeRu_2Si_2$ [12], $CeNi_2Ge_2$ [13], $U_2Pt_2In_2$ [14], $CeCu_{6-x}R_x$ (R=Au, Ag) [15], $YbRh_2Si_2$ [16]. The generic presence of antiferromagnetic QCP in the phase diagrams of these materials can be understood in the following way [17]: at high temperatures the f-electrons form local moments which are mostly decoupled from the conduction electrons. The coupling J grows as the temperature is lowered. It also gives rise to interaction between the moments which is mediated by the conduction electrons. This

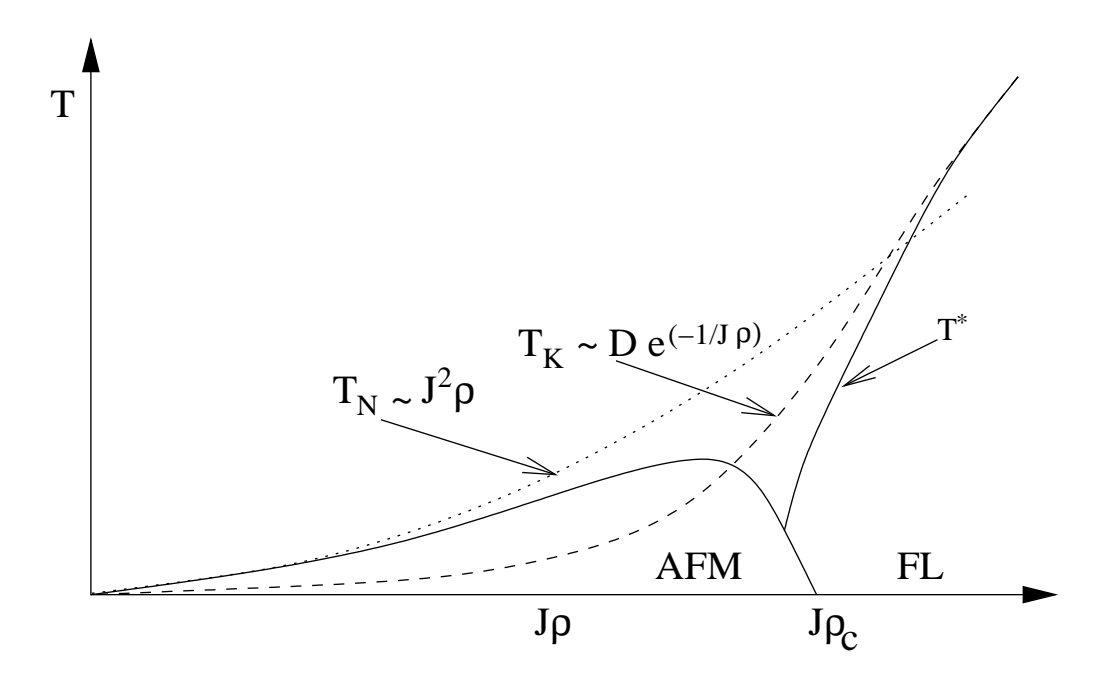


Figure 1.2: The competition between the Kondo effect and the RKKY interaction give rise to magnetic quantum phase transitions in heavy-fermion systems.

is known as the RKKY interaction [18]. In a perturbative calculation the RKKY interaction $J_{RKKY} \sim J^2 \rho$, where ρ is the conduction electron density of states at the Fermi level. This estimate of J_{RKKY} is valid only when $J\rho < 1$. The tendency of the RKKY interaction is to magnetically order the spins, usually in an antiferromagnetic order with Néel temperature $T_N \sim J_{RKKY}/k_B$. On the other hand the Kondo coupling J tends to screen the local moments (Kondo effect) by the formation of singlet bound states between the local moments and the conduction electrons below the Kondo temperature $T_K \sim \rho^{-1} \exp(-1/(J\rho))$. When the moments are screened, they hybridize with the conduction electrons to form a heavy Landau Fermi liquid. The ground state of the system is non-magnetic. The existence of antiferromagnetic QCP in heavy-fermion systems can be understood as a competition between the RKKY interaction J_{RKKY} and the Kondo energy scale T_K (see Fig. 1.2). It is the point in the phase diagram where the balance between J_{RKKY} and T_K is just right to drive the Néel temperature T_N to zero.

Heavy fermion materials with antiferromagnetic QCP have attracted the attention of theorists as well experimentalists in the last several years. At low temperature and close to the QCP these materials, which are metallic, exhibit remarkable non-Fermi liquid (NFL) behaviour. For example, the temperature dependence of resistivity is either linear or quasi-linear, i.e., $\rho \sim T^r$, where $1 \le r < 2$. The specific heat coefficient diverges logarithmically with temperature with $\gamma \sim \log(T_0/T)$. Recently in YbRh₂Si₂, one of the most well-studied materials in this context, it has been observed [19] that as temperature is lowered the divergence of the specific heat coefficient enhances and it becomes a power law with $\gamma \sim T^{-(1/3)}$. The spin susceptibility (χ) of another well-studied material CeCu_{5.9}Au_{0.1} (whose Néel temperature is believed to be zero), measured by inelastic neutron scattering, seem to scale with frequency over temperature (ω/T) with an anomalous exponent $\alpha \sim 0.75$ [20]. There is general consensus that the origin of the NFL behaviour is due to proximity to the QCP (the quantum critical regime), and that the quantum fluctuations in this regime are responsible for the destruction of the Landau Fermi liquid. However, a satisfactory microscopic description of this phenomena and a clear understanding of the NFL properties is still an enigma and therefore constitutes an active area of theoretical and experimental research.

1.3 Landau Ginzburg Description of Magnetic QCP : Spin Fluctuation Theory

The spin fluctuation theory [21,22] is the generalization of the Landau Ginzburg theory for a second order classical phase transition, to describe a quantum phase transition. In a classical phase transition the dynamics can be separated from statics, and so time does not enter in the description of the phase transition. But for a quantum phase transition this separation is not possible. When temperature is the lowest energy scale in the system, i.e., $\hbar\omega_{\rm typ}\gg T$, the dynamics of the long range fluctuations close to the QCP is important. Due to this, the effective dimension of a d dimensional system is

enhanced to (d + z), where z is the dynamical exponent.

In the context of magnetic QCP in heavy-fermion systems, the spin fluctuation theory is constructed to describe the phase transition from the non-magnetic side. The assumption is that T^* is a high energy cut-off, and the spin fluctuation picture is valid for temperature much below this cut-off. In this low temperature regime the local moments are completely screened and are hybridized with the conduction electrons. In other words, in this regime a heavy Fermi liquid has already formed. The spin fluctuation theory describes the phase transition by a spin density wave (SDW) instability of this Fermi liquid. The long wavelength collective spin fluctuations of the fermions condense at the critical point at a particular wave-vector, giving rise to magnetic order.

The starting point of the theory is an interacting fermion system with short range Hubbard interaction. This is written as

$$\mathcal{H} = \sum_{\mathbf{k},\sigma} \epsilon_{\mathbf{k}} c_{\mathbf{k},\sigma}^{\dagger} c_{\mathbf{k},\sigma} + U \sum_{i} n_{i,\uparrow} n_{i,\downarrow}. \tag{1.5}$$

Here $n_{i,\sigma}=c_{i,\sigma}^{\dagger}c_{i,\sigma}$ is the number operator for fermions with spin σ at the lattice site i. $c^{\dagger}(c)$ are fermion creation (annihilation) operators, and $c_{\mathbf{k},\sigma}=(\sum_{i}e^{-i\mathbf{k}\cdot\mathbf{R}_{i}}c_{i,\sigma})/\sqrt{N}$. \mathbf{R}_{i} is the position of the site i and N is the number of lattice sites. $\epsilon_{\mathbf{k}}$ is the spectrum of the free fermions. Since the system is close to a SDW instability, the long wavelength collective spin fluctuations (the paramagnons) are important low-energy degrees of freedom. In a functional integral formalism the spin fluctuations are introduced by a Hubbard Stratonovich transformation. The partition function (Z) is expressed as a functional integral in terms of Grassman fields which represent the fermions. The temperature in this formalism plays the role of imaginary time (τ) . The fermion interaction term, which is quartic in the Grassman fields, is decoupled into Grassman bilinears by introducing a bosonic Hubbard Stratonovich field (ϕ) . This field is identified with the collective spin fluctuation degrees of freedom. The fermionic part of the action is now quadratic, and can be integrated out. The resulting action (S) is expressed entirely in terms of the spin fluctuations, and has a structure which is similar to the Landau

Ginzburg free energy functional for second order classical phase transition. The important difference, as mentioned earlier, is that in the quantum case the order parameter fields are dynamical variables. The spin fluctuation theory is expressed as

$$Z = Z_0 \int \mathcal{D}\phi(\mathbf{k}, \omega_n) e^{-S[\phi(\mathbf{k}, \omega_n)]}, \qquad (1.6)$$

where the action S has the form

$$S[\phi(\mathbf{k},\omega_n)] = \frac{1}{2} \sum_{\mathbf{k},\omega_n} \left(\delta + k^2 + \frac{|\omega_n|}{\Gamma_k} \right) |\phi(\mathbf{k},\omega_n)|^2 + \frac{u}{4\beta} \sum_{\mathbf{k}_i,\omega_i} \phi(\mathbf{k}_1,\omega_1) \phi(\mathbf{k}_2,\omega_2) \times \phi(\mathbf{k}_3,\omega_3) \phi(-\mathbf{k}_1 - \mathbf{k}_2 - \mathbf{k}_3, -\omega_1 - \omega_2 - \omega_3).$$
(1.7)

Here Z_0 is the partition function of the non-interacting fermions, δ is a mass term for the paramagnons which goes to zero at the QCP, and $\beta=1/(k_BT)$. $\omega_n=(2\pi n)/\beta$ is bosonic Matsubara frequency obtained by Fourier transform of the imaginary time τ . In terms of the parameters of the original fermionic theory $\delta=1-U\rho(E_F)$ and $u=U^2\rho''(E_F)/12$, where $\rho(E_F)$ is the density of states of the non-interacting fermions at the Fermi energy. The $|\omega_n|/\Gamma_k$ term in the quadratic part of the action gives damping to the paramagnons. Since the spectrum of the spin fluctuations lies within the continuum of particle-hole excitations, they can decay into particle-hole pairs and are therefore overdamped. For a ferromagnetic instability $\Gamma_k \sim k$, and for an antiferromagnetic instability $\Gamma_k \sim \text{const.}$ In this description of the quantum phase transition the only role of the conduction electrons is to provide damping to the critical collective spin excitations.

The above action can be studied using the renormalization group (RG) approach [21, 22]. This is a powerful conceptual framework [23] in which one studies how the coupling constants (δ and u for the above action, and also T at finite temperature) of the action change as the energy and momentum cut-off of the theory is lowered. From studying the flow of the coupling constants (which are functions of the cut-off scale) one can identify the fixed point action S^* . This is the action which remains unchanged

under RG transformation. Identifying the fixed point action that governs a phase transition gives information about the various critical exponents. These exponents are universal in the sense that they are properties of the fixed point theory S^* and do not depend on the microscopic details of the original action S. RG transformation proceeds in three steps. First, the phase space is separated into slow and fast variables. The modes with low frequency and momentum are the slow modes $\phi_{<}=\phi(k,\omega)$ with $0 < k < \Lambda/s$ and $0 < \omega < \Omega/s_{\omega}$. The modes with high momentum and/or frequency are the fast modes $\phi_>=\phi(k,\omega)$ with $\Lambda/s\leq k\leq \Lambda$ and/or $\Omega/s_\omega\leq \omega\leq \Omega$. After the separation of scales, the fast modes are integrated out (mode elimination). This procedure generates contributions to the slow sector from the fast sector while preserving the form of the action. It is also possible that entirely new couplings are generated by the mode elimination. In the second step, the momenta and frequencies are rescaled by defining k' = sk and $\omega' = s_{\omega}\omega$, such that the cut-offs (for the rescaled parameters) are restored to their original value. The final step is to perform field rescaling by defining new fields, $\phi'(k',\omega')=\xi^{-1}\phi_<(k'/s,\omega'/s_\omega)$, such that certain terms in the quadratic part of the action remains invariant.

In the action given by Eq. (1.7) momentum and frequency enter differently, as a result they are scaled differently. One finds that $s_{\omega}=s^z$ where z is the dynamical critical exponent. This scaling is necessary to keep both the k^2 and the $|\omega_n|/\Gamma_k$ terms in the action unchanged. At the level of bare scaling (i.e., ignoring loop corrections) one finds that $\delta \to \delta s^2$, $T \to T s^z$ and $u \to u s^\epsilon$ where $\epsilon = 4 - (d+z)$. Thus, (d+z) appears as the effective dimension of the system. When (d+z) > 4 the coupling between the spin fluctuation modes diminishes as the cut-off is lowered, and goes to zero at the fixed point. The fixed point theory is given by the quadratic part of the action (with $\delta = 0$). This is known as the Gaussian fixed point, and the system is said to be above its upper critical dimension (= 4). In such a case the critical exponents are correctly given by a mean-field theory. When (d+z) < 4 the coupling u grows as the cut-off is lowered and it becomes relevant. This is a strong coupling problem.

The ultimate fate of the flow of the couplings cannot be determined by perturbative RG (expansion in powers of u). When (d+z)=4, u goes to zero logarithmically as $1/\log(\Lambda_0/\Lambda)$ (u is said to be marginally irrelevant). This is determined by the sign of the $\mathcal{O}(u^2)$ correction to the flow of u. A detailed RG analysis of the above action gives information about the various regimes and the associated phase transition and cross-over lines in the T- δ phase diagram [22].

1.4 Application of Spin Fluctuation Theory to Heavy-Fermion Quantum Criticality

The application of the theory of spin fluctuations to understand magnetic quantum criticality in heavy-fermion materials is not straight-forward and has proven to be only partially successful [10]. For an antiferromagnetic QCP, z=2. If one considers three-dimensional spin fluctuations (since the materials are three-dimensional), the corresponding spin fluctuation model is above the upper critical dimension. Using this model has the following difficulties: (1) it predicts specific heat coefficient $\gamma \sim \gamma_0 + T^{1/2}$, i.e., the corrections to the leading Fermi liquid behaviour are nonanalytic. But experimentally it has been observed [24] that $\gamma \sim \log(T_0/T)$ for materials such as $CeCu_{6-x}Au_x$, $CeNi_2Ge_2$ and $YbRh_2Si_2$. (2) In this model the Landau quasiparticles are well defined on most of the Fermi surface except on the "hot lines" which are lines on the Fermi surface that are connected by the magnetic ordering wave-vector Q. Though the hot electrons have lower lifetime due to scattering with the critical fluctuations, the normal electrons (which form the bulk) contribute the most in transport processes. As a result this model will predict the same temperature dependence of resistivity as does Fermi liquid theory. However, in practice one observes linear or quasi-linear temperature dependence.

The above difficulties can be removed with the postulation that the spin fluctuations are two-dimensional [25]. The two-dimensional nature of the spin fluctuations

has been observed in elastic neutron scattering experiment on $CeCu_{5.9}Au_{0.1}$ [26]. The d=2 and z=2 spin fluctuation theory correctly predicts the logarithmic temperature dependence of the specific heat coefficient. In addition, the entire Fermi surface becomes hot because the spin fluctuation spectrum is insensitive in a third direction. This provides a possible explanation for the linear temperature dependence of resistivity [25]. In a later chapter we will show that this postulation is consistent with the observed temperature dependence of thermopower in $CeCu_{5.9}Au_{0.1}$.

However, the two-dimensional spin fluctuation theory leaves the following issues unexplained: (1) The dynamical spin susceptibility of $\text{CeCu}_{5.9}\text{Au}_{0.1}$ at the ordering wave-vector has been experimentally observed [20] to have the form $\chi(\mathbf{Q},\omega)^{-1}\sim (\omega/T)^{0.75}$. This would suggest a dynamical critical exponent z=2.7 which is different from that given by a Gaussian fixed point. This observation cannot be reconciled with the two-dimensional spin fluctuation theory since it is at the upper critical dimension [27]. (2) Recently the specific heat coefficient of YbRh_2Si_2 has been observed to diverge with a power law as $\gamma \sim T^{-1/3}$ [19]. Currently there is no proper understanding of this behaviour. (3) The microscopic origin of the generic occurrence of two-dimensional spin fluctuations in materials which are three-dimensional is not known.

The attempt to get a complete picture of magnetic quantum criticality in heavy-fermion materials still is an active area of research in condensed matter physics. The failure of the spin fluctuation theory in its current formulation has led to the suggestion that a more basic model, one that will incorporate the physics of the Kondo effect close to a QCP, is necessary [10]. It has been speculated that T^* , the temperature below which the heavy Fermi liquid forms, goes to zero at the QCP [20,28]. This would imply a failure of Kondo effect to take place and the existence of the local moments down to the lowest temperature at the QCP. This idea is currently a topic of investigation.

1.5 Brief Introduction to Dynamical Mean Field Theory

In the last decade dynamical mean field theory (DMFT) has emerged as a successful non-perturbative approximation scheme to deal with problems involving strongly correlated electrons [29, 30]. It is a generalization of the Weiss mean field theory, which was developed for classical systems, to quantum problems. The main idea of DMFT is to describe a many-body system defined on a lattice in terms of a single site quantum impurity in the presence of an effective medium which is self-consistently determined. One can show that this description is exact in the limit of infinite co-ordination number Z (or infinite dimension d). Hence it is a controlled approximation in which various physical quantities can be expanded in powers of 1/Z.

As an illustration of DMFT, we will consider the Hubbard Hamiltonian. It is written as

$$\mathcal{H} = -t \sum_{\langle ij \rangle, \sigma} c_{i,\sigma}^{\dagger} c_{i,\sigma} + U \sum_{i} n_{i\uparrow} n_{i\downarrow}. \tag{1.8}$$

Here $\langle ij \rangle$ denote nearest neighbour summation, $c_{i,\sigma}^{\dagger}$ ($c_{i,\sigma}$) create (annihilate) electrons with spin σ on lattice site \mathbf{R}_i , t is the hopping integral between neighbouring sites, $n_{i,\sigma} = c_{i,\sigma}^{\dagger} c_{i,\sigma}$ is the number operator, and U is the on-site interaction between the electrons. It can be thought of as the local part of the screened Coulomb interaction between the electrons. We will imagine the lattice to be a d-dimensional hypercube which has a co-ordination number Z=2d.

In the limit of infinite dimension the interaction term, which has no information about neighbouring sites, need not be changed. But the hopping term has to be scaled appropriately in order to get a sensible theory. This is done in the following way. We define the one-particle density matrix $g_{ij,\sigma}^0 = \langle c_{i,\sigma}^\dagger c_{j,\sigma} \rangle_0$, where $\langle \ \rangle_0$ implies average with respect to the non-interacting system. $g_{ij,\sigma}^0$ gives the transition amplitude between site \mathbf{R}_i and \mathbf{R}_j . Then $|g_{ij,\sigma}^0|^2$, summed over those \mathbf{R}_j which are nearest neighbour sites to \mathbf{R}_i , gives the probability for an electron to escape from a site \mathbf{R}_i to its nearest neighbour sites. Since the number of nearest neighbour sites is Z, and $g_{ij,\sigma}^0 = t$, when

 \mathbf{R}_i and \mathbf{R}_j are nearest neighbours, this probability is Zt^2 . We have to scale t such that this probability remains finite and the electrons stay mobile in the limit of infinite dimensions. Thus the correct scaling is given by

$$t = \frac{t^*}{Z^{1/2}}, t^* = \text{constant.}$$
 (1.9)

As a result of this scaling, one can show that the electron self-energy becomes local, i.e.,

$$\Sigma_{ij,\sigma}(\omega) \stackrel{d\to\infty}{=} \Sigma_{ii,\sigma}(\omega)\delta_{ij}. \tag{1.10}$$

In other words, self-energy becomes momentum independent, and only a function of frequency. Thus, DMFT ignores fluctuations in space but retains the local quantum fluctuations. In this sense, even in the limit of infinite dimensions, the system has a many-body nature. The above idea can be made more concrete in the functional integral language. This formulation, and the DMFT equations for the Hubbard model are discussed in appendix A.

However, like any other local approximation, DMFT is basis dependent. One has to choose a suitably localized basis in order to ignore all non-local interactions. This topic will be discussed in chapter 2. In recent times DMFT, in conjunction with band theory, is being developed as a numerical tool for predicting properties of correlated materials. For this purpose the accuracy of the DMFT approximation, which is related to the issue of choice of basis, is quite important.

Finally, the calculation of various transport coefficients acquire certain simplifying features in the DMFT formulation. This, and rigorous expressions for the transport coefficients are discussed in chapter 3.

Chapter 2

Basis Dependence and Choice of Basis for DMFT

In this chapter we discuss the basis dependence inherent in all local approximation schemes including dynamical mean field theory (DMFT). From the point of view of improving the numerical accuracy in the implementation of DMFT, choosing an appropriate basis is important. We will suggest a procedure for making this choice. We will test this proposal on an analytically tractable toy model. A few concepts from linear algebra used here, expressed in the language of a non-orthogonal basis, are discussed in appendix B.

2.1 Basis Dependence of Local Approximations

We consider a system of interacting electrons on a lattice whose Hamiltonian is expressed in the basis of atomic orbitals. The single particle states are denoted by $\langle \mathbf{r}|n\alpha\rangle=\phi_{\alpha}(\mathbf{r}-\mathbf{R}_n)$, where α is a symmetry (say, orbital) index and \mathbf{R}_n is a lattice position. We will assume that there are m orbitals such that the index $\alpha=1,\cdots,m$, and there are N lattice sites with the lattice index $n=0,\cdots,N-1$. We will also impose the periodic boundary condition $|n,\alpha\rangle=|n+N,\alpha\rangle$. The states defining the basis, unlike those in a Wannier basis, are not orthogonal. We will denote the overlap between any two states by $O_{\alpha\beta}(n-m)\equiv\langle n\alpha|m\beta\rangle$. As described in appendix B, the second quantized many body Hamiltonian can be written as

$$\mathcal{H} = \sum_{\substack{nm \\ \alpha\beta}} t_{\alpha\beta}^{nm} c_{n,\alpha}^{\dagger} c_{m,\beta} + \sum_{\substack{nmlk \\ \alpha\beta\gamma\delta}} V_{\alpha\beta\delta\gamma}^{nmkl} c_{n,\alpha}^{\dagger} c_{m,\beta}^{\dagger} c_{k,\delta} c_{l,\gamma}, \tag{2.1}$$

where $t_{\alpha\beta}^{nm} \equiv \langle n\alpha | \mathcal{H}_0 | m\beta \rangle$, and $V_{\alpha\beta\delta\gamma}^{nmkl} \equiv \langle n\alpha, m\beta | \hat{V} | l\gamma, k\delta \rangle$. In dynamical mean field theory (DMFT) only the on-site interaction terms are kept, i.e.,

$$\mathcal{H}_{DMFT} = \sum_{\substack{nm \\ \alpha\beta}} t_{\alpha\beta}^{nm} c_{n,\alpha}^{\dagger} c_{m,\beta} + \sum_{\substack{n \\ \alpha\beta\gamma\delta}} V_{\alpha\beta\delta\gamma}^{nnnn} c_{n,\alpha}^{\dagger} c_{n,\beta}^{\dagger} c_{n,\delta} c_{n,\gamma}. \tag{2.2}$$

We now consider an invertible transformation of the single particle basis $|n\alpha\rangle \rightarrow |n'\alpha'\rangle = \sum_{m\beta} T_{\beta\alpha}(m-n)|m\beta\rangle$. Expressed in the new basis the Hamiltonian, say \mathcal{H}' , has the same form as in Eq. (2.1) except with all indices primed. We know that $\mathcal{H}' = \mathcal{H}$ since they are the same operator expressed in two different bases. However, if we perform the DMFT approximation on \mathcal{H}' and neglect the non-local interaction terms in the new basis, the corresponding new DMFT Hamiltonian $\mathcal{H}'_{DMFT} \neq \mathcal{H}_{DMFT}$. The approximation involved in DMFT, namely the neglect of non-local interaction terms, makes this scheme basis dependent. This is a feature of any theory that involves local approximations because a local interaction term in one basis becomes non-local when expressed in another basis. This observation also implies that ignoring non-local interaction terms is a good approximation only if the single particle basis is sufficiently localized. This is the motivation for choosing an appropriate basis in which DMFT can be used as a meaningful approximation.

2.2 Choice of a Localized Basis for DMFT

The two important questions for formulating the problem of choosing an appropriate basis are: (1) what should be the criterion that picks out a suitably localized set of orbitals as the preferred basis, and (2) what type of transformations of the basis should we allow. The problem of choosing an appropriate basis set has been studied earlier in quantum chemistry and in band structure calculations [31]. Usually such problems are formulated by defining an appropriate functional (this provides the aforementioned criterion) which is basis dependent and whose extremization by transformation of basis provides a well-defined scheme for choosing a preferred basis set. For example, "localized molecular orbitals" have been studied extensively in quantum chemistry. These are

the analogues, for finite systems, of the Wannier functions defined for infinite periodic systems. Among the several criteria that have been proposed for defining the localized molecular orbitals, one of the most widely accepted criterion is the maximization of the Coulomb self-interaction of the molecular orbitals by unitary transformations of the basis states [32]. For band structure calculations the use of "maximally-localized" Wannier functions has been proposed [31]. The Wannier functions are defined by

$$W_{\alpha}(\mathbf{r} - \mathbf{R}) = \sum_{\mathbf{k}} e^{i\mathbf{k}\cdot(\mathbf{r} - \mathbf{R})} \phi_{\alpha\mathbf{k}}(\mathbf{r}),$$

where $\phi_{\alpha \mathbf{k}}(\mathbf{r})$ are the Bloch orbitals which have the periodicity of the lattice. However, there is freedom in the choice of phase of the Bloch orbitals. More generally, the basis of Bloch orbitals can be changed by unitary transformations

$$\phi_{\alpha \mathbf{k}}(\mathbf{r}) \to \phi_{\alpha' \mathbf{k}}(\mathbf{r}) = \sum_{\beta} U_{\beta \alpha}(\mathbf{k}) \phi_{\beta \mathbf{k}}(\mathbf{r}),$$

where $U_{etalpha}(\mathbf{k})$ is unitary. This produces a new basis of Wannier functions

$$W_{\alpha'}(\mathbf{r} - \mathbf{R}) = \sum_{\mathbf{k}} e^{i\mathbf{k}\cdot(\mathbf{r} - \mathbf{R})} \sum_{\beta} U_{\beta\alpha}(\mathbf{k}) \phi_{\beta\mathbf{k}}(\mathbf{r}).$$

The criterion for choosing this particular basis of Wannier functions involves the minimization of the "spread functional" which is the sum of the second moments of the Wannier functions. It is given by

$$\Omega[U_{\beta\alpha}(\mathbf{k})] = \sum_{\alpha'} [\langle 0\alpha' | r^2 | 0\alpha' \rangle - \langle 0\alpha' | \mathbf{r} | 0\alpha' \rangle^2].$$

The spread functional is maximized with respect to the unitary transformation $U_{\beta\alpha}(\mathbf{k})$. This criterion is the exact analogue, for a lattice system, of one of the criteria suggested for choosing localized molecular orbitals [33].

In our problem it seems *a priori* there is no unique criterion, and only by comparing the results of different criteria one can conclude what is appropriate. A possible criterion, for example, is to choose the basis in which the sum of the square of the on-site interaction terms is maximum. For this one has to define a functional

$$F_1[\{|n\alpha\rangle\}] = \sum_{\alpha\beta\gamma\delta} |V_{\alpha\beta\delta\gamma}^{0000}|^2 = \sum_{\alpha\beta\gamma\delta} V_{\alpha\beta\delta\gamma}^{0000} V_{\gamma\delta\beta\alpha}^{0000},$$

and find a basis in which the functional is maximum. If it can be implemented, will this procedure allow us to say that the sum of the square of the non-local interaction terms have been minimized as well? Also, should one include weight factors from the overlap matrix in the case of non-orthogonal bases? To answer these questions we will first identify a quantity which is invariant under invertible transformations of the basis states. As discussed in appendix B, the trace of an operator is such a quantity. We define

$$I = \operatorname{Tr}(\hat{V}^{2}) = \sum_{\substack{nmlkrspq\\ \alpha\beta\gamma\delta\sigma\rho\eta\nu}} O_{\alpha\beta}^{-1}(n-m)O_{\gamma\delta}^{-1}(l-k)O_{\sigma\rho}^{-1}(r-s)O_{\eta\nu}^{-1}(p-q)V_{\beta\delta\eta\sigma}^{mkpr}V_{\rho\nu\gamma\alpha}^{sqln}.$$
(2.3)

This invariant quantity has two basis-dependent parts: terms that involve only the local interaction, and those that involve the non-local interaction. Keeping only the local interaction terms we can define the functional

$$F[\{|n\alpha\rangle\}] = \sum_{\alpha\beta\gamma\delta\sigma\rho\eta\nu} O_{\alpha\beta}^{-1}(0)O_{\gamma\delta}^{-1}(0)O_{\sigma\rho}^{-1}(0)O_{\eta\nu}^{-1}(0)V_{\beta\delta\eta\sigma}^{0000}V_{\rho\nu\gamma\alpha}^{0000}, \tag{2.4}$$

which we will call the "local interaction functional". Now if we can find a basis in which F is maximum, then we are guaranteed that simultaneously the part of I which contains non-local interaction terms is minimized. Thus, the functional F is a more suitable quantity to work with than F_1 . We note that the two functionals are identical in the case where the basis is orthonormal.

To elucidate the structure of the functional we will consider a basis transformation of the form $|n\alpha\rangle \to |n'\alpha'\rangle = T|n\alpha\rangle$. In general the transformation of the overlap is given by $O' = T^\dagger OT$, and the transformation of the interaction is $V' = T^\dagger T^\dagger VTT$. Supressing indices for clarity, the functional in the new basis can be expressed as

$$\begin{split} F[\{|n'\alpha'\rangle\}] &= \sum_{\alpha'\beta'\gamma'\delta' \atop \sigma'\rho'\eta'\nu'} O_{\alpha'\beta'}^{-1}(0)O_{\gamma'\delta'}^{-1}(0)O_{\sigma'\rho'}^{-1}(0)V_{\eta'\nu'}^{0000}(0)V_{\beta'\delta'\eta'\sigma'}^{0000}V_{\rho'\nu'\gamma'\alpha'}^{0000} \\ &= \left[T^{-1}O^{-1}\left(T^{\dagger}\right)^{-1}\right]^{4} \left[T^{\dagger}T^{\dagger}VTT\right]^{2} \\ &= F[T]. \end{split}$$

The scheme is to maximize F[T] with respect to the transformations T.

The next question is what kind of transformations of the basis states should we consider under which the local interaction functional will be maximized. We will study two possibilities: (1) unitary transformations, and (2) general invertible transformations with suitable constraints. The overlap matrix remains unchanged under unitary transformations, therefore in this scheme we will maximize F within a family of bases which have the same overlap matrix. The motivation for using general invertible transformations is to probe bases which have different overlap matrices. However, without appropriate constraints, the functional becomes unbounded when non-unitary transformations are allowed. In particular, we will discuss the constraint that the basis states remain normalized under a change of basis. But we find that this scheme still fails to make the functional bounded. We will conclude that the proper way to constrain the non-unitary transformations is to keep the ratio of the singular-value decompositions of the transformations within a certain range.

2.3 Maximization of Local Interaction Functional by Unitary Transformations

Given a basis $\{|n\alpha\rangle\}$ with the overlap matrix $\langle n\alpha|m\beta\rangle\equiv O_{\alpha\beta}(n-m)$, we consider unitary transformation

$$|n\alpha\rangle \to |n\alpha\rangle + \delta|n\alpha\rangle = U|n\alpha\rangle = \sum_{m\beta} U_{\beta\alpha}(m-n)|m\beta\rangle$$
 (2.5)

to a new set of basis states $\{|n'\alpha'\rangle\}$, where $|n'\alpha'\rangle = |n\alpha\rangle + \delta|n\alpha\rangle$. The unitary transformation can be represented as $U = e^{i\epsilon H}$, where H is hermitian and ϵ is a small parameter. The action of H on the states is given by $H|n\alpha\rangle = \sum_{m\beta} H_{\beta\alpha}(m-n)|m\beta\rangle$ such that

$$U_{\alpha\beta}(n-m) = \delta_{\alpha\beta}\delta_{nm} + (i\epsilon)H_{\alpha\beta}(n-m) + \frac{(i\epsilon)^2}{2!}\sum_{l\gamma}H_{\alpha\gamma}(n-l)H_{\gamma\beta}(l-m) + \cdots$$

The hermiticity of H implies that $[\langle n\alpha|H|m\beta\rangle]^* = \langle m\beta|H|n\alpha\rangle$, i.e.,

$$\sum_{l\gamma} H_{\gamma\beta}^*(l-m)O_{\gamma\alpha}(l-n) = \sum_{l\gamma} O_{\beta\gamma}(m-l)H_{\gamma\alpha}(l-n), \tag{2.6}$$

where we have used $O_{\alpha\gamma}^*(n-l)=O_{\gamma\alpha}(l-n)$ (which follows from the definition of O). Using the above equation it is easy to check that the overlap matrix remains unchanged, i.e., $\langle n'\alpha'|m'\beta'\rangle=\langle n\alpha|m\beta\rangle=O_{\alpha\beta}(n-m)$. If there are m orbitals per site, and the lattice has N sites with periodic boundary condition, then $H_{\gamma\alpha}(l-n)$ has Nm^2 real independent parameters. The transformation of the two-particle states is given by

$$|n\alpha, m\beta\rangle \to |n\alpha, m\beta\rangle + (i\epsilon) \sum_{l\gamma} \{H_{\gamma\alpha}(l-n)|l\gamma, m\beta\rangle + H_{\gamma\beta}(l-m)|n\alpha, l\gamma\rangle\} + \mathcal{O}(\epsilon^2),$$

and the variation of the on-site interaction term is

$$\delta V_{\beta\delta\eta\sigma}^{0000} = (i\epsilon) \sum_{t\mu} \left\{ V_{\beta\delta\eta\mu}^{000t} H_{\mu\sigma}(t) + V_{\beta\delta\mu\sigma}^{00t0} H_{\mu\eta}(t) - H_{\mu\beta}^*(t) V_{\mu\delta\eta\sigma}^{t000} - H_{\mu\sigma}^*(t) V_{\beta\mu\eta\sigma}^{0t00} \right\} + \mathcal{O}(\epsilon^2).$$

The variation of the functional F under the unitary transformation is given by

$$\delta F = 2 \sum_{\alpha\beta\gamma\delta\sigma\rho\nu\nu} O_{\alpha\beta}^{-1}(0) O_{\gamma\delta}^{-1}(0) O_{\sigma\rho}^{-1}(0) O_{\eta\nu}^{-1}(0) \delta V_{\beta\delta\eta\sigma}^{0000} V_{\rho\nu\gamma\alpha}^{0000}.$$

In the following we will assume that $\hat{V}(\mathbf{r}_1, \mathbf{r}_2) = \hat{V}(\mathbf{r}_2, \mathbf{r}_1)$, so that $V_{\alpha\beta\delta\gamma}^{nmkl} = V_{\beta\alpha\gamma\delta}^{mnlk}$. For the convenience of notation we define the quantity

$$L_{\sigma\mu}(t) \equiv \sum_{\alpha\beta\gamma\delta\rho\eta\nu} O_{\alpha\beta}^{-1}(0) O_{\gamma\delta}^{-1}(0) O_{\sigma\rho}^{-1}(0) O_{\eta\nu}^{-1}(0) V_{\rho\nu\gamma\alpha}^{0000} V_{\beta\delta\eta\mu}^{000t}.$$
 (2.7)

After some algebra we get

$$\delta F = (4i\epsilon) \sum_{t,\sigma\mu} \left\{ L_{\sigma\mu}(t) H_{\mu\sigma}(t) - L_{\sigma\mu}^*(t) H_{\mu\sigma}^*(t) \right\} + \mathcal{O}(\epsilon^2)$$

$$= (4i\epsilon) \sum_{t,\sigma\mu} \left\{ L_{\sigma\mu}(t) - \sum_{\substack{nm \\ \alpha\beta}} O_{\sigma\beta}^{-1}(m-n) L_{\alpha\beta}^*(-m) O_{\alpha\mu}(n-t) \right\} H_{\mu\sigma}(t)$$

$$+ \mathcal{O}(\epsilon^2). \tag{2.8}$$

We define

$$A_{\sigma\mu}(t) \equiv L_{\sigma\mu}(-t) - \sum_{\substack{nm\\\alpha\beta}} O_{\sigma\beta}^{-1}(m-n) L_{\alpha\beta}^*(-m) O_{\alpha\mu}(n+t), \tag{2.9}$$

and we note that $A_{\sigma\mu}(t)$ is anti-hermitian, i.e.,

$$\sum_{l,\gamma} O_{\beta\gamma}(m-l) A_{\gamma\alpha}(l-n) = -\sum_{l,\gamma} A_{\gamma\beta}^*(l-m) O_{\gamma\alpha}(l-n). \tag{2.10}$$

The condition for the functional F to have a local maxima is

$$\frac{\delta F}{\delta H_{\mu\sigma}(t)} = A_{\sigma\mu}(-t) = 0. \tag{2.11}$$

This anti-hermitian condition has to be satisfied by the preferred basis. In other words, the preferred basis is the one in which $L_{\sigma\mu}(t)$ is hermitian. This condition gives Nm^2 real independent conditions, which is the same as the number of real independent parameters in the hermitian transformation matrix $H_{\sigma\mu}(t)$.

The following is a simple ansatz for maximizing F by successive unitary transformations: starting with a basis $\{|n\alpha\rangle\}$, we calculate $A_{\mu\sigma}(t)$ in that basis using Eqs. (2.7) and (2.9). We then change the basis using the transformation

$$H_{\mu\sigma}(t) = iA_{\mu\sigma}(t), \tag{2.12}$$

and follow this procedure successively till the condition for maxima is achieved. We assert that with this ansatz, to $\mathcal{O}(\epsilon)$

$$\delta F = -(4\epsilon) \sum_{t,\sigma\mu} A_{\sigma\mu}(-t) A_{\mu\sigma}(t) \ge 0. \tag{2.13}$$

This will ensure that with successive transformations the value of the functional increases till maxima is attained.

Next we will prove the above assertion. First, if the basis is orthonormal to begin with, i.e., $O_{\alpha\beta}(n-m)=\delta_{\alpha\beta}\delta_{nm}$, it is easy to see that $A_{\mu\sigma}(t)=L_{\mu\sigma}(-t)-L_{\sigma\mu}^*(t)=-A_{\sigma\mu}^*(t)$. Then, $\delta F=(4\epsilon)\sum_{t,\sigma\mu}|A_{\sigma\mu}(-t)|^2\geq 0$. If the basis $\{|n\alpha\rangle\}$ is non-orthogonal, we will assume there exists an orthonormal basis $\{|a\tau\rangle\rangle\}$ (say a Wannier basis) to which it is related by

$$|a\tau\rangle\rangle = \sum_{n,\alpha} S(n,\alpha;a,\tau)|n\alpha\rangle$$
 and $\langle\langle a\tau| = \sum_{n,\alpha} \langle n\alpha|S(n,\alpha;a,\tau)^*$. (2.14)

From a generalization of Eq. (B.3) we get

$$O_{\alpha\beta}^{-1}(n-m) = \sum_{a,\tau} S(n,\alpha;a,\tau)S(m,\beta;a,\tau)^*.$$
 (2.15)

Using Eq. (2.10) we can rewrite

$$\delta F = (4\epsilon) \sum_{\substack{nmt \\ \alpha\beta\sigma\mu}} O_{\sigma\beta}^{-1}(m-n) A_{\alpha\beta}^*(m) O_{\alpha\mu}(n-t) A_{\mu\sigma}(t)$$

$$= \frac{1}{N} (4\epsilon) \sum_{\substack{nmtk \\ \alpha\beta\sigma\mu}} O_{\sigma\beta}^{-1}(m-n) A_{\alpha\beta}^*(k-n) O_{\alpha\mu}(k-t) A_{\mu\sigma}(t-m),$$
(2.16)

where in the last line we have rearranged the lattice indices in a more symmetric way. Now, using the matrix Eq. (2.15) and its inverse, we get

$$\delta F = \frac{1}{N} (4\epsilon) \sum_{\substack{nmtk \\ \alpha\beta\sigma\mu}} \left[\sum_{a,\tau} S(m,\sigma;a,\tau) S(n,\alpha;a,\tau)^* \right] A_{\alpha\beta}^*(k-n) \times \left[\sum_{b,\kappa} S^{-1}(b,\kappa;k,\alpha)^* S^{-1}(b,\kappa;t,\mu) \right] A_{\mu\sigma}(t-m)$$

$$= \frac{1}{N} (4\epsilon) \sum_{\substack{ab \\ \tau\kappa}} \left| \sum_{\substack{tm \\ \mu\sigma}} S^{-1}(b,\kappa;t,\mu) A_{\mu\sigma}(t-m) S(m,\sigma;a,\tau) \right|^2$$

$$> 0.$$

2.4 Example: Lattice with Two Sites and Two Orbitals

In this section we study the problem of choosing a localized basis for an analytically tractable case, namely a lattice with two sites and two orbitals on each site. For this case we examine the result of maximizing the local interaction functional by unitary transformations. In particular, we will investigate: (1) whether the criterion that we have proposed for choosing a suitably localized basis for DMFT is a mathematically well-defined procedure, and (2) whether the result of maximizing the functional gives a unique basis.

We consider a lattice with two sites (N=2), namely n=0,1. On each site there are two orbitals (m=2) a and b. We assume that the initial basis with the four states $\langle \mathbf{r}|0a\rangle = \phi_a(\mathbf{r}), \langle \mathbf{r}|0b\rangle = \phi_b(\mathbf{r}), \langle \mathbf{r}|1a\rangle = \phi_a(\mathbf{r}-\mathbf{R}), \langle \mathbf{r}|1b\rangle = \phi_b(\mathbf{r}-\mathbf{R})$ is orthonormal. We consider an interacting electron Hamiltonian of the form

$$\mathcal{H} = \sum_{\substack{nm \\ \alpha\beta}} t_{\alpha\beta}^{nm} c_{n,\alpha}^{\dagger} c_{m,\beta} + U\left(n_0^2 + n_1^2\right) + \frac{V}{2} \left(n_0 n_1 + n_1 n_0\right). \tag{2.17}$$

Here n, m are site indices and α, β are orbital indices. $t_{\alpha\beta}^{nm} \equiv \langle n\alpha | \mathcal{H}_0 | m\beta \rangle$ is the hopping term, and $n_i = \sum_{\alpha} c_{i,\alpha}^{\dagger} c_{i,\alpha}$ is the occupancy of the site i. We parameterize the non-local interaction term by $V = \lambda U$.

For the basis defined above the local interaction functional F=4, in units of U^2 (which we will set as 1 from now on). In the following we will examine whether the functional can be maximized by unitary transformations of the starting basis.

We order the initial basis states $\{|0a\rangle, |0b\rangle, |1a\rangle, |1b\rangle\}$, and consider unitary transformation of the form $|n\alpha\rangle \to |n'\alpha'\rangle = \sum_{n,\alpha} U_{\alpha\alpha'}(n-n')|n\alpha\rangle$. The transformation is defined by $Nm^2=8$ independent parameters. Due to lattice translation symmetry, the 4×4 transformation matrix U and its adjoint U^\dagger can be written in terms of 2×2 blocks of the form

$$U = \begin{bmatrix} U(0) & U(1) \\ U(1) & U(0) \end{bmatrix} \quad \text{and} \quad U^{\dagger} = \begin{bmatrix} U^{\dagger}(0) & U^{\dagger}(1) \\ U^{\dagger}(1) & U^{\dagger}(0) \end{bmatrix}.$$
 (2.18)

We note that the 2×2 matrices U(0) and U(1) are not unitary, but the 4×4 matrix U is. The most general form of the blocks can be expressed as

$$U(0) = \frac{1}{2} \left\{ e^{iu_0} \left[\cos(u) \mathbf{1} + i \sin(u) (\hat{u} \cdot \bar{\sigma}) \right] + e^{iv_0} \left[\cos(v) \mathbf{1} + i \sin(v) (\hat{v} \cdot \bar{\sigma}) \right] \right\},$$
(2.19)

and

$$U(1) = \frac{1}{2} \left\{ e^{iu_0} \left[\cos(u) \mathbf{1} + i \sin(u) (\hat{u} \cdot \bar{\sigma}) \right] - e^{iv_0} \left[\cos(v) \mathbf{1} + i \sin(v) (\hat{v} \cdot \bar{\sigma}) \right] \right\}.$$
(2.20)

Here 1 is the 2×2 identity matrix and $\bar{\sigma}$ are the Pauli sigma matrices. $\hat{u}=u_1\hat{x}+u_2\hat{y}+u_3\hat{z}$ and $\hat{v}=v_1\hat{x}+v_2\hat{y}+v_3\hat{z}$ are unit vectors. The parameters of the transformation are $u_0,v_0=(0,2\pi),\ u,v=(0,\pi),\ u_1,u_2$ (with $u_3=\pm\sqrt{1-u_1^2-u_2^2}$), and v_1,v_2 (with $v_3=\pm\sqrt{1-v_1^2-v_2^2}$). The transformations belong to the symmetry group $SU(2)\times SU(2)\times U(1)\times U(1)$. One U(1), which we will associate with the parameter u_0 , is a trivial transformation by a global phase. We will disregard this and set $u_0=0$, and define $v_0-u_0=\theta$. The transformations U are then defined by $\bar{u},\ \bar{v},\ \theta$ (seven parameters), i.e., $U=U(\bar{u},\bar{v},\theta)$.

The local interaction term in the new basis $V^{0000}_{\alpha'\beta'\gamma'\delta'} \equiv \langle 0\alpha', 0\beta' | \hat{V} | 0\delta', 0\gamma' \rangle$ is given by

$$V_{\alpha'\beta'\gamma'\delta'}^{0000} = \sum_{\substack{nmlk \\ \alpha\beta\gamma\delta}} U_{\alpha'\alpha}^{\dagger}(N-n)U_{\beta'\beta}^{\dagger}(N-m)V_{\alpha\beta\gamma\delta}^{nmlk}U_{\gamma\gamma'}(l)U_{\delta\delta'}(k). \tag{2.21}$$

Since the transformation is unitary, the orthonormality of the original basis is preserved in the new one. Since, $O_{\alpha\beta}^{-1}(0) = \delta_{\alpha\beta}$, the form of the functional defined in Eq. (2.4) reduces to

$$F[U] = \sum_{\alpha'\beta'\gamma'\delta'} \left| V_{\alpha'\beta'\gamma'\delta'}^{0000} \right|^{2}$$

$$= \sum_{\alpha'\beta'\gamma'\delta'} \left| \sum_{\substack{nmlk \\ \alpha\beta\gamma\delta}} U_{\alpha'\alpha}^{\dagger}(N-n) U_{\beta'\beta}^{\dagger}(N-m) V_{\alpha\beta\gamma\delta}^{nmlk} U_{\gamma\gamma'}(l) U_{\delta\delta'}(k) \right|^{2} . (2.22)$$

The above expression is simplified because in the original basis we have only two types of interaction matrix elements: $U^{nnnn}_{\alpha\beta\beta\alpha}=1$ (in units of U) for n=(0,1) and $\alpha,\beta=(a,b)$; and $U^{nmmn}_{\alpha\beta\beta\alpha}=\lambda/2,\,n\neq m,\,n,m=(0,1)$ and $\alpha,\beta=(a,b)$. Since the transformation is unitary, it is easy to verify that $U^{\dagger}(0)U(0)+U^{\dagger}(1)U(1)=1$. For convenience we define the matrix $Y=U^{\dagger}(0)U(0)-U^{\dagger}(1)U(1)$. One can show that

$$Y = \cos(\theta) \left[\cos(u) \cos(v) + \sin(u) \sin(v) (\hat{u} \cdot \hat{v}) \right] \mathbf{1} + \sin(\theta) \sin(u) \cos(v) (\hat{u} \cdot \bar{\sigma})$$
$$-\sin(\theta) \cos(u) \sin(v) (\hat{v} \cdot \bar{\sigma}) - \sin(\theta) \sin(u) \sin(v) (\hat{u} \times \hat{v}) \cdot \bar{\sigma}. \tag{2.23}$$

After some algebra one can show that the functional has the form

$$F[U] = \left(1 + \frac{\lambda}{2}\right)^2 + \frac{1}{4}\left(1 - \frac{\lambda}{2}\right)^2 \left[Tr(Y^2)\right]^2 + \frac{1}{2}\left(1 - \frac{\lambda^2}{4}\right) \left[Tr(Y)\right]^2. \tag{2.24}$$

From Eq. (2.23) we get,

$$Tr(Y) = 2\cos(\theta) \left[\cos(u)\cos(v) + \sin(u)\sin(v)(\hat{u}\cdot\hat{v})\right],\tag{2.25}$$

and one can further show that

$$Tr(Y^2) = 2\sin^2(\theta) + 2\cos(2\theta)\left[\cos(u)\cos(v) + \sin(u)\sin(v)(\hat{u}\cdot\hat{v})\right]^2$$
. (2.26)

Since $|\hat{u} \cdot \hat{v}| \leq 1$, one can show that $|\cos(u)\cos(v) + \sin(u)\sin(v)(\hat{u} \cdot \hat{v})| \leq 1$. We define $\cos(u)\cos(v) + \sin(u)\sin(v)(\hat{u} \cdot \hat{v}) = \sin(\phi)$. Then,

$$F[U] = \left(1 + \frac{\lambda}{2}\right)^2 + \frac{1}{4}\left(1 - \frac{\lambda}{2}\right)^2 (1 - \cos(2\theta)\cos(2\phi))^2 + \frac{1}{2}\left(1 - \frac{\lambda^2}{4}\right) (1 - \cos(2\phi)) (1 + \cos(2\theta)).$$
 (2.27)

Before we discuss the transformations that maximize the functional, it is useful to identify the symmetry transformations that leave the interacting part of the Hamiltonian (\mathcal{H}_I) invariant. Since the functional considers only interaction terms, we do not worry about the transformation properties of the non-interacting part. Suppose U_s is a transformation of the form given by Eq. (2.18) which leaves \mathcal{H}_I invariant. Now, if U_m is a transformation that maximizes the functional, then so does U_mU_s . In this context we note: (a) \mathcal{H}_I is invariant under transformations that generate SU(2) rotations of the two orbitals on each site. We will call such transformations $U_{SU(2)}$. They have the form $U(0) = \exp(i\bar{n} \cdot \bar{\sigma})$, U(1) = 0, i.e., $U(\bar{n}, \bar{n}, 0)$. (b) \mathcal{H}_I is invariant under trivial re-labeling of the two sites, i.e., $0 \leftrightarrow 1$. We will call this transformation U_{RL} . It is given by U(0) = 0, U(1) = 1, i.e., $U(0, 0, \pi)$. (c) For $\lambda = 2$, \mathcal{H}_I has SU(4) symmetry and is invariant under any U.

The result of maximizing the functional depends on the strength of the non-local interaction λ in the starting basis. We identify the following different cases:

1. $|\lambda| < 2$.

The maximum value of the functional is $F_{\rm max}=4$ (same as in the original basis), and at the maxima we have the solution $\cos(2\phi)=-1$, i.e., $\phi=\pi/2$, $(3\pi)/2$, and $\cos(2\theta)=1$, i.e., $\theta=0,\pi$. For $\phi=\pi/2$ we have the equation

$$\cos(u)\cos(v) + \sin(u)\sin(v)(\hat{u}\cdot\hat{v}) = 1. \tag{2.28}$$

This has solutions $((\hat{u}\cdot\hat{v})=0,u=v=0), ((\hat{u}\cdot\hat{v})=0,u=v=\pi)$, and $((\hat{u}\cdot\hat{v})=1,u=v)$. Similarly for $\phi=(3\pi)/2$ we have the solutions $(\hat{u}\cdot\hat{v})=0,u=0,v=\pi)$, $(\hat{u}\cdot\hat{v})=0,u=\pi,v=0)$ and $((\hat{u}\cdot\hat{v})=-1,v=\pi-u)$. All these solutions can be put into two categories of transformations: (a) $U(\bar{n},\bar{n},0)$. This gives the identity transformation, and rotations between the two orbitals on each lattice site. Since the identity transformation, which chooses the original basis, maximizes the functional, so does $U_{SU(2)}$. (b) $U(0)\leftrightarrow U(1)$, which is the same as (a) with an additional relabeling of the lattice sites (i.e., $U_{RL}U_{SU(2)}=U(\bar{n},\bar{n},\pi)$). All these transformations are trivial in the sense they do not mix between orbitals on different sites. Up to these trivial transformations the result of maximizing the functional is unique, and we conclude that the original basis is the most localized one.

2. $\lambda = 2$.

In this case the functional becomes constant with F=4 and independent of the choice of basis. This is because \mathcal{H}_I has SU(4) symmetry.

3. $|\lambda| > 2$.

 $F_{\rm max}=2+\lambda^2/2$ and the solution for the maxima is $\cos(2\theta)=-1$, i.e., $\theta=\pi/2, (3\pi)/2$, and $\cos(2\phi)=1$, i.e., $\phi=0,\pi$. For either value of ϕ we get the equation

$$\cos(u)\cos(v) + \sin(u)\sin(v)(\hat{u}\cdot\hat{v}) = 0. \tag{2.29}$$

The vectors \bar{u} and \bar{v} are defined by six independent parameters. The above equation fixes one of the parameters. This defines a family of transformations (S)

with five independent parameters. To understand the composition of this family we note that $u=0,\ v=\pi/2$ satisfy the above equation and belongs to this family. This defines a two parameter set (S_0) of transformations of the form $U(0)=(1-\hat{v}\cdot\sigma)/2,\ U(1)=(1+\hat{v}\cdot\sigma)/2,\ \text{i.e.},\ S_0=\{U(0,(\pi\hat{v})/2,\pi/2)\}.$ The two parameters fix the direction of \hat{v} . The remaining transformations belonging to S are generated by the action of a transformation belonging to S_0 on a symmetry transformation $U_{SU(2)}$ (which accounts for three independent parameters). To prove this let $U(\bar{u}_n,\bar{v}_n,\pi/2)$ be the result of acting $U(0,(\pi\hat{v})/2,\pi/2)$ on a $U_{SU(2)}$ of the form $U(\bar{n},\bar{n},0)$. Then, one can check that $\bar{u}_n=\bar{n}$, and \bar{v}_n is defined by

$$\cos(v_n) = \sin(n)(\hat{n} \cdot \hat{v})$$

and

$$\hat{v}_n = -\frac{\cos(n)\hat{v} + \sin(n)(\hat{n} \times \hat{v})}{\sqrt{1 - \sin^2(n)(\hat{n} \cdot \hat{v})^2}}.$$

Using the above relations one can show that $\cos(u_n)\cos(v_n)+\sin(u_n)\sin(v_n)(\hat{u}_n\cdot\hat{v}_n)=0$, for all \hat{v} (two parameters) and for all \bar{n} (three parameters). Thus, $U(\bar{u}_n,\bar{v}_n,\pi/2)$ constitutes the set S, and furthermore, it is enough to consider only transformations $U(0,(\pi\hat{v})/2,\pi/2)$ as solutions. They define a family of non-trivial transformations (in the sense that the transformations mix orbitals on different sites). Thus, there is no unique most localized basis in this case. As an example, when $\hat{v}=\hat{x},U(0)=(1-\sigma_x)/2$, and $U(1)=(1+\sigma_x)/2$. Then, $\mathcal{H}_I\to \frac{1}{2}(1+\frac{\lambda}{2})n_0^2+\frac{1}{2}(1-\frac{\lambda}{2})(c_{0,a}^{\dagger}c_{0,b}+c_{0,b}^{\dagger}c_{0,a})^2+\text{local terms on site }1+\text{non-local terms.}$ This gives $F=4\times(1+\lambda/2)^2/4+4\times(1-\lambda/2)^2/4=2+\lambda^2/2$. And when $\hat{v}=\hat{y},\mathcal{H}_I\to \frac{1}{2}(1+\frac{\lambda}{2})n_0^2-\frac{1}{2}(1-\frac{\lambda}{2})(c_{0,a}^{\dagger}c_{0,b}+c_{0,b}^{\dagger}c_{0,a})^2+\text{local terms on site }1+\text{non-local terms}$. This too gives $F=2+\lambda^2/2$. It is also important to note that identity does not belong to this family. In other words, the starting basis is not among the most localized bases.

4. $\lambda = -2$.

 $F_{\rm max}=4$ and there are two sets of solutions for the maxima. One set of solution is $\cos(2\phi)=-1$, $\cos(2\theta)=1$, which has been discussed in case 1. The second set of solution is $\cos(2\theta)=-1$, and $\cos(2\phi)=1$, i.e., $\phi=0,\pi$ which has been discussed in case 3.

We conclude that the scheme of maximizing the local interaction functional is mathematically well-defined. The result of maximization, at least for the case that we have studied explicitly, chooses a localized basis uniquely when the non-local interaction terms are sufficiently small in the original basis. However, an unsatisfactory feature of the solution is that it changes discontinuously, like in a first order transition. For small enough values of λ the functional gives no mixing of orbitals and prefers the original basis. But beyond a certain value of λ it mixes orbitals on the two sites equally, and in the preferred basis the wavefunctions are delocalized over the two sites. It remains to be investigated what gives rise to this behaviour. It is possible that the source of the first order transition is due to the high symmetry of the toy Hamiltonian. In that case a more generic model will exhibit second order transition. The other question that remains to be investigated is whether in a lattice the preferred orbitals will be delocalized if the strength of the non-local interactions become large enough. The study of the toy model, but with four sites, will shed some light on these questions.

2.5 Attempt to Include Non-Unitary Transformations

In this section we extend the group of the allowed transformations to include non-unitary transformations as well. We will consider the same system we have studied in the previous section, namely a lattice with two sites and two orbitals and a starting basis which is orthonormal with a Hamiltonian given by Eq. (2.17).

We consider non-unitary transformation of the form $|n\alpha\rangle \to |n'\alpha'\rangle = \sum_{n,\alpha} T_{\alpha\alpha'}(n-n')|n\alpha\rangle$. The transformation is defined by $2Nm^2=16$ independent parameters. The general form of the transformation matrix T and its adjoint T^{\dagger} can be written in terms

of 2×2 blocks of the form

$$T = \begin{bmatrix} T(0) & T(1) \\ T(1) & T(0) \end{bmatrix} \quad \text{and} \quad T^{\dagger} = \begin{bmatrix} T^{\dagger}(0) & T^{\dagger}(1) \\ T^{\dagger}(1) & T^{\dagger}(0) \end{bmatrix}, \quad (2.30)$$

with

$$T(0) = \frac{1}{2} \left\{ e^{iu_0} \left[\cos(u) \mathbf{1} + i \sin(u) (\hat{u} \cdot \bar{\sigma}) \right] + e^{iv_0} \left[\cos(v) \mathbf{1} + i \sin(v) (\hat{v} \cdot \bar{\sigma}) \right] \right\},$$
(2.31)

and

$$T(1) = \frac{1}{2} \left\{ e^{iu_0} \left[\cos(u) \mathbf{1} + i \sin(u) (\hat{u} \cdot \bar{\sigma}) \right] - e^{iv_0} \left[\cos(v) \mathbf{1} + i \sin(v) (\hat{v} \cdot \bar{\sigma}) \right] \right\}.$$
(2.32)

All the parameters in the above transformation are complex (when the parameters are real we have unitary transformations that we have discussed before). Let $u_0 = a_0 + ib_0$, $v_0 = c_0 + id_0$, u = a + ib, v = c + id. $\hat{u} = u_1\hat{x} = u_2\hat{y} + u_3\hat{z}$ and $\hat{v} = v_1\hat{x} = v_2\hat{y} + v_3\hat{z}$ are complex "unit vectors" with $u_i = a_i + ib_i$, and $v_i = c_i + id_i$ for i = (1, 2, 3). Each "unit vector" is determined by six parameters, only four of which are independent since two of the parameters are determined by the complex valued equation $\hat{u} \cdot \hat{u} = 1$. To keep the calculation manageable for the rest of the discussion we will consider only real unit vectors, i.e., $b_i = d_i = 0$, $\forall i$. Thus we are considering only a subclass of non-unitary transformations. For this subclass we have

$$T^{\dagger}(0) = \frac{1}{2} \left\{ e^{-iu_0^*} \left[\cos(u^*) \mathbf{1} - i \sin(u^*) (\hat{u} \cdot \bar{\sigma}) \right] + e^{-iv_0^*} \left[\cos(v^*) \mathbf{1} - i \sin(v^*) (\hat{v} \cdot \bar{\sigma}) \right] \right\},$$

and

$$T^{\dagger}(1) = \frac{1}{2} \left\{ e^{-iu_0^*} \left[\cos(u^*) \mathbf{1} - i \sin(u^*) (\hat{u} \cdot \bar{\sigma}) \right] - e^{-iv_0^*} \left[\cos(v^*) \mathbf{1} - i \sin(v^*) (\hat{v} \cdot \bar{\sigma}) \right] \right\}.$$

Though the starting basis is orthonormal, since the transformation is not unitary, the new basis $\{|n'\alpha'\rangle\}$ is not orthonormal. The overlap matrix for the new basis is given by

$$O = \begin{bmatrix} O(0) & O(1) \\ O(1) & O(0) \end{bmatrix} = T^{\dagger}T, \tag{2.33}$$

where $O(0)=T^{\dagger}(0)T(0)+T^{\dagger}(1)T(1)$, and $O(1)=T^{\dagger}(0)T(1)+T^{\dagger}(1)T(0)$. It will be useful to define the inverse of the transformation T^{-1} and the adjoint of it $(T^{-1})^{\dagger}$ as

$$T^{-1} = \begin{bmatrix} T^{-1}(0) & T^{-1}(1) \\ T^{-1}(1) & T^{-1}(0) \end{bmatrix} \quad \text{and} \quad (T^{-1})^{\dagger} = \begin{bmatrix} (T^{-1})^{\dagger}(0) & (T^{-1})^{\dagger}(1) \\ (T^{-1})^{\dagger}(1) & (T^{-1})^{\dagger}(0) \end{bmatrix}.$$
(2.34)

One can show that

$$T^{-1}(0) = \frac{1}{2} \left\{ e^{-iu_0} \left[\cos(u) \mathbf{1} - i \sin(u) (\hat{u} \cdot \bar{\sigma}) \right] + e^{-iv_0} \left[\cos(v) \mathbf{1} - i \sin(v) (\hat{v} \cdot \bar{\sigma}) \right] \right\},$$
(2.35)

and

$$T^{-1}(1) = \frac{1}{2} \left\{ e^{-iu_0} \left[\cos(u) \mathbf{1} - i \sin(u) (\hat{u} \cdot \bar{\sigma}) \right] - e^{-iv_0} \left[\cos(v) \mathbf{1} - i \sin(v) (\hat{v} \cdot \bar{\sigma}) \right] \right\}.$$
(2.36)

 $(T^{-1})^\dagger(0)$ and $(T^{-1})^\dagger(1)$ are the adjoints of $T^{-1}(0)$ and $T^{-1}(1)$ respectively. Note that $T^{-1}(0)$ and $T^{-1}(1)$ are not the inverses of the matrices T(0) and T(1) respectively as the notation might suggest. The inverse of the overlap matrix is given by

$$O^{-1} = \begin{bmatrix} O^{-1}(0) & O^{-1}(1) \\ O^{-1}(1) & O^{-1}(0) \end{bmatrix} = T^{-1}(T^{-1})^{\dagger}, \tag{2.37}$$

where $O^{-1}(0)=T^{-1}(0)(T^{-1})^{\dagger}(0)+T^{-1}(1)(T^{-1})^{\dagger}(1)$, and $O^{-1}(1)=T^{-1}(0)(T^{-1})^{\dagger}(1)+T^{-1}(1)(T^{-1})^{\dagger}(0)$.

The functional given by Eq. (2.4) can be written in terms of the transformation matrix as

$$F[T] = \sum_{\substack{\alpha'\beta'\gamma'\delta'\\\sigma'\rho'\eta'\nu'}} O_{\nu'\alpha'}^{-1}(0)O_{\eta'\beta'}^{-1}(0)O_{\gamma'\rho'}^{-1}(0)O_{\delta'\sigma'}^{-1}(0)$$

$$\times \left[\sum_{\substack{nmlk\\\alpha\beta\gamma\delta}} T_{\alpha'\alpha}^{\dagger}(N-n)T_{\beta'\beta}^{\dagger}(N-m)V_{\alpha\beta\gamma\delta}^{nmlk}T_{\gamma\gamma'}(l)T_{\delta\delta'}(k) \right]$$

$$\times \left[\sum_{\substack{rspq\\\sigma\rho\eta\nu}} T_{\sigma'\sigma}^{\dagger}(N-r)T_{\rho'\rho}^{\dagger}(N-s)V_{\sigma\rho\eta\nu}^{rspq}T_{\eta\eta'}(p)T_{\nu\nu'}(q) \right], \quad (2.38)$$

where O^{-1} is given by Eq. (2.37). Since in the original basis the interaction matrix elements are simple and symmetric, the above expression simplifies considerably. It is useful to define the matrices $\tilde{X} = O^{-1}(0)[T^{\dagger}(0)T(0) + T^{\dagger}(1)T(1)]$ and $\tilde{Y} = O^{-1}(0)[T^{\dagger}(0)T(0) - T^{\dagger}(1)T(1)]$. The expressions for \tilde{X} and \tilde{Y} are given in appendix C.

One can show that the functional reduces to the form

$$F[T] = \frac{1}{4} \left(1 + \frac{\lambda}{2} \right)^2 \left[Tr(\tilde{X}^2) \right]^2 + \frac{1}{4} \left(1 - \frac{\lambda}{2} \right)^2 \left[Tr(\tilde{Y}^2) \right]^2 + \frac{1}{2} \left(1 - \frac{\lambda^2}{4} \right) \left[Tr(\tilde{X}\tilde{Y}) \right]^2. \tag{2.39}$$

We note that the above equation reduces to the unitary case, i.e. Eq. (2.24), if we put the non-unitary parameters b_0 , d_0 , b, d to zero. The evaluation of the traces of \tilde{X}^2 , \tilde{Y}^2 and $\tilde{X}Y$ are given in appendix C.

It is quite clear that without imposing constraints the functional F is unbounded with respect to the non-unitary parameters b_0 , d_0 , b and d. The rest of this section is devoted to examining what constraints will be appropriate to keep F bounded.

First, we consider the transformation where the orbitals are multiplied by a scale factor (dilatation). This transformation has the form $T(0) = l_{\alpha}\delta_{\alpha\beta}$, T(1) = 0, where l_{α} is the scale by which the orbital α is multiplied. Then $O^{-1}(0) = |l_{\alpha}|^{-2}\delta_{\alpha\beta}$, and $\tilde{X} = \tilde{Y} = 1$. Using Eq. (2.39) we get F = 4 for this transformation, which is the same as in the original basis. Thus, we note that the functional stays constant under dilatation.

Next we consider the transformation where only the non-unitary parameter b_0 is non-zero, i.e. $a_0 = c_0 = d_0 = a = b = c = d = 0$ and $b_0 \neq 0$. This transformation has the form $T(0) = ((e^{-b_0} + 1)/2)\mathbf{1}$ and $T(1) = ((e^{-b_0} - 1)/2)\mathbf{1}$. This is a non-trivial transformation since it mixes the orbitals on different sites. It is easy to check that $\tilde{X} = \cosh^2(b_0)\mathbf{1}$ and $\tilde{Y} = \cosh(b_0)\mathbf{1}$, and F as a function of b_0 is

$$F(b_0) = \left(1 + \frac{\lambda}{2}\right)^2 \cosh^8(b_0) + \left(1 - \frac{\lambda}{2}\right)^2 \cosh^4(b_0) + 2\left(1 - \frac{\lambda^2}{4}\right) \cosh^6(b_0),$$

which is unbounded for any value of λ . As $b_0 \to \infty$, the functional F blows up and the

transformation becomes singular. It is easy to check that the behaviour of the functional is the same for transformations where any one of the non-unitary parameters d_0 , b and d is the only non-zero parameter. Thus, each of the non-unitary parameters enter the functional in a way that makes it unbounded and when the functional goes to infinity the transformation becomes singular as well.

Next we will examine what kind of constraint will keep the functional bounded. First we will consider the constraint that the basis states remain normalized after the transformation, i.e. we want the transformation to satisfy $O_{\alpha\alpha}(0)=1$. To keep the calculation simple we will put the unitary parameters $a_0=c_0=a=c=0$. The constraint gives two equations involving the non-unitary parameters b_0 , d_0 , b and d. Solving for b_0 and b in terms of d_0 and d we get

$$b_0 = -\frac{1}{4} \ln \left[\left(e^{-2d_0} \cosh(2d) - 2 \right)^2 - \left(e^{-2d_0} (l_3) \sinh(2d) \right)^2 \right],$$

$$b = \operatorname{arctanh} \left[\frac{e^{-2d_0} (l_3) \sinh(2d)}{e^{-2d_0} \cosh(2d) - 2} \right],$$

where $l_3 = v_3/u_3$. Since we have put the parameters a_0 and a to zero, we need real solutions of the constraint equations. This imposes some bound on the possible values of the parameters d_0 , d and l_3 . However, it is easy to verify that over the range in which real solutions exist the functional still blows up. As an example, say $l_3 = 0.1$ and $d_0 = 1$. Then over the range $2 \le d < \infty$ we get real solutions for b_0 and b. Over this range we find that the functional F, now a function of d, is monotonically increasing and is still unbounded.

By studying the above examples we find that the functional is unbounded in terms of the non-unitary parameters. Since the group of invertible transformations is non-compact, the parameters themselves do not have an upper bound. Any attempt to maximize the functional has to be supplemented by a suitable constraint that will keep the non-unitary parameters within some bound and not allow them to flow to infinity. This idea can be implemented more concretely in terms of the singular value decomposition of the transformation matrix. In this decomposition the transformation is expressed as

 $T=V^\dagger DW$, where W and V are unitary matrices and D is diagonal with positive definite eigenvalues (the singular values). It is easy to check that the singular values are nothing but the square roots of the eigenvalues of the overlap matrix $T^\dagger T$. For example, for transformations in which $a_0=c_0=a=c=0$ (to keep the calculation simple), the singular value decomposition gives $\exp(d_0-d)$, $\exp(d_0+d)$, $\exp(b_0-b)$ and $\exp(b_0+b)$. When any of the non-unitary parameters flow to infinity one or more of the singular values become zero or infinity. This is the point where the functional blows up and the transformation becomes singular. Thus, a suitable way of imposing constraints would be to keep the ratio of the maximum and minimum singular values within a specified bound. This will ensure that the singular values do not become too large or too small, and that the non-unitary parameters stay within a finite bound. The local interaction functional can now be maximized by non-unitary transformations.

Chapter 3

Thermal and Charge Transport for Many Body Tight-Binding Models

3.1 Introduction

The theoretical description of the thermoelectric response of correlated materials is a fundamental problem in condensed matter physics, and a breakthrough in this area has potential technological useful implications [34]. The materials, which have been studied as likely candidates for useful thermoelectric properties, are mostly semiconductor alloys and compounds. Materials such as Bi₂Te₃/Sb₂Te₃ and Si-Ge, which are currently favoured for room temperature application, belong to this category. Another class of materials, with potentially useful thermoelectric properties, are Ce and La filled skutterudites such as LaFe₃CoSb₁₂ and CeFe₃CoSb₁₂ [34]. Theoretically these materials have been studied successfully using band theory [35]. Recently Mahan and Sofo [36] have shown that the best thermoelectric materials could well be correlated metals and semiconductors (i.e., rare earth intermetallic compounds). The development of the dynamical mean field theory (DMFT)[for reviews see Refs. [29, 37]] has allowed new studies of the effects of correlation on the thermoelectric response using this method on model Hamiltonians [38, 39, 40]. More recent combinations of band theory and many-body methods such as the LDA+DMFT method [41] [for reviews see Refs. [42, 43]] or the LDA++ method [44] offers the exciting possibility of predicting the thermoelectric properties of materials starting from first principles [45]. This revival of interest in the thermoelectric response motivates us to re-analyze in this chapter the following issues: (1) what is the form of the thermal current and the charge current which should be used in realistic calculations, and (2) how it should be approximated in a DMFT calculation.

The first question is subtle for two reasons. First, as noted early on by Jonson and Mahan [46], the electronic part of the thermal current operator contains a quadratic and a quartic piece (if the electron-electron interaction is non-local) in the electron creation and annihilation operators. The contribution of this quartic interaction term to the current has continued to be the subject of discussion [47]. Second, while the form of the thermal current and the charge current in the continuum is unambiguous, and can be calculated using Noether's theorem [48,49], DMFT calculations require the projection of these currents on a restricted lattice model. This involves the computation of complicated matrix elements, and in practice an approximation which is analogous to the Peierls substitution [50] for the electrical current is carried out. It is well known that the results of this construction depend on the basis set of orbitals used [51]. This raises the practical question of how to optimize the basis of orbitals to be used in transport calculations.

The second question is subtle due to the presence of interaction terms in the current. This raises the issue of how it should be simplified in the evaluation of the various current-current correlation functions and the transport coefficients. This question was first addressed by Schweitzer and Czycholl [52] and by Pruschke and collaborators [37] who stated that within the relaxation time approximation, this term can be expressed in terms of a time derivative, and the vertex corrections can be ignored. In the review of Georges et. al. [29] it was stated that the results of Pruschke et. al. hold beyond the relaxation time approximation in the limit of large dimensionality when DMFT becomes exact but no detailed proof of this statement was presented.

The following are our main results. (1) In section 3.2 we address the question of the optimization of the basis of localized orbitals for transport calculations, following the ideas of Marzari and Vanderbilt [31]. For completeness and for pedagogical reasons

we discuss in parallel work on the charge current, which is simpler and better understood [53] than the thermal current. Our conclusions in this context have applications for the computation of Born charges in empirical tight-binding models [54]. (2) In section 3.3 we derive the form of the thermal current to be used in tight-binding models, and its dependence on the orbitals, using the equation of motion technique introduced in Ref. [55]. Our final expression differs in one term from the results of Ref. [47]. (3) In section 3.4 we describe in detail the diagrammatic analysis of correlation functions of the current operators. We demonstrate explicitly that in the DMFT limit of the transport calculation, the vertex corrections (even for those involving the thermal current) can be completely neglected, thereby justifying the current practice used in all previous DMFT work.

3.2 Charge Current

We consider a system of electrons in a periodic potential V(r), in the presence of an external vector potential $\mathbf{A}(r)$, and with coulomb interaction between them. The Lagrangian is given by

$$L = \frac{i}{2} \int d^3r \left(\psi^{\dagger} \dot{\psi} - \dot{\psi}^{\dagger} \psi \right) + \frac{1}{2m} \int d^3r \psi^{\dagger} \left(\nabla - ie\mathbf{A}(r) \right)^2 \psi$$
$$- \int d^3r V(r) \psi^{\dagger} \psi - \frac{e^2}{2} \int \int d^3r d^3r' \psi^{\dagger}(\mathbf{r}) \psi^{\dagger}(\mathbf{r}') \frac{1}{|\mathbf{r} - \mathbf{r}'|} \psi(\mathbf{r}') \psi(\mathbf{r}). \quad (3.1)$$

Here $\psi^{\dagger}(\mathbf{r})$ and $\psi(\mathbf{r})$ are the electron field operators with usual anticommutation properties. We have ignored the spin of the electrons only to simplify the notation. Including spin in the following analysis is quite straightforward. In field theory, when both high and low energy degrees of freedom are retained, Noether's theorem provides a robust procedure to identify the various currents [49]. The theorem associates with every symmetry of the action a conserved charge and a corresponding current. The charge current is determined by the invariance of the action $S = \int dt L(t)$, under U(1) gauge transformation given by $\psi(\mathbf{r}) \to \psi(\mathbf{r})e^{i\phi(\mathbf{r})}$ and $\psi^{\dagger}(\mathbf{r}) \to \psi^{\dagger}(\mathbf{r})e^{-i\phi(\mathbf{r})}$. The transformation does not produce any variation from the interaction term, and the well known

expression for the charge current is

$$\mathbf{j} = -\frac{ie}{m} \int d^3r \psi^{\dagger}(\mathbf{r}) \left(\nabla - ie\mathbf{A}(r)\right) \psi(\mathbf{r}). \tag{3.2}$$

The above expression is gauge invariant. The part which is proportional to the vector potential gives the diamagnetic current.

In order to facilitate further discussion we will perform the standard Noether construction in the Wannier basis. In this basis the action (which includes both low and high energy degrees of freedom) is

$$S = \int dt \qquad \left\{ \frac{i}{2} \sum_{n\mu} \left(c_{n}^{\dagger \mu} \dot{c}_{n}^{\mu} - \dot{c}_{n}^{\dagger \mu} c_{n}^{\mu} \right) - \sum_{\substack{nm \\ \mu\nu}} t_{nm}^{\mu\nu} c_{n}^{\dagger \mu} c_{m}^{\nu} + \frac{e}{2m} \sum_{\substack{nml \\ \mu\nu\gamma}} \mathbf{p}_{nl}^{\mu\gamma} \cdot \mathbf{A}_{lm}^{\gamma\nu} c_{n}^{\dagger \mu} c_{m}^{\nu} + \frac{e}{2m} \sum_{\substack{nml \\ \mu\nu\gamma}} \mathbf{p}_{nl}^{\mu\gamma} \cdot \mathbf{A}_{lm}^{\gamma\nu} c_{n}^{\dagger \mu} c_{m}^{\nu} - \frac{e^{2}}{2m} \sum_{\substack{nml \\ \mu\nu\gamma}} \mathbf{A}_{nl}^{\mu\gamma} \cdot \mathbf{A}_{lm}^{\gamma\nu} c_{n}^{\dagger \mu} c_{m}^{\nu} - \frac{1}{2m} \sum_{\substack{nml \\ \mu\nu\gamma}} \mathbf{p}_{nl}^{\mu\gamma} \cdot \mathbf{p}_{nl}^{\gamma\nu} c_{n}^{\mu} c_{n}^{\nu} + \frac{1}{2m} \sum_{\substack{nml \\ \mu\nu\gamma}} \mathbf{p}_{nl}^{\mu\gamma} \cdot \mathbf{p}_{nl}^{\gamma\nu} c_{n}^{\mu} c_{n}^{\nu} + \frac{1}{2m} \sum_{\substack{nml \\ \mu\nu\gamma}} \mathbf{p}_{nl}^{\mu\gamma} \cdot \mathbf{p}_{nl}^{\gamma\nu} c_{n}^{\mu} c_{n}^{\nu} c_{n}^{\nu} + \frac{1}{2m} \sum_{\substack{nml \\ \mu\nu\gamma}} \mathbf{p}_{nl}^{\mu\gamma} \cdot \mathbf{p}_{nl}^{\gamma\nu} c_{n}^{\mu} c_{n}^{\nu} c_{n}^$$

where $t_{nm}^{\mu\nu} = \langle n\mu|\mathcal{H}_0|m\nu\rangle$, $\mathbf{p}_{nm}^{\mu\nu} = \langle n\mu|\mathbf{p}|m\nu\rangle$, $\mathbf{A}_{nm}^{\mu\nu} = \langle n\mu|\mathbf{A}(r)|m\nu\rangle$, and $U_{n_1...n_4}^{\mu_1...\mu_4} = \langle n_1\mu_1, n_2\mu_2|e^2/|\mathbf{r}-\mathbf{r}'||n_4\mu_4, n_3\mu_3\rangle$. Here $\mathcal{H}_0 = \mathbf{p}^2/2m + V(r)$ is the non-interacting part of the Hamiltonian, μ is the band index, and \mathbf{R}_n defines the lattice positions. $W_{\mu}(\mathbf{r}-\mathbf{R}_n) = \langle \mathbf{r}|n\mu\rangle$ form a complete set of orthonormal Wannier functions. The creation and annihilation operators satisfy the anticommutation relation $\{c_n^{\mu}, c_m^{\dagger\nu}\} = \delta_{nm}\delta_{\mu\nu}$. The gauge transformation of the fermionic field operators is equivalent to the variation $\delta c_n^{\mu} = i\int d^3r\phi(\mathbf{r})\psi(\mathbf{r})W_{\mu}^*(\mathbf{r}-\mathbf{R}_n)$ and $\delta c_n^{\dagger\mu} = -i\int d^3r\phi(\mathbf{r})\psi^{\dagger}(\mathbf{r})W_{\mu}(\mathbf{r}-\mathbf{R}_n)$. Expanding $\phi(\mathbf{r})$ about the point \mathbf{R}_n and keeping only up to $\nabla\phi$ (which is all we need to construct the Noether current) we get

$$\delta c_n^{\mu} = i\phi(\mathbf{R}_n)c_n^{\mu} + i\nabla\phi \sum_{m\nu} \mathbf{L}_{nm}^{\mu\nu}c_m^{\nu},$$

$$\delta c_n^{\dagger\mu} = -i\phi(\mathbf{R}_n)c_n^{\dagger\mu} - i\nabla\phi \sum_{m\nu} c_m^{\dagger\nu}\mathbf{L}_{mn}^{\nu\mu},$$
(3.4)

where $\mathbf{L}_{nm}^{\mu\nu}=\int d^3r W_{\mu}^*(\mathbf{r}-\mathbf{R}_n)(\mathbf{r}-\mathbf{R}_n)W_{\nu}(\mathbf{r}-\mathbf{R}_m)$ are the connection coefficients. The matrix \mathbf{L} is hermitian. We note first that the variation from the interaction term is

exactly zero. Next, using the operator identity $[r_i, A_j(r)] = 0$, we find that the variation from the term quadratic in $\mathbf{A}(r)$ is zero. To get the correct diamagnetic part we make use of $[r_i, p_j] = i\delta_{ij}$. From the invariance of the action we can identify the charge current as

$$\mathbf{j} = ie \sum_{\substack{nm \\ \mu\nu}} (\mathbf{R}_m - \mathbf{R}_n) t_{nm}^{\mu\nu} c_n^{\dagger\mu} c_m^{\nu} + ie \sum_{\substack{nml \\ \mu\nu\gamma}} c_n^{\dagger\mu} \left(t_{nl}^{\mu\gamma} \mathbf{L}_{lm}^{\gamma\nu} - \mathbf{L}_{nl}^{\mu\gamma} t_{lm}^{\gamma\nu} \right) c_m^{\nu}$$

$$- \frac{e^2}{m} \sum_{\substack{nm \\ \mu\nu}} \mathbf{A}_{nm}^{\mu\nu} c_n^{\dagger\mu} c_m^{\nu}$$

$$= ie \sum_{\substack{nm \\ \mu\nu}} c_n^{\dagger\mu} c_m^{\nu} \langle n\mu | [\mathcal{H}_0(\mathbf{A}), \mathbf{r}] | m\nu \rangle. \tag{3.5}$$

 $\mathcal{H}_0(\mathbf{A}) = (\mathbf{p} - e\mathbf{A})^2/(2m) + V(r)$. This is just Eq. (3.2) expressed in the Wannier basis. The charge current is related to the electronic polarization operator [56]

$$\mathbf{P}_{\mathrm{el}} = e \sum_{\substack{nm \\ \mu\nu}} c_n^{\dagger\mu} c_m^{\nu} \langle n\mu | \mathbf{r} | m\nu \rangle$$

by $\partial \mathbf{P}_{\rm el}/\partial t = \mathbf{j}$. The change in polarization $\Delta \mathbf{P}_{\rm el}$ (which is a well defined and measurable bulk quantity, rather than polarization itself) between an initial and a final state of a sample is the integrated current flowing through the sample during an adiabatic transformation connecting the two states [57].

Theoretical models of the tight-binding type are effective low energy models described in terms of those bands which are close to the Fermi surface [58]. The question, which is non-trivial and which is still debated, is what should be the form of the current for such low energy models. The low energy Hamiltonian is obtained by eliminating or integrating out the degrees of freedom corresponding to the high energy bands. This is easily formulated in the functional integral language and the procedure generates many interaction terms that are not present in the original action. In a Hamiltonian formulation this is equivalent to making a canonical transformation to decouple the low energy and the high energy sectors [59]. That is, given a full many body Hamiltonian \mathcal{H} , we perform unitary transformation U such that $U\mathcal{H}U^{-1}$ is diagonal (for a

system of interacting particles, in general, this can be done only approximately), and then consider only $PU\mathcal{H}U^{-1}P$, where P is the operator projecting on the low energy bands. To obtain the expression for the current in the low energy sector one has to perform the same canonical transformation used to transform the original Hamiltonian into the effective Hamiltonian on the operator representing the current. In other words, we first calculate the current (say, **J**) for the full theory (using the symmetry of the full theory), make the same unitary transformation and then project the current on the low energy sector of interest. The exact low energy current is then given by $PUJU^{-1}P$. This method of calculating the current for the low energy theory is motivated by renormalization group ideas. But, to implement this in practice is usually a formidable task. However, if we consider a system of non-interacting electrons (in a periodic potential) with a subset M of bands that defines the low energy subspace, the low energy current is obtained by projecting the full current in Eq. (3.5) on the low energy subspace. This is given by $P\mathbf{j}P$, where $P=\sum_{n,\mu\in M}|n\mu\rangle\langle n\mu|$ is the projection operator. We note that the calculation of the exact current requires knowledge of the matrix elements of the position operator in addition to that of \mathcal{H}_0 (the tight-binding parameters) [60].

Sometimes, to avoid calculating the matrix elements of the position operator, one makes the approximation known as Peierls substitution. There are two types of approximations involved with this procedure. First, terms involving the connection coefficients are dropped out, and one considers an approximate gauge transformation given by $\delta c_n^{\mu} = i\phi(\mathbf{R}_n)c_n^{\mu}$ and $\delta c_n^{\dagger\mu} = -i\phi(\mathbf{R}_n)c_n^{\dagger\mu}$. Putting the connection coefficients to zero is equivalent to the approximation $\langle n\mu|\mathbf{r}|m\nu\rangle \approx \mathbf{R}_n\delta_{nm}\delta_{\mu\nu}$ for the matrix elements of the position operator, and $\langle n\mu|\mathbf{p}|m\nu\rangle = im\langle n\mu|[\mathcal{H}_0,\mathbf{r}]|m\nu\rangle \approx im(\mathbf{R}_m-\mathbf{R}_n)t_{nm}^{\mu\nu}$ for the matrix elements of the momentum operator. Second, with this approximate gauge transformation, the variation from the interaction term is non-zero (though, as already noted, it is zero for the exact gauge transformation). However, contribution to the current from the interaction term is neglected. It will be further

assumed that the vector potential is constant, i.e., $\mathbf{A}_{nm}^{\mu\nu} = \mathbf{A}\delta_{nm}\delta_{\mu\nu}$. With these simplifications the approximate current (\mathbf{j}_P) is given by

$$\mathbf{j}_{P} = ie \sum_{\substack{nm\\\mu\nu\in M}} (\mathbf{R}_{m} - \mathbf{R}_{n}) t_{nm}^{\mu\nu} c_{n}^{\dagger\mu} c_{m}^{\nu} + e^{2} \sum_{\substack{nm\\\mu\nu\in M}} (\mathbf{R}_{m} - \mathbf{R}_{n}) \left((\mathbf{R}_{m} - \mathbf{R}_{n}) \cdot \mathbf{A} \right) t_{nm}^{\mu\nu} c_{n}^{\dagger\mu} c_{m}^{\nu}.$$
(3.6)

The second term is the approximate diamagnetic contribution. The usefulness of \mathbf{j}_P lies in the fact that it can be calculated from the tight-binding parameters alone.

The construction of the Peierls current in terms of the atomic orbitals is *a priori* not obvious for the case when there is more than one atom per unit cell. It is worthwhile to clarify this issue here. We will denote the atomic wavefunctions by $|\alpha \tau \mathbf{R}_n\rangle$, where α is a symmetry index, \mathbf{R}_n is the lattice position of a unit cell, and \mathbf{R}_τ is the position of the atom τ within a unit cell. It is desirable to define the Bloch basis wavefunctions by $|\alpha \tau \mathbf{k}\rangle = \frac{1}{\sqrt{N}} \sum_{\mathbf{R}_n} e^{-i\mathbf{k}\cdot(\mathbf{R}_n+\mathbf{R}_\tau)} |\alpha \tau \mathbf{R}_n\rangle$, though the phase factor $e^{-i\mathbf{k}\cdot\mathbf{R}_\tau}$ is quite innocuous for the definition of the Hamiltonian matrix $\mathcal{H}(\mathbf{k})_{\alpha_1\tau_1;\alpha_2\tau_2}$ and for the subsequent calculation of the energy bands. The question, whether to keep the phase factor or not, is however important for the definition of the Peierls current $\mathbf{j}_P(\mathbf{k})_{\alpha_1\tau_1;\alpha_2\tau_2} = \frac{\partial}{\partial \mathbf{k}}\mathcal{H}(\mathbf{k})_{\alpha_1\tau_1;\alpha_2\tau_2}$. It is easy to verify that, with the above definition of the Bloch basis, one gets the same form for the Peierls current if one considers a lattice with one atom per unit cell (for which case the definition of the Peierls current is unambiguous), and compare it with the same lattice with its period doubled (and therefore now with two identical atoms per unit cell).

We will examine the behaviour of the exact current and the approximate one under infinitesimal unitary transformation $U_{nm}^{\mu\nu}=\delta_{nm}\delta_{\mu\nu}+W_{nm}^{\mu\nu}$ (where W is antihermitian) of the Wannier functions defined by $|n\mu\rangle\to\sum_{m\nu}U_{mn}^{\nu\mu}|m\nu\rangle$. The variation of a matrix element $(\mathbf{j})_{nm}^{\mu\nu}=ie\langle n\mu|[\mathcal{H}_0(\mathbf{A}),\mathbf{r}]|m\nu\rangle$ of the exact current is given by

$$(\mathbf{j})_{nm}^{\mu\nu} \to (\mathbf{j})_{nm}^{\mu\nu} + \sum_{k,\gamma} \{ (\mathbf{j})_{nk}^{\mu\gamma} W_{km}^{\gamma\nu} - W_{nk}^{\mu\gamma} (\mathbf{j})_{km}^{\gamma\nu} \}.$$
 (3.7)

This is the usual transformation of matrix elements of operators that remain invariant under unitary transformation. In fact, the paramagnetic and the diamagnetic parts of the operator \mathbf{j} are separately invariant. The behaviour of \mathbf{j}_P is, however, different. The variation of $(\mathbf{j}_P)_{nm}^{\mu\nu}=ie(\mathbf{R}_m-\mathbf{R}_n)t_{nm}^{\mu\nu}+e^2(\mathbf{R}_m-\mathbf{R}_n)((\mathbf{R}_m-\mathbf{R}_n)\cdot A)t_{nm}^{\mu\nu}$ is given by

$$(\mathbf{j}_{P})_{nm}^{\mu\nu} \rightarrow (\mathbf{j}_{P})_{nm}^{\mu\nu} + \sum_{k,\gamma} \left\{ (\mathbf{j}_{P})_{nk}^{\mu\gamma} W_{km}^{\gamma\nu} - W_{nk}^{\mu\gamma} (\mathbf{j}_{P})_{km}^{\gamma\nu} \right\} + ie \sum_{k,\gamma} (\mathbf{R}_{m} - \mathbf{R}_{k}) t_{nk}^{\mu\gamma} W_{km}^{\gamma\nu}$$

$$-ie \sum_{k,\gamma} (\mathbf{R}_{k} - \mathbf{R}_{n}) W_{nk}^{\mu\gamma} t_{km}^{\gamma\nu} + e^{2} \sum_{k,\gamma} \left\{ (\mathbf{R}_{k} - \mathbf{R}_{n}) ((\mathbf{R}_{m} - \mathbf{R}_{k}) \cdot \mathbf{A}) + (\mathbf{R}_{m} - \mathbf{R}_{k}) ((\mathbf{R}_{m} - \mathbf{R}_{n}) \cdot \mathbf{A}) \right\} t_{nk}^{\mu\nu} W_{km}^{\gamma\nu} - e^{2} \sum_{k,\gamma} \left\{ (\mathbf{R}_{m} - \mathbf{R}_{k}) ((\mathbf{R}_{k} - \mathbf{R}_{n}) \cdot \mathbf{A}) + (\mathbf{R}_{k} - \mathbf{R}_{n}) ((\mathbf{R}_{m} - \mathbf{R}_{n}) \cdot \mathbf{A}) \right\} W_{nk}^{\mu\gamma} t_{km}^{\gamma\nu}. \tag{3.8}$$

The paramagnetic and the diamagnetic parts of j_P are both basis dependent operators.

The basis dependence of j_P raises the practical question as to what basis one should choose while making the Peierls construction. For example, there have been efforts to calculate polarization properties, like effective charges of semiconductors, using the empirical tight-binding theory [54]. In this scheme a natural approximation is the "diagonal" ansatz which assumes that the position operator is diagonal in the tightbinding basis with expectation values equal to the atomic positions. This is equivalent to a Peierls substitution, and the polarization calculated with this ansatz is related to the Peierls current j_P . The effective charges calculated in this procedure depends on the choice of the underlying Wannier basis. In order to improve the results one should first make an appropriate choice of a basis. One possibility is to use the basis of the "maximally localized" Wannier functions that was introduced by Marzari and Vanderbilt [31]. This is obtained by minimizing a functional which measures the spread of the Wannier functions. Intuitively, it seems plausible that the approximation in which the connection coefficients are neglected, will work better in a basis where the Wannier functions are more localized. A second possibility, suggested by Millis [51], is to choose that basis in which the charge stiffness calculated using the Peierls current will be closest to the one obtained from band theory. We note that this criterion is already satisfied by the Bloch basis in which the effective one-electron Hamiltonian is diagonal in the band indices. This can be seen easily in the following manner. We consider the scenario of band theory where electrons are in an effective periodic potential. Let $\epsilon_{\mathbf{k}\mu}$ denote the single particle energy levels. It can be shown that the charge stiffness is given by $D_{\alpha\beta} = \sum_{\mathbf{k}\mu} f(\epsilon_{\mathbf{k}\mu})(\partial^2 \epsilon_{\mathbf{k}\mu}/(\partial k_\alpha \partial k_\beta))$ [61]. Here $f(\epsilon)$ is the Fermi function and α , β denote spatial directions. The Peierls current constructed in the Bloch basis does not have any interband term since the basis is already diagonal in the band indices. The paramagnetic part of the current is given by $(j_P)_{\mathrm{para},\alpha} = \sum_{\mathbf{k}\mu} (\partial \epsilon_{\mathbf{k}\mu}/\partial k_\alpha) c_{\mathbf{k}}^{\dagger\mu} c_{\mathbf{k}}^{\mu}$. Since the paramagnetic part has no interband matrix element, it does not contribute to the charge stiffness. The diamagnetic part, given by $(j_P)_{\mathrm{dia},\alpha} = -\sum_{\mathbf{k}\mu\beta} (\partial^2 \epsilon_{\mathbf{k}\mu}/(\partial k_\alpha \partial k_\beta)) A_\beta c_{\mathbf{k}}^{\dagger\mu} c_{\mathbf{k}}^{\mu}$, gives a charge stiffness exactly equal to that obtained from band theory. It is possible, though, that there are other bases which satisfy this criterion.

In passing we note that if the matrix elements of the exact current j are known by some means, say, from first principles calculation, then it is possible to define the functional

$$\Omega = \sum_{\substack{nm\\\mu\nu\in M}} \langle n\mu|\mathbf{j} - \mathbf{j}_P|m\nu\rangle \cdot \langle m\nu|\mathbf{j} - \mathbf{j}_P|n\mu\rangle$$
 (3.9)

and choose the basis which minimizes Ω , and thereby the difference between the exact current and the approximate one. Using Eqs. (3.7) and (3.8) we can calculate the variation of Ω under infinitesimal unitary transformation. The gradient, defined as $G_{nm}^{\mu\nu} = d\Omega/dW_{nm}^{\mu\nu}$, is given by

$$G_{nm}^{\mu\nu} = (\mathbf{R}_{m} - \mathbf{R}_{n}) \cdot \langle n\mu | [\mathcal{H}_{0}, (\mathbf{j} - \mathbf{j}_{P})] | m\nu \rangle$$

$$+ ie ((\mathbf{R}_{m} \cdot \mathbf{A}) \mathbf{R}_{m} - (\mathbf{R}_{n} \cdot \mathbf{A}) \mathbf{R}_{n}) \cdot \langle n\mu | \{\mathcal{H}_{0}, (\mathbf{j} - \mathbf{j}_{P})\} | m\nu \rangle$$

$$- ie \sum_{k\gamma} \{ (\mathbf{R}_{m} - \mathbf{R}_{n}) (\mathbf{R}_{k} \cdot \mathbf{A}) + ((\mathbf{R}_{m} - \mathbf{R}_{n}) \cdot \mathbf{A}) \mathbf{R}_{k} \}$$

$$\cdot \{ \langle n\mu | \mathbf{j} - \mathbf{j}_{P} | k\gamma \rangle \langle k\gamma | \mathcal{H}_{0} | m\nu \rangle + \langle n\mu | \mathcal{H}_{0} | k\gamma \rangle \langle k\gamma | \mathbf{j} - \mathbf{j}_{P} | m\nu \rangle \}$$
(3.10)

The optimum basis is the one for which the gradient vanishes. The choice of basis will depend on the vector potential, but the physical quantities calculated in that basis will

not. In general, this criterion will give a basis which is different from that of the "maximally localized" Wannier functions. The above method of choosing an appropriate basis is not very useful for doing charge transport calculations because to define the method one needs to know the matrix elements of the exact current, knowing which makes the Peierls construction redundant. However, one can use this optimization procedure for doing thermal transport calculation. As we will see in the next section, the matrix elements of the exact thermal current are quite complicated, and a Peierls formulation of the thermal current is desirable (in some suitable basis). The rationale for our suggestion is that the basis which optimizes the Peierls construction for electric transport will be a good basis for doing the Peierls construction for thermal transport as well.

3.3 Thermal Current

In field theory, the energy current (which is same as the thermal current, except for the latter the single particle energies are measured from the chemical potential) is determined from the invariance of the action under the transformation of time $t \to t - \phi(\mathbf{r}, t)$. This shifts the field operators by $\delta \psi = \dot{\psi} \phi$, and $\delta \psi^{\dagger} = \dot{\psi}^{\dagger} \phi$. From the variation of the action defined in Eq.(3.1), the energy current (\mathbf{j}_E) is given by

$$\mathbf{j}_{E} = -\frac{1}{2m} \int d^{4}r \left\{ \dot{\psi}^{\dagger} \nabla \psi + \nabla \psi^{\dagger} \dot{\psi} \right\} + \frac{1}{4} \int d^{3}\mathbf{r}_{1} \int d^{3}\mathbf{r}_{2} \left(\mathbf{r}_{2} - \mathbf{r}_{1} \right) U(r_{1} - r_{2})$$

$$\times \left\{ \dot{\psi}^{\dagger}(\mathbf{r}_{1}) \rho(\mathbf{r}_{2}) \psi(\mathbf{r}_{1}) - \psi^{\dagger}(\mathbf{r}_{1}) \dot{\rho}(\mathbf{r}_{2}) \psi(\mathbf{r}_{1}) + \psi^{\dagger}(\mathbf{r}_{1}) \rho(\mathbf{r}_{2}) \dot{\psi}(\mathbf{r}_{1}) \right\}.$$
(3.11)

Here $\rho(\mathbf{r}) = \psi^{\dagger}(\mathbf{r})\psi(\mathbf{r})$, and U(r) is the two-particle interaction energy (Coulomb potential, in our case). The second term above, which is formally quartic in the field operators, is the contribution to energy current from the non-local (in space) interaction. This term was missed by Langer [48], but noted in a different context by Jonson and Mahan [46]. More recently, it has been discussed by Moreno and Coleman [47].

We have discussed in the previous section that for an effective low-energy model any current is obtained correctly by projecting the current for the full theory (where both high and low energy degrees of freedom are present) on the low-energy bands. To implement this for the energy current one has to consider variations of the Wannier operators $\delta c_i^{\mu} = \phi(\mathbf{R}_i)\dot{c}_i^{\mu} + \nabla\phi\sum_{j,\nu}\mathbf{L}_{ij}^{\mu\nu}\dot{c}_j^{\nu}$ and $\delta c_i^{\dagger\mu} = \phi(\mathbf{R}_i)\dot{c}_i^{\dagger\mu} + \nabla\phi\sum_{j,\nu}\dot{c}_j^{\dagger\nu}\mathbf{L}_{ji}^{\nu\mu}$ under translation of time. If we ignore the terms with the connection coefficients, we get an approximate current which is equivalent to a Peierls substitution. The same approximate current can be derived from the low-energy effective Hamiltonian using the equations of motion [55]. Although we are emphasizing the importance of the exact low-energy current, in practice, calculating the exact thermal current is fairly complicated. Therefore, we will restrict the derivation to that of a Peierls type of energy current for a generalized Hubbard model described by the Hamiltonian

$$\mathcal{H} = \sum_{\substack{ij\\\mu\nu\\\sigma}} t_{ij}^{\mu\nu} c_{i\sigma}^{\dagger\mu} c_{j\sigma}^{\nu} + \sum_{\substack{ij\\\mu\nu\\\sigma\sigma'}} V_{ij,\sigma\sigma'}^{\mu\nu} n_{i\sigma}^{\mu} n_{j\sigma'}^{\nu}, \tag{3.12}$$

using the equation of motion technique. Here $n_{i\sigma}^{\mu}=c_{i\sigma}^{\dagger\mu}c_{i\sigma}^{\mu}$. The local energy density (h_i) is given by

$$h_{i} = \frac{1}{2} \sum_{\substack{j \\ \mu\nu \\ \sigma}} \left(t_{ij}^{\mu\nu} c_{i\sigma}^{\dagger\mu} c_{j\sigma}^{\nu} + t_{ji}^{\nu\mu} c_{j\sigma}^{\dagger\nu} c_{i\sigma}^{\mu} \right) + \frac{1}{2} \sum_{\substack{j \\ \mu\nu \\ \sigma\sigma'}} \left(V_{ij,\sigma\sigma'}^{\mu\nu} n_{i\sigma}^{\mu} n_{j\sigma'}^{\nu} + V_{ji,\sigma'\sigma}^{\nu\mu} n_{j\sigma'}^{\mu} n_{i\sigma}^{\mu} \right).$$

We can show that

$$\dot{h}_{i} = \frac{1}{2} \sum_{\substack{j \\ \mu\nu \\ \sigma}} \left\{ t_{ij}^{\mu\nu} \left(c_{i\sigma}^{\dagger\mu} \dot{c}_{j\sigma}^{\nu} - \dot{c}_{i\sigma}^{\dagger\mu} c_{j\sigma}^{\nu} \right) + t_{ji}^{\nu\mu} \left(\dot{c}_{j\sigma}^{\dagger\nu} c_{i\sigma}^{\mu} - c_{j\sigma}^{\dagger\nu} \dot{c}_{i\sigma}^{\mu} \right) \right\}$$

$$+ \frac{1}{2} \sum_{\substack{j \\ \mu\nu \\ \sigma\sigma'}} V_{ij,\sigma\sigma'}^{\mu\nu} \left(-\dot{c}_{i\sigma}^{\dagger\mu} c_{j\sigma'}^{\dagger\nu} c_{j\sigma'}^{\nu} c_{i\sigma}^{\mu} + c_{i\sigma}^{\dagger\mu} \dot{c}_{j\sigma'}^{\dagger\nu} c_{j\sigma'}^{\nu} c_{i\sigma}^{\mu} + c_{i\sigma}^{\dagger\mu} c_{j\sigma'}^{\dagger\nu} \dot{c}_{j\sigma'}^{\nu} c_{i\sigma}^{\mu} \right.$$

$$- c_{i\sigma}^{\dagger\mu} c_{j\sigma'}^{\dagger\nu} c_{i\sigma}^{\nu} \dot{c}_{i\sigma}^{\mu} \right) + \frac{1}{2} \sum_{\substack{j \\ \mu\nu \\ \sigma\sigma'}} V_{ji,\sigma'\sigma}^{\mu\mu} \left(\dot{c}_{j\sigma'}^{\dagger\nu} c_{i\sigma}^{\dagger\mu} c_{i\sigma}^{\mu} c_{j\sigma'}^{\nu} - c_{j\sigma'}^{\dagger\nu} \dot{c}_{i\sigma}^{\mu} c_{j\sigma'}^{\nu} \right.$$

$$- c_{j\sigma'}^{\dagger\nu} c_{i\sigma}^{\dagger\mu} \dot{c}_{i\sigma}^{\mu} c_{j\sigma'}^{\nu} + c_{j\sigma'}^{\dagger\nu} c_{i\sigma}^{\dagger\mu} c_{i\sigma}^{\nu} \dot{c}_{j\sigma'}^{\nu} \right), \qquad (3.13)$$

where $\dot{\hat{O}}=i[\mathcal{H},\hat{O}]$. The energy current (\mathbf{j}_E) is related to the energy density by the continuity equation $\dot{h}_i+\nabla\cdot\mathbf{j}_E(i)=0$. We define $h(\mathbf{q})=\sum_i e^{-i\mathbf{q}\cdot\mathbf{R}_i}h_i$, and similarly $\mathbf{j}_E(\mathbf{q})$. The Fourier transform of the Wannier operators are defined by $c_{\mathbf{k}\sigma}^{\mu}=0$

 $\frac{1}{\sqrt{N}}\sum_{i}e^{-i\mathbf{k}\cdot\mathbf{R}_{i}}c_{i\sigma}^{\mu}$, and similarly for $c_{\mathbf{k}\sigma}^{\dagger\mu}$. Here N is the size of the lattice. Comparing with the continuity equation we get the energy current

$$\mathbf{j}_{E} = \frac{i}{2} \sum_{\substack{\mathbf{k} \\ \mu\nu}} \nabla_{\mathbf{k}} \epsilon_{\mathbf{k}}^{\mu\nu} \left(c_{\mathbf{k},\sigma}^{\dagger\mu} \dot{c}_{\mathbf{k},\sigma}^{\nu} - \dot{c}_{\mathbf{k},\sigma}^{\dagger\mu} c_{\mathbf{k},\sigma}^{\nu} \right) + \frac{i}{2} \sum_{\substack{\mathbf{k}\mathbf{k}' \\ \mu\nu} \\ \sigma\sigma'}} \nabla_{\mathbf{k}} V_{\mathbf{k},\sigma\sigma'}^{\mu\nu} \left(c_{\mathbf{k}',\sigma}^{\dagger\mu} \dot{n}_{\mathbf{k},\sigma'}^{\nu} c_{\mathbf{k}'-\mathbf{k},\sigma}^{\mu} \right) - \dot{c}_{\mathbf{k}',\sigma}^{\dagger\mu} n_{\mathbf{k},\sigma'}^{\nu} c_{\mathbf{k}'-\mathbf{k},\sigma}^{\mu} - c_{\mathbf{k}',\sigma}^{\dagger\mu} n_{\mathbf{k},\sigma'}^{\nu} \dot{c}_{\mathbf{k}'-\mathbf{k},\sigma}^{\mu} \right),$$

$$(3.14)$$

where $n_{\mathbf{k},\sigma}^{\mu} = \sum_{\mathbf{k'}} c_{\mathbf{k'},\sigma}^{\dagger\mu} c_{\mathbf{k'}+\mathbf{k},\sigma}^{\mu}$. The first two terms (the quadratic part) in the above equation are contributions to the energy current from the electron hopping and from the local part of the interactions. The last three terms (the quartic part) are additional contributions to energy flow from the long range interactions. Moreno and Coleman [47] have calculated the quartic part using Noether's theorem for classical fields, and their result is $\frac{i}{2} \sum_{\mathbf{k},\mu\nu,\sigma\sigma'} \nabla_{\mathbf{k}} V_{\mathbf{k},\sigma\sigma'}^{\mu\nu} \left(n_{-\mathbf{k},\sigma}^{\mu} \dot{n}_{\mathbf{k},\sigma'}^{\nu} - \dot{n}_{-\mathbf{k},\sigma}^{\mu} n_{\mathbf{k},\sigma'}^{\nu} \right)$. We want to argue that this result is incorrect. We note that for classical fields the issue of correct arrangement of operators is not present. Indeed, if we could commute the third operator with the second in each of the last three terms of Eq. (3.14) we would get the result derived in Ref. [47]. However such commutation will generate an additional term $\sum_{\mathbf{k}\mathbf{k}',\mu\nu,\sigma} \nabla_{\mathbf{k}} V_{\mathbf{k},\sigma\sigma}^{\mu\nu} \epsilon_{\mathbf{k}'-\mathbf{k}}^{\mu\nu} c_{\mathbf{k}',\sigma}^{\nu} c_{\mathbf{k}',\sigma}^{\nu}$. Thus, proper arrangement of operators is important to get the correct form of the energy current, which is naturally captured in an equation of motion technique but not while using Noether's theorem for classical fields.

The heat current (\mathbf{j}_Q) is related to the energy current by $\mathbf{j}_Q = \mathbf{j}_E - \mu \mathbf{j}$, where μ is the chemical potential [55]. The chemical potential enters only to shift the single particle energies, i.e., right hand side of Eq. (3.14) gives the heat current with the re-definition $\dot{\hat{O}} = i[\mathcal{H} - \mu \mathcal{N}, \hat{O}]$, where \mathcal{N} is the total particle operator.

3.4 Transport Coefficients

In this section we will examine in detail the derivation of the correlation functions of the current operators. We will consider only the Peierls type of (charge and thermal)

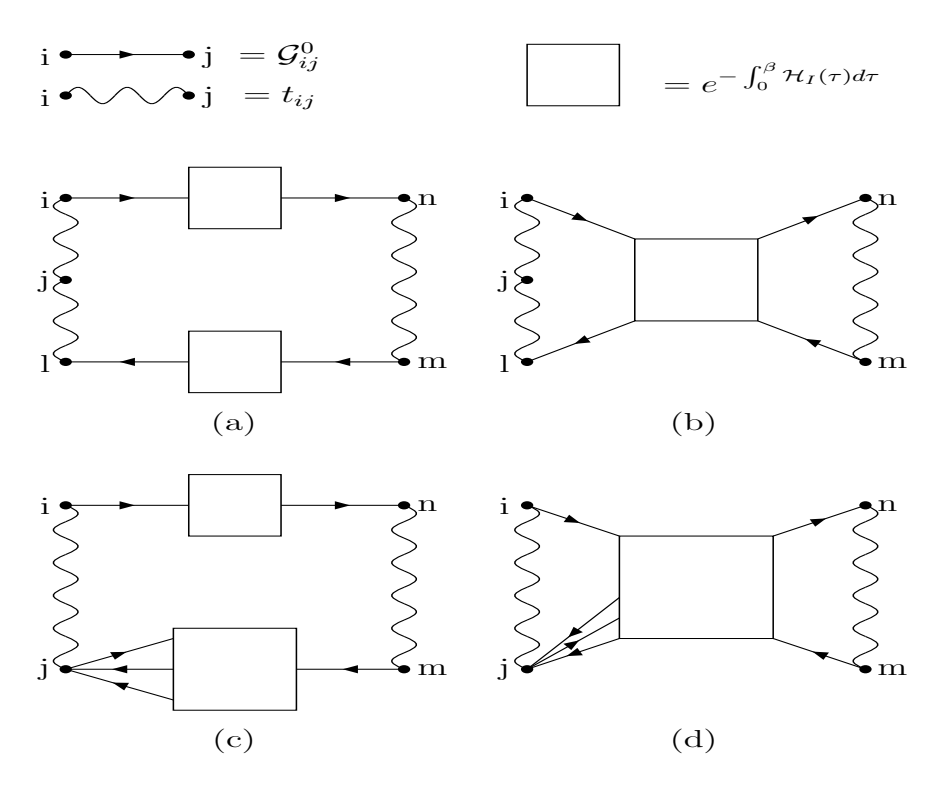


Figure 3.1: Diagrams in configuration space for thermoelectric power. \mathcal{H}_I is the interaction term. In (a) and (b) the thermal current is a two-point vertex, while in (c) and (d) it is a four-point vertex. In the limit of infinite d contribution from (b) and (d) can be neglected.

currents to keep things analytically tractable. In Kubo formalism the correlation functions are related to the corresponding response functions (the transport coefficients). In the framework of DMFT [29] it is possible to derive exact expressions for the transport coefficients. The essential simplification in the limit of infinite dimensions (d) is that the self energy and the vertex terms are local. For the single-band Hubbard model, defined by the Hamiltonian

$$\mathcal{H} = \sum_{\langle ij\rangle,\sigma} \left(t_{ij} c_{i,\sigma}^{\dagger} c_{j,\sigma} + \text{h.c.} \right) + U \sum_{i} n_{i,\uparrow} n_{i,\downarrow},$$

we will demonstrate that this allows the correlation functions to be factorized into products of single particle Green's functions and their time derivatives. The terms that are ignored by such factorization are $\mathcal{O}(1/d)$ smaller and can be neglected in the limit of infinite d. Using a slightly different approach, the expressions for the transport coefficients for the Falikov-Kimball model have been derived recently [40].

The correlation functions of the current operators are defined as [55]

$$L_{ab}(i\omega_n) = \frac{1}{\beta i\omega_n V} \int_0^\beta d\tau e^{i\omega_n \tau} \langle T_\tau \mathbf{j}_a(\tau) \mathbf{j}_b(0) \rangle, \tag{3.15}$$

where a, b = (1, 2), and $\mathbf{j}_1 = \mathbf{j}$ is the charge current and $\mathbf{j}_2 = \mathbf{j}_Q$ is the heat current. Here V is the volume of the system, $\beta = 1/k_BT$ is inverse temperature, and $i\omega_n$ is bosonic Matsubara frequency. The transport coefficients (that enter the formula for DC conductivity, thermoelectric power and thermal conductivity) are given by,

$$L_{ab} = \lim_{\omega \to 0} \text{Im} L_{ab}(i\omega_n \to \omega + i\delta). \tag{3.16}$$

For the single band Hubbard model the charge current is given by,

$$\mathbf{j} = e \sum_{\mathbf{k}, \sigma} \mathbf{v}_{\mathbf{k}} c_{\mathbf{k}, \sigma}^{\dagger} c_{\mathbf{k}, \sigma} = e \sum_{\langle ij \rangle} i \left(\mathbf{R}_{j} - \mathbf{R}_{i} \right) t_{ij} c_{i, \sigma}^{\dagger} c_{j, \sigma}, \tag{3.17}$$

and the heat current is given by

$$\mathbf{j}_{Q} = \frac{i}{2} \sum_{\mathbf{k},\sigma} \mathbf{v}_{\mathbf{k}} \left(c_{\mathbf{k},\sigma}^{\dagger} \dot{c}_{\mathbf{k},\sigma} - \dot{c}_{\mathbf{k},\sigma}^{\dagger} c_{\mathbf{k},\sigma} \right) = \frac{1}{2} \sum_{\langle ij \rangle} \left(\mathbf{R}_{i} - \mathbf{R}_{j} \right) t_{ij} \left(c_{i,\sigma}^{\dagger} \dot{c}_{j,\sigma} - \dot{c}_{i,\sigma}^{\dagger} c_{j,\sigma} \right).$$
(3.18)

Here $\mathbf{v_k} = \nabla_{\mathbf{k}} \epsilon_{\mathbf{k}}$ is the electron velocity. Since the interaction is purely local, there is no contribution from the long range interactions.

The derivation of L_{11} is discussed extensively in the literature on DMFT [37, 52]. In infinite d the particle-hole vertex becomes momentum independent [62], and the dressed correlation function becomes equal to the bare one. This implies the correlation function can be factorized into a product of single particle Green's functions, i.e., $\langle T_{\tau}\mathbf{j}(\tau)\mathbf{j}(0)\rangle = -\frac{e^2}{d}\sum_{\mathbf{k},\sigma}v_{\mathbf{k}}^2\mathcal{G}_{\sigma}(\mathbf{k},\tau)\mathcal{G}_{\sigma}(\mathbf{k},-\tau)$, where $\mathcal{G}_{\sigma}(\mathbf{k},\tau) = -\langle T_{\tau}c_{\mathbf{k},\sigma}(\tau)c_{\mathbf{k},\sigma}^{\dagger}(0)\rangle$ is the fermionic Matsubara Green's function. We define the Fourier transform $\mathcal{G}_{\sigma}(\mathbf{k},\tau) = \frac{1}{\beta}\sum_{n}e^{-i\omega_{n}\tau}\mathcal{G}_{\sigma}(\mathbf{k},i\omega_{n})$, in terms of which

$$L_{11}(i\omega_n) = -\left(\frac{e^2}{d}\right) \left(\frac{1}{\beta i\omega_n V}\right) \sum_{\mathbf{k},\sigma} v_{\mathbf{k}}^2 \frac{1}{\beta} \sum_{ip_n} \mathcal{G}_{\sigma}(\mathbf{k}, i\omega_n + ip_n) \mathcal{G}_{\sigma}(\mathbf{k}, ip_n).$$

 $\mathcal{G}_{\sigma}(\mathbf{k},z)$ has a possible branch cut at $z=\epsilon$ and $\mathcal{G}_{\sigma}(\mathbf{k},z+i\omega_n)$ has one at $z=\epsilon-i\omega_n$ [55]. Following Mahan [46,55] one can show

$$\frac{1}{\beta} \sum_{ip_n} \mathcal{G}_{\sigma}(\mathbf{k}, i\omega_n + ip_n) \mathcal{G}_{\sigma}(\mathbf{k}, ip_n) = \int_{-\infty}^{\infty} \frac{d\epsilon}{2\pi} n_F(\epsilon) A_{\sigma}(\mathbf{k}, \epsilon) \left[\mathcal{G}_{\sigma}(\mathbf{k}, \epsilon + i\omega_n) + \mathcal{G}_{\sigma}(\mathbf{k}, \epsilon - i\omega_n) \right],$$

where $A_{\sigma}(\mathbf{k}, \epsilon) = -2 \mathrm{Im} G_{\sigma}^{R}(\mathbf{k}, \epsilon)$ is the spectral function and $n_{F}(\epsilon)$ is the Fermi function. After analytic continuation $i\omega_{n} \to \omega + i\delta$, and after taking the static limit we get

$$L_{11} = \frac{e^2}{2d\beta V} \sum_{\mathbf{k},\sigma} v_{\mathbf{k}}^2 \int_{-\infty}^{\infty} \frac{d\epsilon}{2\pi} \left(-\frac{\partial n_F(\epsilon)}{\partial \epsilon} \right) A_{\sigma}^2(\mathbf{k}, \epsilon). \tag{3.19}$$

The derivation of L_{21} is more involved, and is not well discussed in the literature. Since the heat current has a part which is a four-point vertex, a priori it is not clear whether a factorization of the correlation function into products of single particle Green's functions and their time derivatives is possible. We have $\dot{c}_{i,\sigma} = -i\sum_l t_{il}c_{l,\sigma} - iUc_{i,\sigma}n_{i,\bar{\sigma}} + i\mu c_{i,\sigma}$ (and similarly for $\dot{c}_{i,\sigma}^{\dagger}$). We ignore the term with the chemical potential for the time being (the result remains unchanged). Due to the first term the heat current is a two-point vertex, and the corresponding diagrams for L_{21} are of the type (a) and (b) of Fig. 3.1. The heat current is a four-point vertex due to the second term. The corresponding diagrams are of the type (c) and (d) of Fig. 3.1. In the limit of infinite d the scaling of the hopping term is $t_{ij} = t_{ij}^*/\sqrt{d}$ (Ref. 4). This implies that $\mathcal{G}_{ij}^0 \sim (1/\sqrt{d})^{|i-j|}$ (Ref. [29]). One can show explicitly that diagrams (a) and (c) are $\mathcal{O}(1/d)$ (and higher), and diagrams (b) and (d) are $\mathcal{O}(1/d^2)$ (and higher). In Fig. 3.1, $\mathcal{H}_I = U \sum_i n_{i,\uparrow} n_{i,\downarrow}$ is the interaction term of the Hubbard Hamiltonian. In the limit of infinite d the latter drops out, and the factorization of the correlation function is possible. In imaginary time

$$\langle T_{\tau} \mathbf{j}_{Q}(\tau) \mathbf{j}(0) \rangle \stackrel{d \to \infty}{=} \frac{e}{2d} \sum_{\mathbf{k}, \sigma} v_{\mathbf{k}}^{2} \left\{ \langle T_{\tau} \dot{c}_{\mathbf{k}, \sigma}(\tau) c_{\mathbf{k}, \sigma}^{\dagger}(0) \rangle \langle T_{\tau} c_{\mathbf{k}, \sigma}(0) c_{\mathbf{k}, \sigma}^{\dagger}(\tau) \rangle + \text{h.c.} \right\}.$$

Using $\frac{\partial}{\partial \tau} \mathcal{G}(\tau) = \langle T_{\tau} \frac{\partial}{\partial \tau} c(\tau) c^{\dagger}(0) \rangle - \delta(\tau)$ (in imaginary time), we get

$$L_{21}(i\omega_n) = -\left(\frac{2}{d\beta i\omega_n V}\right) \sum_{\mathbf{k},\sigma} v_{\mathbf{k}}^2 \left\{ \frac{1}{\beta} \sum_{ip_n} \left(ip_n + \frac{i\omega_n}{2} \right) \mathcal{G}_{\sigma}(\mathbf{k}, ip_n) \mathcal{G}_{\sigma}(\mathbf{k}, ip_n + i\omega_n) - n_{\mathbf{k},\sigma} \right\}.$$

We drop the second term within braces because it does not contribute to $\text{Im}L_{21}(\omega+i\delta)$. The rest is evaluated like $L_{11}(i\omega_n)$. It can be shown that

$$\frac{1}{\beta} \sum_{ip_n} \left(ip_n + \frac{i\omega_n}{2} \right) \mathcal{G}_{\sigma}(\mathbf{k}, ip_n) \mathcal{G}_{\sigma}(\mathbf{k}, ip_n + i\omega_n) =$$

$$\int_{-\infty}^{\infty} \frac{d\epsilon}{2\pi} n_F(\epsilon) A_{\sigma}(\mathbf{k}, \epsilon) \left[\left(\epsilon + \frac{i\omega_n}{2} \right) \mathcal{G}_{\sigma}(\mathbf{k}, \epsilon + i\omega_n) + \left(\epsilon - \frac{i\omega_n}{2} \right) \mathcal{G}_{\sigma}(\mathbf{k}, \epsilon - i\omega_n) \right].$$

After analytic continuation and taking the static limit we get,

$$L_{21} = \frac{e}{2d\beta V} \sum_{\mathbf{k},\sigma} v_{\mathbf{k}}^2 \int_{-\infty}^{\infty} \frac{d\epsilon}{2\pi} \epsilon \left(-\frac{\partial n_F(\epsilon)}{\partial \epsilon} \right) A_{\sigma}^2(\mathbf{k}, \epsilon). \tag{3.20}$$

The derivation of L_{22} is analogous to that of L_{21} . In the limit of infinite d, $\langle T_{\tau} \mathbf{j}_{Q}(\tau) \mathbf{j}_{Q} \rangle$ factorizes into products of (imaginary) time derivatives of single particle Green's functions (plus terms which do not contribute to $\mathrm{Im}L_{22}(\omega)$). As in the case of L_{11} and L_{21} , the terms which are dropped out by such factorization are at least $\mathcal{O}(1/d)$ smaller. In other words,

$$\langle T_{\tau} \mathbf{j}_{Q}(\tau) \mathbf{j}_{Q} \rangle \stackrel{d \to \infty}{=} \frac{1}{4d} \sum_{\mathbf{k}, \sigma} v_{\mathbf{k}}^{2} \left\{ \langle T_{\tau} \dot{c}_{\mathbf{k}, \sigma}(\tau) c_{\mathbf{k}, \sigma}^{\dagger}(0) \rangle \langle T_{\tau} c_{\mathbf{k}, \sigma}(0) \dot{c}_{\mathbf{k}, \sigma}^{\dagger}(\tau) \rangle - \langle T_{\tau} \ddot{c}_{\mathbf{k}, \sigma}(\tau) c_{\mathbf{k}, \sigma}^{\dagger}(0) \rangle \langle T_{\tau} c_{\mathbf{k}, \sigma}(0) c_{\mathbf{k}, \sigma}^{\dagger}(\tau) \rangle + \text{h.c.} \right\}.$$

With this simplification it can be shown that

$$L_{22}(i\omega_n) = -\left(\frac{1}{d\beta i\omega_n V}\right) \sum_{\mathbf{k},\sigma} v_{\mathbf{k}}^2 \left\{ \frac{1}{\beta} \sum_{ip_n} \left(ip_n + \frac{i\omega_n}{2} \right)^2 \mathcal{G}_{\sigma}(\mathbf{k}, ip_n) \mathcal{G}_{\sigma}(\mathbf{k}, ip_n + i\omega_n) + \cdots \right\}.$$

The terms in the ellipses do not contribute to $\text{Im}L_{22}(\omega)$. Finally we get,

$$L_{22} = \frac{e}{2d\beta V} \sum_{\mathbf{k},\sigma} v_{\mathbf{k}}^2 \int_{-\infty}^{\infty} \frac{d\epsilon}{2\pi} \epsilon^2 \left(-\frac{\partial n_F(\epsilon)}{\partial \epsilon} \right) A_{\sigma}^2(\mathbf{k}, \epsilon). \tag{3.21}$$

We reiterate the observation made in Ref. [40] that the above expressions for the transport coefficients are correct for any model with local interaction (for which Eq. (3.18) is correct), in infinite dimensions.

3.5 Conclusion

The current (charge or thermal) obtained by Peierls substitution or by the equation of motion technique is an approximation to the exact low energy current for an effective tight-binding Hamiltonian. In particular, the approximate current is not invariant under a unitary transformation of the Wannier basis. We have suggested a simple criteria by which one can choose a set of Wannier functions where the difference between the exact and the approximate current is minimum. The minimization procedure is well defined provided the matrix elements of the exact current are known from first principles calculation. Using the equations of motion we have derived the thermal current for a very general tight-binding Hamiltonian, correcting the result of a previous work. Finally, using the Peierls currents, we have established the correctness of known expressions for the transport coefficients for the Hubbard model in infinite d. The simplification in the limit of large coordination is that the current (charge and thermal) correlation functions can be factorized into products of single particle Green's functions and their time derivatives. These expressions are correct for any model with local interaction and in infinite dimensions.

Chapter 4

The Charge Current Operator in Down-folding Scheme

4.1 Introduction

The notion of effective low-energy Hamiltonians, or model Hamiltonians, is central to the conceptual framework of condensed matter theory. The motivation and the justification for using model Hamiltonians is the following: The microscopic details of an interacting many-body system come into play only when we probe the system over a wide range of energy. But if we restrict ourselves to examining only low-energy properties of the system then much of the microscopic details can be forgotten. This allows us to replace a more complicated full Hamiltonian, which describes both low- as well as high-energy modes of the system, by a simpler Hamiltonian (usually with fewer microscopic parameters) which describes only the low-energy degrees of freedom. The Hilbert space for the latter is smaller and hence has a better chance of being tractable, both analytically as well as numerically. This procedure is implemented rigorously within the formalism of the renormalization group (RG).

The scheme of down-folding is a formal procedure by which a Hamiltonian, which has a clear and well-separated low(L)- and high(H)-energy subspaces, is expressed entirely in the low-energy sector. This procedure can be used to construct low-energy effective Hamiltonians, and the scheme is motivated by the idea of RG mentioned above. To illustrate the scheme we consider solving Schroedinger equation $\mathcal{H}\psi=E\psi$. The wave-function has low- and high-energy projections ψ_L and ψ_H respectively. The Hamiltonian has low- and high-energy pieces and also some mixing terms. In matrix

notation we write

$$\mathcal{H}\psi = \begin{bmatrix} \mathcal{H}_L & \mathcal{H}_M^{\dagger} \\ \mathcal{H}_M & \mathcal{H}_H \end{bmatrix} \begin{bmatrix} \psi_L \\ \psi_H \end{bmatrix} = E \begin{bmatrix} \psi_L \\ \psi_H \end{bmatrix}. \tag{4.1}$$

Formally one can write

$$\psi_H = \frac{1}{(E - \mathcal{H}_H)} \mathcal{H}_M \psi_L \tag{4.2}$$

and eliminate the high-energy subspace completely. The "Schroedinger equation" in the low-energy subspace is

$$\mathcal{H}_D(E)\psi_L = \left(\mathcal{H}_L + \mathcal{H}_M^{\dagger} \frac{1}{(E - \mathcal{H}_H)} \mathcal{H}_M\right) \psi_L = E\psi_L. \tag{4.3}$$

Note that the down-folded "Hamiltonian" \mathcal{H}_D is energy dependent and that the above equation is non-linear. Let us suppose that E_L and E_H are typical energy scales of the low- and high-energy manifolds respectively, i.e., typical matrix elements of the operators \mathcal{H}_L and \mathcal{H}_H respectively. We want the down-folded theory to reproduce the spectrum of the low-energy manifold. In principle this can be done by writing $E = E_L + \delta E$ and expanding the above equation in the small parameter $\delta E/(E_H - E_L)$.

Let us suppose that for the original theory (in which both the low- and high- energy degrees of freedom are present) the form of the charge current operator \mathbf{j} is known from the symmetry of the original theory and by the application of Noether's theorem. Let us assume that the current operator is given by $\mathbf{j} = ((\delta \mathcal{H}(\mathbf{A}))/(\delta \mathbf{A}))_{\mathbf{A}=0}$. For the down-folded theory it is not possible to reconstruct Noether's theorem since the Hilbert space has been truncated to exclude the high-energy states. The questions, then, are: what is the form of the charge current operator (\mathbf{j}_{eff}) for the down-folded theory that reproduces the low-energy part of the current correctly? Also, if we can write down a low-energy effective Hamiltonian $\mathcal{H}_{\text{eff}}(E_L)$ (and which does not depend on E like $\mathcal{H}_D(E)$), then will $\mathbf{j}_{\text{eff}} = ((\delta \mathcal{H}_{\text{eff}}(\mathbf{A}))/(\delta \mathbf{A}))_{\mathbf{A}=0}$.

This issue was recently revisited by Millis [51]. He assumed that the wavefunction in the low-energy sector is normalized, i.e., $\langle \psi_L | \psi_L \rangle = 1$. With this normalization convention, the basis states of the full theory acquire energy dependent normalization factor, i.e., the normalized states are $\psi_N = \psi/N(E)$ where $N(E) = \sqrt{1 + \langle \psi_L | \mathcal{H}_M^{\dagger}(E - \mathcal{H}_H)^{-2}\mathcal{H}_M | \psi_L \rangle}$. By a simple application of the Feynman-Hellman theorem one can show that

$$\langle \psi_N | \left(\frac{\delta \mathcal{H}(\mathbf{A})}{\delta \mathbf{A}} \right)_{\mathbf{A} = 0} | \psi_N \rangle = \left(\frac{\delta E}{\delta \mathbf{A}} \right)_{\mathbf{A} = 0} = \langle \psi_L | \left(\frac{\delta \mathcal{H}_D(E, \mathbf{A})}{\delta \mathbf{A}} \right)_{\mathbf{A} = 0} | \psi_L \rangle. \tag{4.4}$$

From the above equation we find that the diagonal matrix elements of the current operator for the full theory can be expressed in terms of the diagonal matrix elements of the energy-dependent current operator of the down-folded theory. However, Millis observed, for non-diagonal matrix elements there is no such simple relation between the full theory and the down-folded one. The main problem in making such a connection is the energy dependence of the normalization of the basis states in the full theory and the energy dependence of the operators in the down-folded theory.

RG provides a rigorous way of identifying the low-energy theory. In the functional integral language this is done by eliminating or integrating out high-energy degrees of freedom. In a Hamiltonian formulation this is equivalent to making unitary transformations that decouple the high- and low-energy subspaces, and then truncating the Hilbert space to keep only the low-energy subspace. That is, given a Hamiltonian \mathcal{H} , we perform unitary transformations (U) such that $U^{\dagger}\mathcal{H}U$ is block diagonal (i.e., no terms mixing the two subspaces). The effective low-energy Hamiltonian is $\mathcal{H}_{\text{eff}} = PU^{\dagger}\mathcal{H}UP$, where P is the operator projecting on the low-energy subspace. In this scheme the effective low-energy current operator is unambiguous and is $\mathbf{j}_{\text{eff}} = PU^{\dagger}\mathbf{j}UP$. In the following our aim will be to understand down-folding as a formal procedure of performing RG transformation and make a connection between the two schemes.

We make the observation that the problem of the energy dependence in the normalization factor and the energy dependence in the operators of the down-folded theory can be removed if we expand Eq. (4.3) to first order in δE . To this order, and

after a transformation that makes the low-energy basis states orthonormal, the low-energy effective theory can be expressed as a Schroedinger equation with an effective Hamiltonian $\mathcal{H}_{\text{eff}}(E_L)$. We will identify the down-folding transformation D, where $\mathcal{H}_{\text{eff}}(E_L) = D^{\dagger}\mathcal{H}D$, as a combined operation of unitary transformation and projection, i.e., D = UP. With this identification it is clear that in the down-folding scheme the effective current operator is $\mathbf{j}_{\text{eff}} = D^{\dagger}\mathbf{j}D$. However, we will see that the down-folding transformation is energy dependent, i.e., $D = D(\delta E)$. Therefore, in order to write down \mathbf{j}_{eff} we will have to make use of the equation of motion.

4.2 Charge Current Operator in Low-Energy Sector

We begin with Eq. (4.1), and we adopt the normalization that the eigenstates of the full theory are orthonormal, i.e., $\langle \psi_a | \psi_b \rangle = \delta_{ab}$. This implies the projections of the eigenstates on the low-energy sector satisfy the formal relation

$$\langle \psi_{La} \left| \left[1 + \mathcal{H}_M^{\dagger} \left(E_a - \mathcal{H}_H \right)^{-1} \left(E_b - \mathcal{H}_H \right)^{-1} \mathcal{H}_M \right] \right| \psi_{Lb} \rangle = \delta_{ab}. \tag{4.5}$$

Next, we expand Eq. (4.3) to linear order in δE . The corresponding equation can be written as

$$\tilde{\mathcal{H}}(E_L)\psi_L^{(0)} = \delta E O^{-1}(E_L)\psi_L^{(0)},$$
(4.6)

where

$$\tilde{\mathcal{H}}(E_L) = \mathcal{H}_L + \mathcal{H}_M^{\dagger} (E_L - \mathcal{H}_H)^{-1} \mathcal{H}_M - E_L, \tag{4.7}$$

and

$$O^{-1}(E_L) = 1 + \mathcal{H}_M^{\dagger} (E_L - \mathcal{H}_H)^{-2} \mathcal{H}_M. \tag{4.8}$$

The solution of Eq. (4.6), $\psi_L^{(0)}$, coincides with ψ_L to zeroth order in δE , i.e., $\psi_L = \psi_L^{(0)} + \mathcal{O}(\delta E)$. If we expand the normalization Eq. (4.5) to zeroth order in δE , we get

$$\langle \psi_{La}^{(0)} | O^{-1}(E_L) | \psi_{Lb}^{(0)} \rangle = \delta_{ab}.$$
 (4.9)

This suggests that Eq. (4.6) has the structure of Schroedinger equation expressed in a non-orthogonal basis, and the operator $O^{-1}(E_L)$ can be understood as the inverse of

the overlap. This is expected because though the basis states for the full theory (ψ 's) are orthonormal, their projection on the low-energy sector (ψ_L 's) are not orthonormal. In other words, this step in the process of down-folding is a transformation (say T_1) that is a non-unitary followed by the projection P. We write this transformation as

$$\begin{bmatrix} \psi_L \\ \psi_H \end{bmatrix} = T_1 \begin{bmatrix} \psi_L^{(0)} \\ 0 \end{bmatrix} = \begin{bmatrix} 1 & 0 \\ M & 0 \end{bmatrix} \begin{bmatrix} \psi_L^{(0)} \\ 0 \end{bmatrix}$$
(4.10)

where

$$M = (E_L - \mathcal{H}_H)^{-1} \mathcal{H}_M - \delta E(E_L - \mathcal{H}_H)^{-2} \mathcal{H}_M.$$
 (4.11)

In this new basis we have the equation

$$T_1^{\dagger} \left(\mathcal{H} - E_L \right) T_1 \begin{bmatrix} \psi_L^{(0)} \\ 0 \end{bmatrix} = \delta E T_1^{\dagger} T_1 \begin{bmatrix} \psi_L^{(0)} \\ 0 \end{bmatrix}. \tag{4.12}$$

To $\mathcal{O}(\delta E)$ this coincides with Eq. (4.6). We note that the transformation T_1 depends on the spectrum δE .

In the next step we will consider a non-unitary transformation (T_2) in the lowenergy sub-space of the form $\psi_L^{(0)} = T_2 \phi_L$, such that the states ϕ_L are orthonormal. It is easy to check that the general form of the transformation is $T_2 = O^{1/2}U$, where U is unitary, i.e., $U^{\dagger}U = 1$. Using Eq. (4.9) we get

$$\delta_{ab} = \langle \psi_{La}^{(0)} | O^{-1}(E_L) | \psi_{Lb}^{(0)} \rangle = \langle \phi_{La} | U^{\dagger} O^{1/2} O^{-1} O^{1/2} U | \phi_{Lb} \rangle = \langle \phi_{La} | \phi_{Lb} \rangle. \tag{4.13}$$

This establishes the orthonormality of the $\{|\phi_L\rangle\}$ basis. The transformation from the non-orthogonal basis $\{|\psi_L\rangle\}$ to the orthonormal basis $\{|\phi_L\rangle\}$ is not unique. It depends on the choice of U. In the following we will choose U=1. Applying this transformation to Eq. (4.6) we get

$$\mathcal{H}_{\text{eff}}(E_L)\phi_L = \delta E \phi_L,\tag{4.14}$$

where

$$\mathcal{H}_{\text{eff}}(E_L) = O^{1/2}(E_L) \left(\mathcal{H}_L + \mathcal{H}_M^{\dagger} (E_L - \mathcal{H}_H)^{-1} \mathcal{H}_M - E_L \right) O^{1/2}(E_L). \tag{4.15}$$

We identify the down-folding transformation (D) as

$$D = T_1 T_2 = \begin{bmatrix} 1 & 0 \\ M & 0 \end{bmatrix} \begin{bmatrix} O^{1/2} & 0 \\ 0 & 0 \end{bmatrix} = \begin{bmatrix} O^{1/2} & 0 \\ MO^{1/2} & 0 \end{bmatrix}, \tag{4.16}$$

and we can write

$$D^{\dagger} \mathcal{H} D = \begin{bmatrix} \mathcal{H}_{\text{eff}} & 0 \\ 0 & 0 \end{bmatrix} + \mathcal{O}((\delta E)^2). \tag{4.17}$$

It is easy to check that keeping terms to zeroth order in δE (which is consistent since we have maintained accuracy of the wavefunction and the normalization condition to this order) we get

$$D^{\dagger}D = \begin{bmatrix} 1 & 0 \\ 0 & 0 \end{bmatrix}. \tag{4.18}$$

This confirms the identification D = UP. It is important to remember that the transformation D is spectrum dependent.

The effective low-energy current is given by

$$D^{\dagger} \mathbf{j} D = \begin{bmatrix} O^{1/2} & O^{1/2} M^{\dagger} \\ 0 & 0 \end{bmatrix} \begin{bmatrix} \mathbf{j}_{L} & \mathbf{j}_{M}^{\dagger} \\ \mathbf{j}_{M} & \mathbf{j}_{H} \end{bmatrix} \begin{bmatrix} O^{1/2} & 0 \\ MO^{1/2} & 0 \end{bmatrix} = \begin{bmatrix} \mathbf{j}_{\text{eff}} & 0 \\ 0 & 0 \end{bmatrix} + \mathcal{O}((\delta E)^{2}).$$

$$(4.19)$$

The above equation has explicit dependence on δE . This can be removed formally by making use of the equation of motion, i.e., Eq. (4.14). Since the operator D acts on $|\phi_L\rangle$, we will replace δE by $\mathcal{H}_{\mathrm{eff}}$ acting on the right, and for D^{\dagger} we will replace δE by $\mathcal{H}_{\mathrm{eff}}$ acting on the left. We get

$$\mathbf{j}_{\text{eff}} = O^{1/2} \left[\mathbf{j}_{L} + \mathbf{j}_{M}^{\dagger} (E_{L} - \mathcal{H}_{H})^{-1} \mathcal{H}_{M} + \mathcal{H}_{M}^{\dagger} (E_{L} - \mathcal{H}_{H})^{-1} \mathbf{j}_{M} + \mathcal{H}_{M}^{\dagger} (E_{L} - \mathcal{H}_{H})^{-1} \mathbf{j}_{H} (E_{L} - \mathcal{H}_{H})^{-1} \mathcal{H}_{M} \right] O^{1/2} - \left[O^{1/2} \left\{ \mathbf{j}_{M}^{\dagger} + \mathcal{H}_{M}^{\dagger} (E_{L} - \mathcal{H}_{H})^{-1} \mathbf{j}_{H} \right\} (E_{L} - \mathcal{H}_{H})^{-2} \mathcal{H}_{M} O^{1/2} \mathcal{H}_{\text{eff}} + \mathcal{H}_{\text{eff}} O^{1/2} \mathcal{H}_{M}^{\dagger} (E_{L} - \mathcal{H}_{H})^{-2} \left\{ \mathbf{j}_{M} + \mathbf{j}_{H} (E_{L} - \mathcal{H}_{H})^{-1} \mathcal{H}_{M} \right\} O^{1/2} \right]. (4.20)$$

This construction guarantees that

$$\langle \psi_a | \mathbf{j} | \psi_b \rangle = \langle \phi_{La} | \mathbf{j}_{\text{eff}} | \phi_{Lb} \rangle + \mathcal{O}((\delta E)^2).$$

4.3 Downfolding in the Presence of a Vector Potential

We will assume we know how the vector potential \mathbf{A} couples to the original Hamiltonian \mathcal{H} , and that the current operator is given by $\mathbf{j} = ((\delta \mathcal{H}(\mathbf{A}))/(\delta \mathbf{A}))_{\mathbf{A}=0}$. Thus $\mathcal{H}(\mathbf{A}) = \mathcal{H}(0) + \mathbf{j} \cdot \mathbf{A}$. From this information we should be able to find how \mathbf{A} couples to $\mathcal{H}_{\mathrm{eff}}(E_L)$. We will investigate whether $\mathbf{j}_{\mathrm{eff}} = ((\delta \mathcal{H}_{\mathrm{eff}}(E_L, \mathbf{A}))/(\delta \mathbf{A}))_{\mathbf{A}=0}$.

It is instructive to study this issue first for a case where the down-folding is trivial. Let us suppose we have a Hamiltonian which we can diagonalize and which we can cleanly separate into a low- and a high-energy subspace. In obvious notations

$$\mathcal{H}_0 = \mathcal{H}_L \oplus \mathcal{H}_H = \sum_{i \in L} E_L^i |\psi_L^i\rangle \langle \psi_L^i| + \sum_{k \in H} E_H^k |\psi_H^k\rangle \langle \psi_H^k|.$$

In this trivial case the down-folded Hamiltonian is

$$\mathcal{H}_{\text{eff}} = \mathcal{H}_L = \sum_{i \in L} E_L^i |\psi_L^i\rangle\langle\psi_L^i|.$$

However, though \mathcal{H} is diagonal, the current operator $\mathbf{j} = ((\delta \mathcal{H}(\mathbf{A}))/(\delta \mathbf{A}))$, in general, is not diagonal in this basis. In particular, it can have terms mixing between the two subspaces. The current operator can be expressed as

$$\mathbf{j} = \sum_{i,j \in L} \langle \psi_L^i | \frac{\delta \mathcal{H}_0}{\delta \mathbf{A}} | \psi_L^j \rangle | \psi_L^i \rangle \langle \psi_L^j | + \sum_{k,l \in H} \langle \psi_H^k | \frac{\delta \mathcal{H}_0}{\delta \mathbf{A}} | \psi_H^l \rangle | \psi_H^k \rangle \langle \psi_H^l | + \sum_{k \in L \atop k \in H} \langle \psi_H^k | \frac{\delta \mathcal{H}_0}{\delta \mathbf{A}} | \psi_L^i \rangle | \psi_H^k \rangle \langle \psi_L^i | + \sum_{k \in L \atop k \in H} \langle \psi_L^i | \frac{\delta \mathcal{H}_0}{\delta \mathbf{A}} | \psi_H^k \rangle | \psi_L^i \rangle \langle \psi_H^k |.$$

The four terms above are \mathbf{j}_L , \mathbf{j}_M , \mathbf{j}_M and \mathbf{j}_M^{\dagger} respectively. The current for the downfolded theory is

$$\mathbf{j}_{\text{eff}} = P\mathbf{j}P = \mathbf{j}_L = \sum_{i,j \in L} \langle \psi_L^i | \frac{\delta \mathcal{H}_0}{\delta \mathbf{A}} | \psi_L^j \rangle | \psi_L^i \rangle \langle \psi_L^j |.$$

Now the question is whether $\mathbf{j}_L = (\delta \mathcal{H}_L(\mathbf{A}))/(\delta \mathbf{A})$. Using Feynman-Hellman theorem we can express the current matrix elements as

$$\langle \psi^j | \frac{\delta \mathcal{H}}{\delta \mathbf{A}} | \psi^i \rangle = \frac{\partial E^i}{\partial \mathbf{A}} \delta_{ij} + (E^i - E^j) \langle \psi^j | \overrightarrow{\partial_{\mathbf{A}}} | \psi^i \rangle, \qquad i, j \in L, H.$$
 (4.21)

Using the above equation we get

$$\frac{\delta \mathcal{H}_L}{\delta \mathbf{A}} = \mathbf{j}_L + \sum_{\stackrel{i \in L}{k \in H}} E_L^i \left(\langle \psi_H^k | \overrightarrow{\partial_{\mathbf{A}}} | \psi_L^i \rangle | \psi_H^k \rangle \langle \psi_L^i | + \langle \psi_L^i | \overleftarrow{\partial_{\mathbf{A}}} | \psi_H^k \rangle | \psi_L^i \rangle \langle \psi_H^k | \right). \tag{4.22}$$

Similarly, one can show that

$$\frac{\delta \mathcal{H}_{H}}{\delta \mathbf{A}} = \mathbf{j}_{H} + \sum_{\stackrel{i \in L}{k \in H}} E_{H}^{k} \left(\langle \psi_{H}^{k} | \overleftarrow{\partial_{\mathbf{A}}} | \psi_{L}^{i} \rangle | \psi_{H}^{k} \rangle \langle \psi_{L}^{i} | + \langle \psi_{L}^{i} | \overrightarrow{\partial_{\mathbf{A}}} | \psi_{H}^{k} \rangle | \psi_{L}^{i} \rangle \langle \psi_{H}^{k} | \right). \tag{4.23}$$

In general $(\delta \mathcal{H}_{L,H,M}/\delta \mathbf{A}) \neq \mathbf{j}_{L,H,M}$. The difference is due to matrix elements of the type $\langle \psi_H^k | \overrightarrow{\partial_{\mathbf{A}}} | \psi_L^i \rangle$, which gives coupling of the two subspaces due to the vector potential. Thus, we see explicitly in this simple example that $\mathcal{H}_{\mathrm{eff}}(\mathbf{A}) = \mathcal{H}_L + \mathbf{j}_L \cdot \mathbf{A}$, and then of course, $\mathbf{j}_{\mathrm{eff}} = (\delta \mathcal{H}_{\mathrm{eff}}/\delta \mathbf{A})$. In particular, $\mathcal{H}_{\mathrm{eff}}(\mathbf{A}) \neq \mathcal{H}_L + (\delta \mathcal{H}_L(\mathbf{A})/\delta \mathbf{A}) \cdot \mathbf{A}$. In fact, the operator $(\delta \mathcal{H}_L(\mathbf{A})/\delta \mathbf{A})$ is not contained only in the low-energy sector. It has mixing terms as can be seen explicitly from Eq. (4.22). In this context it is useful to note that the approximate low-energy current (\mathbf{j}_P) obtained by Peierls substitution is only the diagonal part of \mathbf{j}_L . It is given by

$$\mathbf{j}_{P} = \sum_{i \in L} \frac{\partial E_{L}^{i}}{\partial \mathbf{A}} |\psi_{L}^{i}\rangle\langle\psi_{L}^{i}|. \tag{4.24}$$

The off-diagonal part of \mathbf{j}_L involve information about the \mathbf{A} dependence of the wavefunctions $|\psi_L\rangle$. The diagonal part contains the \mathbf{A} dependence of the spectrum E_L .

Next we will consider the general case of down-folding in the presence of the vector potential. We generalize Eq. (4.1) to

$$\begin{bmatrix} \mathcal{H}_L + \mathbf{j}_L \cdot \mathbf{A} & \mathcal{H}_M^{\dagger} + \mathbf{j}_M^{\dagger} \cdot \mathbf{A} \\ \mathcal{H}_M + \mathbf{j}_M \cdot \mathbf{A} & \mathcal{H}_H + \mathbf{j}_H \cdot \mathbf{A} \end{bmatrix} \begin{bmatrix} \psi_L \\ \psi_H \end{bmatrix} = E \begin{bmatrix} \psi_L \\ \psi_H \end{bmatrix}. \tag{4.25}$$

As we have discussed before

$$\frac{\delta \mathcal{H}_L(\mathbf{A})}{\delta \mathbf{A}} = \frac{\delta}{\delta \mathbf{A}} [P \mathcal{H}(\mathbf{A}) P] \neq \mathbf{j}_L = P [\frac{\delta \mathcal{H}(\mathbf{A})}{\delta \mathbf{A}}] P.$$

As before we will assume that the eigenstates for the full theory are orthonormal. The

equivalent of Eq. (4.3) in the low-energy sector is

$$\mathcal{H}_{D}(E, \mathbf{A})\psi_{L} = \left[(\mathcal{H}_{L} + \mathbf{j}_{L} \cdot \mathbf{A}) + \left(\mathcal{H}_{M}^{\dagger} + \mathbf{j}_{M}^{\dagger} \cdot \mathbf{A} \right) (E - \mathcal{H}_{H} - \mathbf{j}_{H} \cdot \mathbf{A})^{-1} \right] \times (\mathcal{H}_{M} + \mathbf{j}_{M} \cdot \mathbf{A}) \psi_{L}$$

$$= E(\mathbf{A})\psi_{L}. \tag{4.26}$$

We expand the above equation to linear order in δE and $\bf A$ and also retain terms of the order ($\delta E {\bf A}$). We get, after collecting terms,

$$\tilde{\mathcal{H}}(E_L, \mathbf{A}) |\psi_L^{(0)}\rangle = \delta E O^{-1}(E_L, \mathbf{A}) |\psi_L^{(0)}\rangle, \tag{4.27}$$

where

$$\tilde{\mathcal{H}}(E_L, \mathbf{A}) = \left[\mathcal{H}_L + \mathcal{H}_M^{\dagger} (E_L - \mathcal{H}_H)^{-1} \mathcal{H}_M - E_L \right]
+ \left[\mathbf{j}_L + \mathbf{j}_M^{\dagger} (E_L - \mathcal{H}_H)^{-1} \mathcal{H}_M + \mathcal{H}_M^{\dagger} (E_L - \mathcal{H}_H)^{-1} \mathbf{j}_M \right]
+ \mathcal{H}_M^{\dagger} (E_L - \mathcal{H}_H)^{-1} \mathbf{j}_H (E_L - \mathcal{H}_H)^{-1} \mathcal{H}_M \cdot \mathbf{A},$$
(4.28)

and

$$O^{-1}(E_L, \mathbf{A}) = \left[1 + \mathcal{H}_M^{\dagger} (E_L - \mathcal{H}_H)^{-2} \mathcal{H}_M \right] + \left[\mathbf{j}_M^{\dagger} (E_L - \mathcal{H}_H)^{-2} \mathcal{H}_M \right]$$

$$+ \mathcal{H}_M^{\dagger} (E_L - \mathcal{H}_H)^{-2} \mathbf{j}_M + \mathcal{H}_M^{\dagger} (E_L - \mathcal{H}_H)^{-1} \mathbf{j}_H (E_L - \mathcal{H}_H)^{-2} \mathcal{H}_M$$

$$+ \mathcal{H}_M^{\dagger} (E_L - \mathcal{H}_H)^{-2} \mathbf{j}_H (E_L - \mathcal{H}_H)^{-1} \mathcal{H}_M \right] \cdot \mathbf{A}.$$

$$(4.29)$$

If we expand the normalization condition which is a generalization of Eq. (4.5) to zeroth order in δE and to linear order in \mathbf{A} , we get

$$\langle \psi_{La}^{(0)} | O^{-1}(E_L, \mathbf{A}) | \psi_{Lb}^{(0)} \rangle = \delta_{ab}.$$
 (4.30)

As before we use the transformation T_2 to go to the orthonormal basis $\{|\phi_L\rangle\}$. In this basis we get

$$\mathcal{H}_{\text{eff}}(E_L, \mathbf{A})\phi_L = \delta E(\mathbf{A})\phi_L, \tag{4.31}$$

where

$$\mathcal{H}_{\text{eff}}(E_L, \mathbf{A}) = O^{1/2}(E_L, \mathbf{A})\tilde{\mathcal{H}}(E_L, \mathbf{A})O^{1/2}(E_L, \mathbf{A}). \tag{4.32}$$

From the above equation we get

$$\left(\frac{\delta \mathcal{H}_{\text{eff}}(E_L, \mathbf{A})}{\delta \mathbf{A}}\right)_{\mathbf{A}=0} = O^{1/2}(E_L) \left[\mathbf{j}_L + \mathbf{j}_M^{\dagger} (E_L - \mathcal{H}_H)^{-1} \mathcal{H}_M + \mathcal{H}_M^{\dagger} (E_L - \mathcal{H}_H)^{-1} \mathbf{j}_M \right. \\
+ \left. \mathcal{H}_M^{\dagger} (E_L - \mathcal{H}_H)^{-1} \mathbf{j}_H (E_L - \mathcal{H}_H)^{-1} \mathcal{H}_M \right] O^{1/2}(E_L) \\
+ \left. \left(\frac{\delta O^{1/2}(E_L, \mathbf{A})}{\delta \mathbf{A}}\right)_{\mathbf{A}=0} \tilde{\mathcal{H}}(E_L) O^{1/2}(E_L) \right. \\
+ \left. O^{1/2}(E_L) \tilde{\mathcal{H}}(E_L) \left(\frac{\delta O^{1/2}(E_L, \mathbf{A})}{\delta \mathbf{A}}\right)_{\mathbf{A}=0} \right. \tag{4.33}$$

Now we want to compare the above expression with that of \mathbf{j}_{eff} given by Eq. (4.20). We note that the first term in the above expression, which is zeroth order in δE , coincides with the zeroth order term in \mathbf{j}_{eff} . The difference is in terms which are first order in δE . However, it turns out that there is no simple closed form expression for $((\delta O^{1/2}(E_L, \mathbf{A}))/(\delta \mathbf{A}))_{\mathbf{A}=0}$. So we will expand $O^{1/2}(E_L, \mathbf{A})$ in the parameter $\lambda = E_M/(E_H - E_L)$, where E_M is a typical matrix element of \mathcal{H}_M . We find

$$\left(\frac{\delta \mathcal{H}_{\text{eff}}(E_L, \mathbf{A})}{\delta \mathbf{A}}\right)_{\mathbf{A}=0} - \mathbf{j}_{\text{eff}} = \frac{1}{2} \left[X(E_L) - X^{\dagger}(E_L), \tilde{\mathcal{H}}(E_L) \right] + \mathcal{O}(\lambda^4), \quad (4.34)$$

where

$$X(E_L) = \left[\mathbf{j}_M^{\dagger} + \mathcal{H}_M^{\dagger} (E_L - \mathcal{H}_H)^{-1} \mathbf{j}_H\right] (E_L - \mathcal{H}_H)^{-2} \mathcal{H}_M. \tag{4.35}$$

4.4 Example: Non-Interacting Anderson Lattice Model

In this section we apply the abstract concepts of down-folding discussed in the last two sections to the particular case of the non-interacting Anderson lattice model. The interacting version of this model is used to study heavy-fermion systems. We write the Hamiltonian as

$$\mathcal{H} = \sum_{\mathbf{k}} (\epsilon_F + \epsilon_{\mathbf{k}}) |\mathbf{k}, c\rangle \langle \mathbf{k}, c| + \sum_{\mathbf{k}} \epsilon_f |\mathbf{k}, f\rangle \langle \mathbf{k}, f|$$

$$+ \sum_{\mathbf{k}} (V_{\mathbf{k}} |\mathbf{k}, f\rangle \langle \mathbf{k}, c| + V_{\mathbf{k}}^* |\mathbf{k}, c\rangle \langle \mathbf{k}, f|).$$

The states $|\mathbf{k}, c\rangle$ form a broad band of conduction electrons with a well-defined Fermi sea. The spectrum $\epsilon_{\mathbf{k}}$ is defined with respect to the Fermi energy ϵ_F . The states $|\mathbf{k}, f\rangle$

form a narrow dispersion-less band with energy ϵ_f . In the following we will assume that the two bands are well-separated with large $\epsilon_F - \epsilon_f = \Delta E$. The last two terms in the Hamiltonian represent hybridization between the bands.

The Hamiltonian is diagonal in momentum space, and it is quite elementary to diagonalize it into a low-energy and a high-energy bands. However, in the following we will apply the concept of down-folding and construct a low-energy effective theory which is entirely in terms of the conduction electrons. Since in the low-energy sector all the operators are now scalars (matrices diagonal in k-space), the down-folding is very easy. We get,

$$\mathcal{H}_{\text{eff}} = \sum_{\mathbf{k}} \delta E_{\mathbf{k}} |\mathbf{k}, c'\rangle \langle \mathbf{k}, c'|, \tag{4.36}$$

where

$$\delta E_{\mathbf{k}} = \left(1 + \frac{|V_{\mathbf{k}}|^2}{(\Delta E)^2}\right)^{-1} \left(\epsilon_{\mathbf{k}} + \frac{|V_{\mathbf{k}}|^2}{(\Delta E)}\right),\tag{4.37}$$

and $|\mathbf{k}, c'\rangle$ are the renormalized conduction electron states.

In the following we will assume that the current operator for the full theory is known and is given by $\nabla \mathcal{H}(\mathbf{k})$. Thus,

$$\mathbf{j} = \sum_{\mathbf{k}} \nabla \epsilon_{\mathbf{k}} |\mathbf{k}, c\rangle \langle \mathbf{k}, c| + \sum_{\mathbf{k}} (\nabla V_{\mathbf{k}} |\mathbf{k}, f\rangle \langle \mathbf{k}, c| + \nabla V_{\mathbf{k}}^* |\mathbf{k}, c\rangle \langle \mathbf{k}, f|). \tag{4.38}$$

Following the formalism discussed in section 4.2 we get,

$$\mathbf{j}_{\text{eff}} = \sum_{\mathbf{k}} \left(1 + \frac{|V_{\mathbf{k}}|^2}{(\Delta E)^2} \right)^{-1} \left(\nabla \epsilon_{\mathbf{k}} + \frac{1}{\Delta E} \nabla (|V_{\mathbf{k}}|^2) - \delta E_{\mathbf{k}} \frac{1}{(\Delta E)^2} \nabla (|V_{\mathbf{k}}|^2) \right) |\mathbf{k}, c'\rangle \langle \mathbf{k}, c'|.$$
(4.39)

It is also easy to check that if we do the down-folding in the presence of a vector potential then, in this example,

$$\frac{\delta \mathcal{H}_{\text{eff}}}{\delta \mathbf{A}} \bigg|_{\mathbf{A}=0} = \mathbf{j}_{\text{eff}}.$$
 (4.40)

This is due to the fact that in this example the various operators in the down-folded theory are scalars. As discussed in the previous section, in a more general case, where the low-energy theory has non-trivial matrix structure with respect to the band indices (for this the low-energy theory has to have more than one band), the above equality will not hold.

4.5 Conclusion

We identify down-folding, to linear order in the spectrum, as a formal renormalization group procedure. We construct the current operator for the low-energy theory which gives the correct matrix elements to linear order in the spectrum. We find that while down-folding in the presence of a vector potential, the operator that couples to the linear term in $\bf A$ cannot be interpreted as the current operator for the low-energy theory. In the presence of the vector potential the downfolding transformation is a function of $\bf A$, i.e., $D = D(\bf A)$. As a result the effective low-energy Hamiltonian to linear order in $\bf A$ is

$$\begin{aligned} \mathcal{H}_{\mathrm{eff}}(\mathbf{A}) &= D^{\dagger}(\mathbf{A}) \left(\mathcal{H} + \mathbf{j} \cdot \mathbf{A} \right) D(\mathbf{A}) \\ &= \mathcal{H}_{\mathrm{eff}}(0) + \left[\mathbf{j}_{\mathrm{eff}} + \frac{\delta D^{\dagger}(\mathbf{A})}{\delta \mathbf{A}} \mathcal{H} D(0) + D^{\dagger}(0) \mathcal{H} \frac{\delta D(\mathbf{A})}{\delta \mathbf{A}} \right]_{\mathbf{A} = 0} \cdot \mathbf{A}. \end{aligned}$$

We see explicitly that besides $\mathbf{j}_{\mathrm{eff}}$, there are additional operators that couple to the term linear in \mathbf{A} . We conclude that the correct procedure to obtain the current operator is the one outlined in section 4.2, and that $\mathbf{j}_{\mathrm{eff}} \neq ((\delta \mathcal{H}_{\mathrm{eff}}(\mathbf{A}))/(\delta \mathbf{A}))_{\mathbf{A}=0}$. However, one needs to understand the physical nature of the additional terms. It is possible that the additional terms are divergence-less, and therefore do not contribute to dc transport. To test this conjecture one has to study a more non-trivial example where the low-energy sector retains more than one band.

Chapter 5

Thermoelectric Behaviour of Heavy-Fermion Systems Near Magnetic Quantum Critical Point

5.1 Introduction

Understanding the behaviour of a system close to antiferromagnetic quantum critical point (QCP) is currently an area of active research. The problem is interesting both in the context of high temperature superconductors as well as heavy-fermion materials, especially to understand metallic phases that show non-Fermi liquid (NFL) properties. In recent times several materials have been discovered where it has been possible to demonstrate the existence of magnetic QCP [24, 16, 11]. This has made the problem an exciting ground where theoretical understanding of electrons with strong correlations can be verified experimentally. One central issue in this problem is an appropriate theoretical treatment of electrons interacting with spin fluctuations close to the QCP where magnetic correlation length diverges. A second central issue, is whether the spin-fermion model [25] describes the relevant degrees of freedom, or whether a more basic model, allowing for the disintegration of the binding of local moments to the quasiparticles, is necessary for describing this transition [20, 63].

In this chapter we will discuss two experimentally well-studied heavy fermion materials, $CeCu_{6-x}Au_x$ [24] and $YbRh_2Si_2$ [16], that exhibit antiferromagnetic QCP. In doped $CeCu_6$, replacing Cu with larger Au atoms, favours the formation of long range magnetic order [24]. Beyond a critical doping $x_c = 0.1$, the ground state of the system is antiferromagnetic with finite Néel temperature (T_N) [25]. At the critical doping T_N is zero and the system has a QCP. On the other hand $YbRh_2Si_2$ is undoped and

atomically well-ordered [16]. It is a much cleaner material than $CeCu_{6-x}Au_x$, with residual resistivity (ρ_0) smaller by a factor of about 10. At ambient pressure it develops long range magnetic order at a very low temperature of $T_N \simeq 65$ mK. [16] The ordering temperature can be suppressed to practically zero (less than 20 mK) by applying a magnetic field of only 45 mT [16]. Both these materials show pronounced deviations from Fermi liquid (FL) behaviour, which is believed to be due to closeness to the QCP. For instance, the dependence of electrical resistivity $\Delta \rho = \rho - \rho_0$ to temperature T is $\Delta \rho \propto T$, while that of specific heat C is $C/T \propto -\ln T$ [24, 16]. This is in contrast with FL behaviour which predicts $\Delta \rho \propto T^2$ and $C/T={
m constant.}$ The low temperature NFL behaviour is observed over a decade of temperature, up to about 1 K for $CeCu_{6-x}Au_x$ [24, 25], and up to as high as 10 K for $YbRh_2Si_2$ [16]. The source of the interesting physics in these materials is the localized 4f electrons [20] of Ce^{3+} (in $4f^1$ electronic configuration) and Yb^{3+} (in the configuration $4f^{13}$), and their interaction with the relatively delocalized s, p and d orbital electrons that form a conduction band with a well defined Fermi surface at low temperature. The conduction electrons and the localized 4f electrons carrying magnetic moment are coupled by exchange interaction (J). Below a certain critical value of exchange interaction (J_c), the local moments interact with each other, mediated by conduction electrons, and at sufficiently low temperature form long range antiferromagnetic order. On the other hand, if the exchange coupling is strong $(J > J_c)$, the local moments are quenched below a certain temperature (lattice Kondo temperature). The quenched moments hybridize with the conduction electrons and they participate in the formation of the Fermi sea. The ground state of such a system is non-magnetic. The exchange coupling is usually tuned experimentally by either doping the material or by applying external pressure or external magnetic field.

For $CeCu_{6-x}Au_x$ there are two different views [20] regarding the nature of the system in the non-ordered phase and the corresponding mechanism by which the critical instability occurs. In the first picture (Fig.5.1(a)), the lattice Kondo temperature

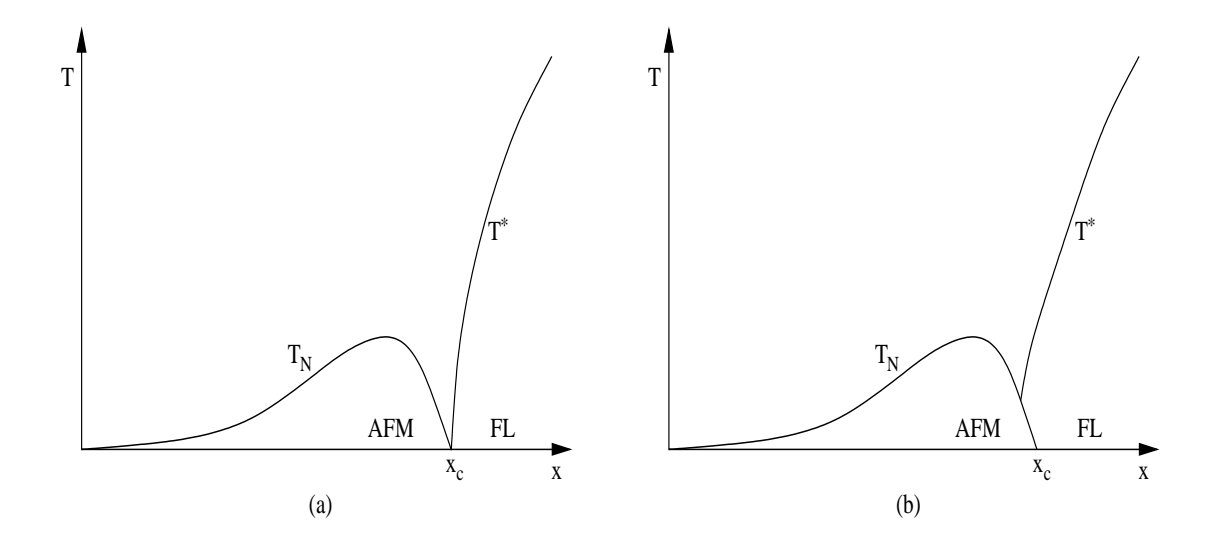


Figure 5.1: Two possible scenarios for heavy-fermion quantum criticality. T^* is the temperature below which heavy Fermi liquid forms. Local moments exist above this temperature. In (a) T^* is zero at the critical point x_c . Local moments exist down to the lowest temperature. In (b) T^* is finite at the critical point. The phase transition is by spin density wave instability of the Fermi liquid.

 (T^*) becomes zero exactly at the critical point $(J=J_c)$. The local moments of the 4f electrons survive at all finite temperature close to the critical point. At the transition point they are critically quenched. The local moments produce the critical magnetic fluctuations that destabilize the Fermi sea. It has been argued, in favour of this mechanism, that the data on magnetic susceptibility shows non-trivial scaling with temperature [64]. At the critical point the susceptibility has the scaling form $\chi = T^{-\alpha}f(\omega/T)$ with an anomalous exponent $\alpha \simeq 0.75$, which is different from conventional insulating magnets which have $\alpha=1$. The alternative picture suggests that T^* is finite at the critical point. Well below this temperature, and close to the critical point, the local moments are quenched by Kondo mechanism. The 4f electrons become part of the Fermi sea. Then, the phase transition occurs by the usual spin-density wave instability of the Fermi surface. In this picture the local moments do not play any role in the

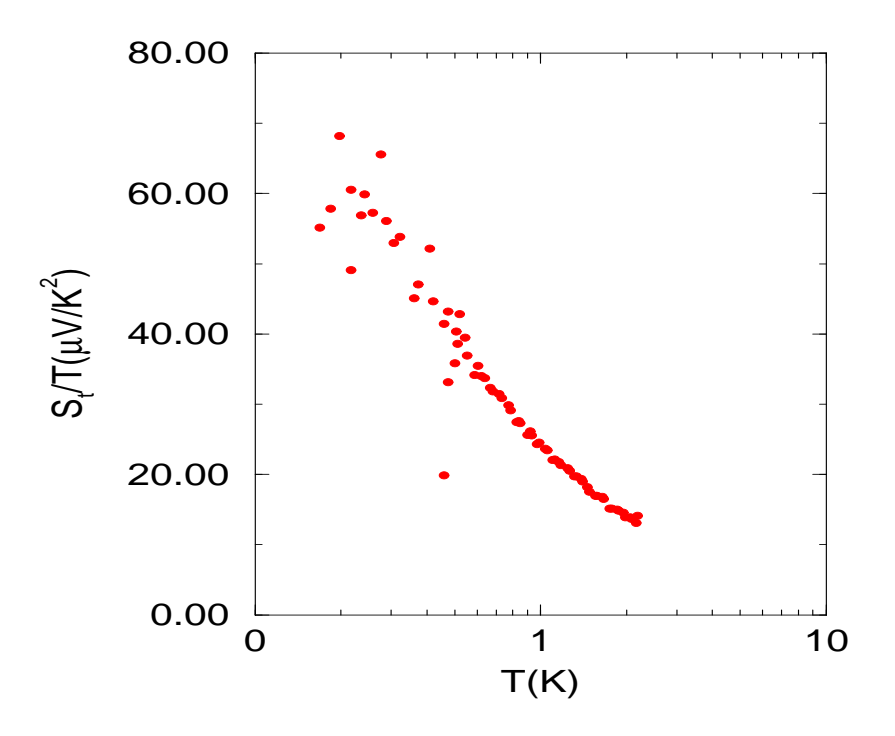


Figure 5.2: Logarithmic temperature dependence of thermopower over tempearture for $CeCu_{5.9}Au_{0.1}$. Data courtesy of C. Pfleiderer and A. Rosch.

phase transition. This theoretical viewpoint, proposed by Rosch and collaborators [25], is motivated by inelastic neutron scattering data on $CeCu_{5.9}Au_{0.1}$ which show that the nearly critical spin fluctuations are two dimensional [26]. But the origin of the quasi 2d behaviour of spin fluctuations is not well understood. However, the same feature is probably also present in $YbRh_2Si_2$, where the structure of the lattice provides a more natural explanation for the spin fluctuations to be two-dimensional [16]. Besides the nature of the magnetic correlations, there are different opinions regarding the dynamics of the spin fluctuations. It has been argued [65] that if the ordering wave-vector spans different points of the Fermi surface, then the dynamics of the spin fluctuations is overdamped, with dynamic exponent z=2. This model of spin fluctuations with d=2 and z=2, coupled with three-dimensional electrons, was used to explain the linearity of resistivity with temperature [25]. Following the method of Hertz [21, 22], in which the system is described entirely in terms of the spin fluctuations, after a formal Hubbard-Stratanovich transformation to integrate the fermion modes, it also explains

the logarithmic temperature dependence of specific heat [25, 22]. In an alternative description [66], in terms of low energy electrons interacting with spin fluctuations, it has been suggested recently that both the frequency and momentum dependence of the spin fluctuation propagator undergo singular corrections such that the propagator acquires an anomalous dimension $\eta \sim 1/4$ [67]. Thus, after nearly a decade, there is still no clear understanding regarding the appropriate model that describes the quantum phase transition.

In this chapter we will study the thermoelectric behaviour of a system in the paramagnetic phase and close to antiferromagnetic QCP. For $CeCu_{5.9}Au_{0.1}$ it is known that thermopower (S_t) has a dependence similar to specific heat over the same range of temperature [68, 69], i.e, $S_t/T \propto -\ln T$. We will show that scattering with nearly critical spin fluctuations give rise to temperature dependent quasiparticle mass (m^*) over much of the Fermi surface. The signature of this can be seen in static response (specific heat) and in transport (thermopower). Finally we will argue that the same mechanism should be relevant for $YbRh_2Si_2$, and so we expect to see the same behaviour for thermopower from future experiments.

5.2 Model

Our model is motivated by the second picture as described above. It assumes that T^* defines a high energy parameter. For $T \sim T^*$ the local nature of the spins of the 4f electrons is important as they participate in some lattice Kondo phenomenon. For $T < T^*$, the 4f electrons become part of the hybridized conduction band. In this regime the nearly critical spin fluctuations of the conduction electrons is important. It is an intermediate temperature range where the system is described by low energy conduction electrons interacting with quasi two-dimensional spin fluctuations. Within the spin-fermion description, at sufficiently low temperature, the three-dimensional nature of the spin fluctuations is retrieved and the model used here ceases to be valid.

In this regime, the model predicts, in pure systems, a crossover to an electronic Fermi liquid with a finite mass. However the physics governing this dimensional crossover, has not been investigated.

The model is described by the Hamiltonian

$$\mathcal{H} = \sum_{\mathbf{k},\sigma} \epsilon_{k} c_{\mathbf{k},\sigma}^{\dagger} c_{\mathbf{k},\sigma} + \frac{g_{0}}{2} \sum_{\mathbf{k},\mathbf{q},\alpha,\beta} c_{\mathbf{k}+\mathbf{q},\alpha}^{\dagger} c_{\mathbf{k},\beta} \boldsymbol{\sigma}_{\alpha,\beta} \cdot \mathbf{S}_{-\mathbf{q}} + \sum_{\mathbf{q}} \left[\chi^{-1}(\mathbf{q}) \mathbf{S}_{\mathbf{q}} \cdot \mathbf{S}_{-\mathbf{q}} \right] + \Pi_{\mathbf{q}} \cdot \Pi_{-\mathbf{q}} + \frac{u_{0}}{4} \sum_{\mathbf{k}_{1},\mathbf{k}_{2},\mathbf{k}_{3},\mathbf{k}_{4}} \left(\mathbf{S}_{\mathbf{k}_{1}} \cdot \mathbf{S}_{\mathbf{k}_{2}} \right) \left(\mathbf{S}_{\mathbf{k}_{3}} \cdot \mathbf{S}_{\mathbf{k}_{4}} \right) \delta(\sum_{i} \mathbf{k}_{i}).$$
(5.1)

Here $c_{\mathbf{k},\sigma}^{\dagger}$ is the electron creation operator, $\mathbf{S}_{\mathbf{q}}$ is the operator for the spin fluctuations, $\mathbf{\Pi}_{\mathbf{q}} = \partial_t \mathbf{S}_{\mathbf{q}}$ is the conjugate momentum field for the spin fluctuations, and $\chi(\mathbf{q})$ is the static magnetic susceptibility. g_0 is the bare coupling between the electrons and the spin fluctuations, and u_0 is the interaction energy of the spin fluctuations. The collective spin fluctuations are formally obtained by integrating out high energy electrons in the band up to a certain cutoff [66]. Thus the typical energies of the spin fluctuations $\omega_s \sim W$, the bandwidth of the conduction electrons. The system is close to an antiferromagnetic instability with ordering wave-vector \mathbf{Q} . We will assume that the dynamics of the spin fluctuations is purely damped with dynamic exponent z=2. The spectrum of the two-dimensional spin fluctuations will be described by [21,22]

$$\chi^{-1}(\mathbf{q},\omega) = \delta + \omega_s(\mathbf{q} - \mathbf{Q})_{\parallel}^2 - i\gamma |\omega|.$$
 (5.2)

Here δ is the mass of the spin fluctuations and measures the deviation from the QCP, the parallel directions are those along the planes of magnetic correlation, and $\gamma \sim (g_0/\epsilon_F)^2$ is an estimate of the damping from the polarization bubble. In the spin fluctuation part of the Hamiltonian, the interaction term u_0 is marginal, since the scaling dimension is zero [21, 22]. The main contribution of this term is to renormalize the mass of the spin fluctuations (δ) and make it temperature dependent. Within a Gaussian approximation, δ is linearly dependent on temperature, up to logarithmic corrections [25, 22]. We will ignore other effects of the u_0 term in our discussion, and will consider only the quadratic term with temperature dependent mass of the spin fluctuations. To simplify

the calculation we will assume a spherical Fermi surface for the non-interacting electrons, with the ordering wave-vector $\mathbf{Q} = (\alpha, 0, 2k_F \cos \theta_0)$. Here $\theta_0 \neq 0$ (i.e. not $2k_F$ ordering), and $\theta_0 \neq \pi/2$ (i.e. not ferromagnetic ordering). We have chosen $\hat{\mathbf{x}}$ as the direction along which the spin fluctuations are uncorrelated, and α , the ordering in the x-direction, varies from one plane of magnetic correlation to another. Since the spectrum of spin fluctuations is two-dimensional, those carrying momentum of the form $\mathbf{Q} + a\hat{\mathbf{x}}$, where a is arbitrary, are all nearly critical. Due to constraints from energymomentum conservation, only those points on the Fermi surface that are connected by the nearly critical spin fluctuations are particularly sensitive to the QCP, since electrons at these points undergo singular scattering with the spin fluctuations. These are the so-called "hot spots". It is important to note that since the spin fluctuations are two-dimensional, there will be a finite area of the Fermi surface that is hot. Though it is worthwhile to estimate the fraction of the Fermi surface that is hot, theoretically it is a daunting task. In our calculation we will assume that most of the Fermi surface is hot. In effect, we are assuming that contribution to static response and also to transport is mostly from the hot regions. It was pointed out by Hlubina and Rice [70] that in transport the hot carriers are less effective than the cold ones. This is because the quasiparticle lifetime of the hot carriers is less than that of the cold carriers, since the former suffer enhanced scattering with the spin fluctuations. As we will show below, the lifetime of the hot electrons $\tau_h \propto 1/T$, while the cold electrons have Fermi liquid characteristics with $\tau_c \propto 1/T^2$. If x is the fraction of the Fermi surface (FS) that is hot, then we can make an estimate of conductivity σ ,

$$\sigma \propto \langle \tau_{\mathbf{k}} \rangle_{\mathrm{FS}} \propto \frac{x}{T/\epsilon_F} + \frac{1-x}{(T/\epsilon_F)^2}.$$

The first term, which is the contribution from the hot region, will dominate to give $\Delta \rho \propto T$ only if $x > 1/(1 + T/\epsilon_F)$. This gives a rough estimate of the fraction necessary for the hot carriers to dominate. In the case of $\text{CeCu}_{6-x}\text{Au}_x$, which is a dirtier material, the above estimation is more involved. It was recently shown [71] that the effect of disorder is to favour isotropic scattering and thereby reduce the effectiveness of

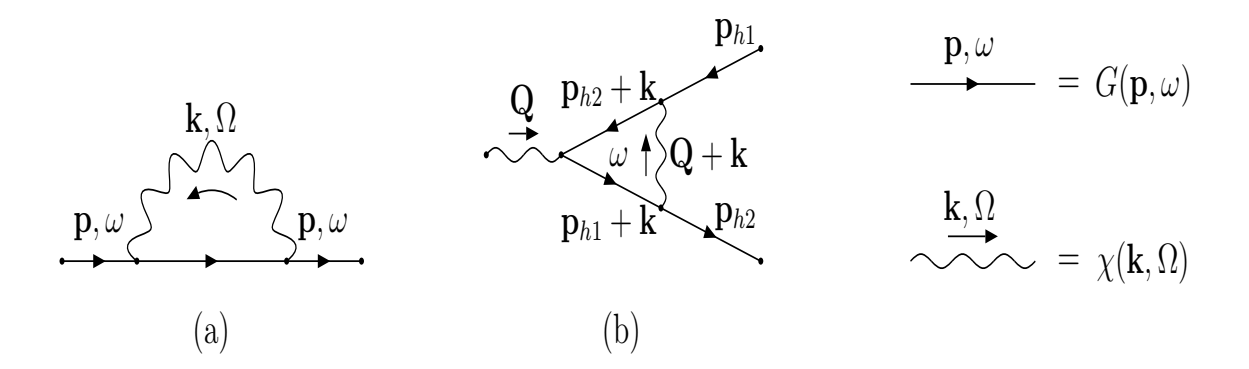


Figure 5.3: Lowest order (a) electron self-energy and (b) spin-fermion vertex correction. For the vertex external frequency has been set to zero.

Hlubina-Rice mechanism. Thus, one should expect a smaller fraction, than estimated above, enough to make the contribution of the hot carriers significant for $CeCu_{6-x}Au_x$.

5.3 Spin-Fermion Vertex and Electron Self-Energy

We will first examine the lowest order correction to the spin-fermion vertex (Fig.5.3(b)). The main purpose of this exercise will be to demonstrate that at the QCP ($\delta \to 0$) the corrections to the vertex is not singular. This is important because otherwise our perturbative calculation will break down at low temperature near the QCP. With a singular vertex, the coupling constant between the electrons and the spin fluctuations will get strongly renormalized at low energy. The qualitative features of the theory will change, in particular the electron self-energy. We will express the lowest order correction to the bare spin-fermion coupling as $g = g_o(1 + \Gamma)$. Since we are interested only in the hot electrons and their low energy interaction with the spin fluctuations, we will calculate

the vertex Γ with zero external frequency. The expression for the vertex is given by,

$$\Gamma = ig_0^2 \sum_{\mathbf{k}} \int_{-\infty}^{\infty} \frac{d\omega}{2\pi} G(\mathbf{p}_1 + \mathbf{k}, \omega) G(\mathbf{p}_2 + \mathbf{k}, \omega) \chi(\mathbf{Q} + a\hat{\mathbf{x}} + \mathbf{k}, \omega).$$
 (5.3)

Here \mathbf{p}_1 and \mathbf{p}_2 are two hot points that are connected by wave-vector $\mathbf{Q} + a\hat{\mathbf{x}}$ and $G(\mathbf{p}, \omega)$ is the free electron propagator given by,

$$G(\mathbf{p},\omega) = \frac{n_p}{\omega - \epsilon_p - i\eta} + \frac{1 - n_p}{\omega - \epsilon_p + i\eta}.$$
 (5.4)

Here n_p is the electron occupation of the momentum state \mathbf{p} at T=0. It is convenient to use the spectral representation of the spin fluctuation propagator

$$\chi(\mathbf{k},\omega) = \int_0^\infty \frac{d\Omega}{\pi} \text{Im} \chi(\mathbf{k},\Omega) \frac{2\Omega}{\Omega^2 - \omega^2 - i\eta}.$$
 (5.5)

The ω -integral is now stright-forward. We get

$$\Gamma = g_0^2 \sum_{\mathbf{k}} \int_0^\infty \frac{d\Omega}{\pi} \frac{2\Omega^2}{\gamma_{\mathbf{Q}+\mathbf{k}}^2 + \Omega^2} \left\{ \frac{\theta(-\epsilon_{1\mathbf{k}})}{(\epsilon_{1\mathbf{k}} - \epsilon_{2\mathbf{k}})(\epsilon_{1\mathbf{k}} - \Omega)(\epsilon_{1\mathbf{k}} + \Omega)} + \frac{\theta(-\epsilon_{2\mathbf{k}})}{(\epsilon_{2\mathbf{k}} - \epsilon_{1\mathbf{k}})(\epsilon_{2\mathbf{k}} - \Omega)(\epsilon_{2\mathbf{k}} + \Omega)} - \frac{1}{2\Omega(\Omega + \epsilon_{1\mathbf{k}})(\Omega + \epsilon_{2\mathbf{k}})} \right\}.$$

In the above equation $\gamma_{\mathbf{k}} = \delta + \omega_s (\mathbf{k} - \mathbf{Q})_{\parallel}^2$, and $\epsilon_{1\mathbf{k}}$, $\epsilon_{2\mathbf{k}}$ are the fermionic spectra near the two hot points \mathbf{p}_1 and \mathbf{p}_2 respectively. The linearized spectra can be expressed as $\epsilon_{1\mathbf{k}} = v_{1i}k_i + v_{1j}k_j$ and $\epsilon_{2\mathbf{k}} = v_{2i}k_i + v_{2j}k_j$, where (k_i, k_j) are co-ordinate axes in the plane defined by the centre of the Fermi sphere and the two hot points. The k-sum can now be simplified by expressing all the terms in the quadrant defined by $\epsilon_{1\mathbf{k}}$, $\epsilon_{2\mathbf{k}} > 0$. After some algebra we get

$$\Gamma = 4g_0^2 \sum_{\mathbf{k}, \atop \epsilon_{1\mathbf{k}}, \epsilon_{0\mathbf{k}} > 0} \int_0^\infty \frac{d\omega}{\pi} \frac{\omega^2}{\left(\gamma_{\mathbf{Q}+\mathbf{k}}^2 + \omega^2\right) \left(\epsilon_{1\mathbf{k}} + \epsilon_{2\mathbf{k}}\right) \left(\omega + \epsilon_{1\mathbf{k}}\right) \left(\omega + \epsilon_{2\mathbf{k}}\right)}.$$
 (5.6)

It is easy to check by simple dimensional analysis that as $\delta \to 0$, the above expression is finite. As an estimate we get $\Gamma \propto g_0^2 \Lambda^{1/2}/(\epsilon_F^{3/2} \omega_s^{1/2})$, where Λ is a dimensionless cutoff in the momentum space.

Next, in order to calculate the effect of the low energy spin fluctuations on the hot electrons, we will examine the electron self-energy. The lowest order term (Fig.5.3(a))

in perturbation gives

$$\Sigma(\mathbf{p},\omega) = -g_0^2 \sum_{\mathbf{k}} \int_{-\infty}^{\infty} \frac{d\Omega}{2\pi i} \, \chi(\mathbf{k},\Omega) \, G(\mathbf{p} + \mathbf{k}, \omega + \Omega) \,. \tag{5.7}$$

As expected, the above expression has different behaviours in the hot and cold regions. But within each region the self-energy is practically momentum independent. The imaginary part of the self-energy gives the quasiparticle lifetime as determined by scattering with the spin fluctuations. For $\omega > 0$ we have,

$$\operatorname{Im}\Sigma\left(\mathbf{p},\omega\right) = -g_0^2 \sum_{0 < \epsilon_k < \omega} \frac{(\omega - \epsilon_{\mathbf{k}+\mathbf{p}})}{\gamma_{\mathbf{k}}^2 + (\omega - \epsilon_{\mathbf{k}+\mathbf{p}})^2}.$$
 (5.8)

If \mathbf{p} is a point in the hot region, then it is connected to another hot spot by a wave-vector of the form $\mathbf{k} = \mathbf{Q} + a\hat{\mathbf{x}}$. We linearize the spectrum about this second hot point, and perform the integral in terms of local coordinates around it. In the hot region we get,

Im
$$\Sigma(\mathbf{p},\omega) \propto -\left(\frac{g_0^2}{\epsilon_F \omega_s}\right) \frac{\omega^2}{\max[\delta,\omega]}$$
. (5.9)

For $\omega > \delta$ the lifetime of the hot electrons is much smaller than that given by Fermi liquid behaviour (Im $\Sigma(\omega) \propto \omega^2$). As we have mentioned above, this is due to more effective scattering with the spin fluctuations in this region. For the cold electrons the behaviour is Fermi liquid like.

Next, we will examine the real part of the self-energy. The dependence of $\mathrm{Re}\Sigma$ on frequency is more important than the dependence on momentum. We get,

$$-\lim_{\omega \to 0} \frac{\partial}{\partial \omega} \operatorname{Re}\Sigma(\mathbf{p}, \omega) = \frac{g_0^2}{\pi} \sum_{\mathbf{k}} \left\{ \frac{1}{\gamma_{\mathbf{k}}^2 + \epsilon_{\mathbf{k}+\mathbf{p}}^2} - \frac{\left(\gamma_{\mathbf{k}}^2 - \epsilon_{\mathbf{k}+\mathbf{p}}^2\right)}{\left(\gamma_{\mathbf{k}}^2 + \epsilon_{\mathbf{k}+\mathbf{p}}^2\right)^2} \ln \left| \frac{\gamma_{\mathbf{k}}}{\epsilon_{\mathbf{k}+\mathbf{p}}} \right| + \frac{\pi (2n_{\mathbf{k}+\mathbf{p}} - 1)\gamma_{\mathbf{k}}\epsilon_{\mathbf{k}+\mathbf{p}}}{\left(\gamma_{\mathbf{k}}^2 + \epsilon_{\mathbf{k}+\mathbf{p}}^2\right)^2} \right\}.$$
(5.10)

If **p** is a point within the hot region, each of the three terms in the above expression is logarithmic. As before, after linearizing the spectrum near the second hot spot, we get,

$$-\lim_{\omega \to 0} \frac{\partial}{\partial \omega} \operatorname{Re}\Sigma\left(\mathbf{p}, \omega\right) \propto \left(\frac{g_0^2}{\pi \epsilon_F \omega_s}\right) \ln\left(\frac{\omega_s}{\delta}\right). \tag{5.11}$$

Due to scattering, the non-interacting electron mass m is renormalized to the quasiparticle mass $m^*=m/Z$ (in the absence of any momentum dependence of the electron self-energy), where

$$Z^{-1} = 1 - \lim_{\omega \to 0} \frac{\partial}{\partial \omega} \text{Re} \Sigma (\mathbf{p}, \omega)$$
 (5.12)

defines the quasiparticle residue. Since δ , which measures the deviation from the critical point, can be written as $\delta = \Gamma(p-p_c) + T$, the quasiparticle mass becomes temperature dependent. Here p is an experimental parameter that can be tuned to the critical value p_c , and Γ is an appropriate energy parameter. As a consequence the entropy of each hot quasiparticle becomes anomalously large. This can be seen from the expression for entropy (S) per particle, [72]

$$\frac{S}{N} = \sum_{\mathbf{p}} \frac{1}{\pi T} \int_{-\infty}^{\infty} d\omega \left(-\frac{\partial f}{\partial \omega} \right) \omega \tan^{-1} \left(\frac{\tau(\omega)}{\epsilon_p - \omega/Z} \right).$$

Here $f(\omega)$ is the Fermi function, and $\tau(\omega)$ is quasiparticle lifetime obtained from the inverse of imaginary part of self energy. From the above expression it is easy to see that $S/N \propto 1/Z$. Over the hot region, keeping only the leading term, $Z^{-1} \sim \ln(1/\delta)$. Then,

$$S/N \propto \mathcal{N}(0)T\left(\frac{g_0^2}{\epsilon_F \omega_s}\right) \ln\left(\frac{\omega_s}{\delta}\right),$$
 (5.13)

where $\mathcal{N}(0)$ is the density of states of the non-interacting system at the Fermi energy. For $T > \Gamma(p-p_c)$, the temperature dependence of entropy is $S \propto T \ln(1/T)$, which is different from Fermi liquid behaviour $(S \propto T)$. This gives rise to the anomalous logarithmic temperature dependence of specific heat. In the past [22,25] this behaviour has been understood from a purely bosonic point of view following the formalism of Hertz and Millis. For the spin fluctuations the Gaussian part of the action gives a free energy $F \propto T^2 \ln T$, which explains the $\ln(1/T)$ behaviour of C/T. Thus, here we find that there is agreement between the results of the spin-fermion model and the pure bosonic model.

5.4 Thermopower

From our discussion on entropy, it is natural to expect that this entropy enhancement should be seen in the measurement of thermopower (S_t) . This is because one can think of thermopower as proportional to the correlation function between the heat current and the particle current, and heat current involves the transport of entropy due to temperature and electric potential gradients in the system. Strictly speaking, thermopower is defined as a ratio of two correlation functions [55], i.e,

$$S_t = \frac{L_{12}}{eTL_{11}},$$

where

$$L_{12} = \lim_{\omega \to 0} \frac{1}{\omega V} \operatorname{Im} \int_0^\beta d\tau e^{i\omega\tau} \langle T_\tau \mathbf{j}_Q(\tau) \cdot \mathbf{j}(0) \rangle,$$

is the correlation function between heat current (\mathbf{j}_Q) and particle current (\mathbf{j}) , and

$$L_{11} = \lim_{\omega \to 0} \frac{1}{\omega V} \operatorname{Im} \int_0^\beta d\tau e^{i\omega \tau} \langle T_\tau \mathbf{j}(\tau) \cdot \mathbf{j}(0) \rangle,$$

is the correlation function between particle currents. L_{11} is a measure of electrical conductivity ($\sigma=e^2L_{11}$). Here we are ignoring the tensor nature of L_{11} and L_{12} , and assuming that temperature and potential gradients and the thermal current are along the major symmetry directions of the lattice so that the tensors are diagonal. We express the single particle energies with respect to the chemical potential and assume that chemical potential in the sample is uniform. The expression for heat current is given by,

$$\mathbf{j}_{Q} = \frac{i}{2} \sum_{\mathbf{p},\sigma} \mathbf{v}_{\mathbf{p}} \left(c_{\mathbf{p},\sigma}^{\dagger} \dot{c}_{\mathbf{p},\sigma} - \dot{c}^{\dagger}_{\mathbf{p},\sigma} c_{\mathbf{p},\sigma} \right).$$

In principle, heat current will have additional terms (see Eq.(3.14)). However, such terms are quartic in fermionic operators and generate only subleading contributions in our calculation. We will also ignore corrections to the particle current and heat current vertices due to exchange of spin fluctuations. These vertex corrections are nonsingular, and change only the numerical prefactor (which we do not attempt to calculate) of our leading term, because the spin fluctuations are peaked around a finite wave-vector.

We note that neglecting the vertex corrections for the transport coefficients is justified rigorously in the limit of infinite dimension (see Sec.(3.4)). With these approximations the expressions for the correlation functions can be re-expressed in a more transparent form as

$$L_{12} = \sum_{\mathbf{p}} v_{\mathbf{p}}^2 \int_{-\infty}^{\infty} d\omega \left(-\frac{\partial f}{\partial \omega}\right) \omega A^2(\mathbf{p}, \omega),$$

$$L_{11} = \sum_{\mathbf{p}} v_{\mathbf{p}}^2 \int_{-\infty}^{\infty} d\omega \left(-\frac{\partial f}{\partial \omega}\right) A^2(\mathbf{p}, \omega).$$

Here $\mathbf{v_p} = \partial \epsilon_p / \partial \mathbf{p}$ is the quasiparticle velocity, and $A\left(\mathbf{p}, \omega\right)$ is the spectral function defined as

$$A(\mathbf{p}, \omega) = \frac{\tau(\omega)^{-1}}{\left(\frac{\omega}{Z} - \epsilon_p\right)^2 + \tau(\omega)^{-2}}.$$

The evaluation of L_{11} is more straightforward and we will examine it first. The momentum sum can be converted into an integral over various energy surfaces. The dominant contribution is from close to the Fermi level, and we get

$$L_{11} = v_F^2 \mathcal{N}(0) \int_{-\infty}^{\infty} d\omega \left(-\frac{\partial f}{\partial \omega}\right) \tau(\omega).$$

We have already noted that over the hot region $\tau(\omega) \propto \omega^{-1}$. For the frequency integral since $\omega \sim T$, we get

$$L_{11} \propto \left(\frac{\epsilon_F \omega_s}{q_0^2}\right) \frac{v_F^2 \mathcal{N}(0)}{T}.$$
 (5.14)

This result [24, 25] simply reiterates what we had noted before, that when the hot carriers dominate transport, $\Delta\sigma\propto 1/T$. Now for L_{12} , we first notice that the expression is odd in frequency. This is because L_{12} is a measure of particle-hole asymmetry in the system. In our calculation we will consider as phenomenological input two different sources of such asymmetry. One such source is from the density of states, so that $\mathcal{N}(\omega) = \mathcal{N}(0) + \omega \mathcal{N}'(0) + O(\omega^2/\epsilon_F^3)$, where $\mathcal{N}'(0) \neq 0$ only if there is particle-hole asymmetry in the bare non-interacting system of electrons. The second source of asymmetry will be from the quasiparticle lifetime which, for the hot carriers, we write as $\tau^{-1}(\omega) = (g_0^2/\epsilon_F\omega_s) |\omega| (1 + \tau\omega)$. Here the second term is a possible particle-hole

asymmetric term in scattering lifetime. τ is a typical scattering time, and $\omega < \tau^{-1}$. After the energy integral around the Fermi surface we get,

$$L_{12} = v_F^2 \int_{-\infty}^{\infty} d\omega \left(-\frac{\partial f}{\partial \omega}\right) \omega \tau(\omega) \mathcal{N}(\omega/Z)$$

$$= \left(\frac{\epsilon_F \omega_s}{g_0^2}\right) v_F^2 \left\{T \mathcal{N}'(0)/Z + T \mathcal{N}(0)\tau\right\}. \tag{5.15}$$

The first term in the above equation is from the asymmetry in density of states, and the second term is from the asymmetry in quasiparticle lifetime. We note that the factor of 1/Z, which leads to entropy enhancement, is associated with the asymmetry in density of states. Thus, the first term is the dominant one and eventually gives anomalous temperature dependence to thermopower. For this leading term we can write

$$S_t \propto \frac{1}{e} \left(\frac{g_0^2 \mathcal{N}'(0)}{\epsilon_F \omega_s \mathcal{N}(0)} \right) T \ln(\omega_s/\delta).$$
 (5.16)

In the regime where $T > \Gamma(p-p_c)$, $S_t/T \propto \ln(1/T)$, as has been observed [68,69] in thermopower measurement on $\text{CeCu}_{6-x}\text{Au}_x$ (see Fig5.2).

5.5 Conclusion

To check the consistency of our model and calculation, we need to estimate the high energy scale (namely, T^*) of $CeCu_{5.9}Au_{0.1}$. For this purpose, we have fitted an approximate form of the free energy function (F) that will match with the experimental results at low temperature and in the presence of magnetic field (H). The function that matches well with the experiment has the form,

$$F(T,H)/k_B = X(T,H) \ln \left[2 \cosh \left(\frac{\mu \lambda H}{Y(T,H)} \right) \right],$$
 (5.17)

where

$$X(T,H) = T^* + C_1 \left(\frac{T^2}{T^*}\right) - C_2 \left(\frac{T^2}{T^*}\right) \ln(T^2 + C_3 H^2),$$

$$Y(T,H) = T^* + (T^2 + C_3 H^2)^{1/2}.$$

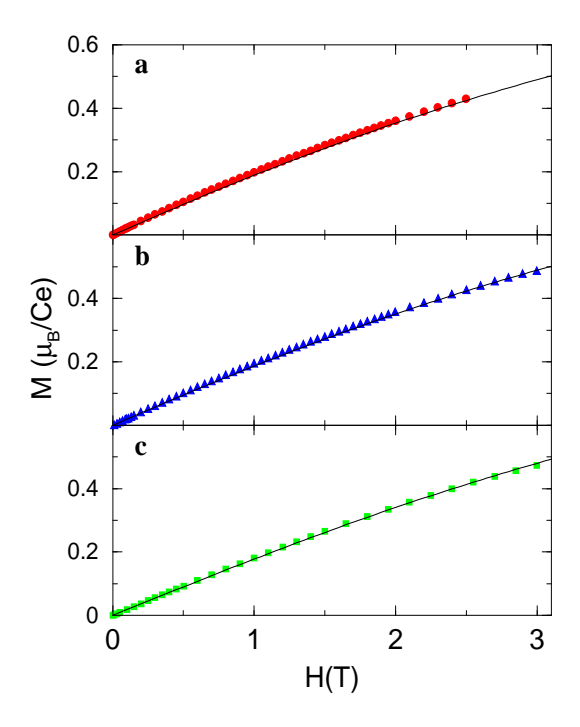


Figure 5.4: Magnetization (M) vs external magnetic field (H) at different temperatures : a) T=0.15K, b) T=0.3K and c) T=0.8K. The discrete points are experimental. The solid lines are fits using equation (10).

Here C_1 - C_3 are parameters of the fitting function, μ is the effective magnetic moment of the Ce³⁺ ions in units of Bohr magneton (μ_B) and $\lambda = \mu_B/k_B = 0.67$. We have chosen a simple possible form of the free energy which, at low temperatures ($T \ll T^*$), is consistent with the critical form of free energy that is suggested by renormalization group calculation for two-dimensional spin fluctuations [22], namely $F \propto T^2 \ln(T_0/T)$. At high temperatures ($T \gg T^*$) it matches smoothly to an impurity model where the 4f cerium electrons act as Kondo impurities. The uniform magnetic susceptibility in this regime is Curie-Weiss like, with $\chi(T) \propto \mu^2/T$. This temperature dependence is cut-off at T^* , below which $\chi \sim \mu^2/T^*$, down to zero temperature. The fitting function is chosen such that at very low temperature ($T \to 0$), $\chi(T) - \chi(0) \propto -T$. [73] This limiting behaviour agrees with the form $\chi \approx a_0 + 1/(a_1 + a_2T)$ which Rosch et. al. [25] used to fit susceptibility data up to 1.4 K. We also find that susceptibility derived from equation (10) can describe reasonably well (with a difference of at most twenty percent) the data [64] up to 6 K. The

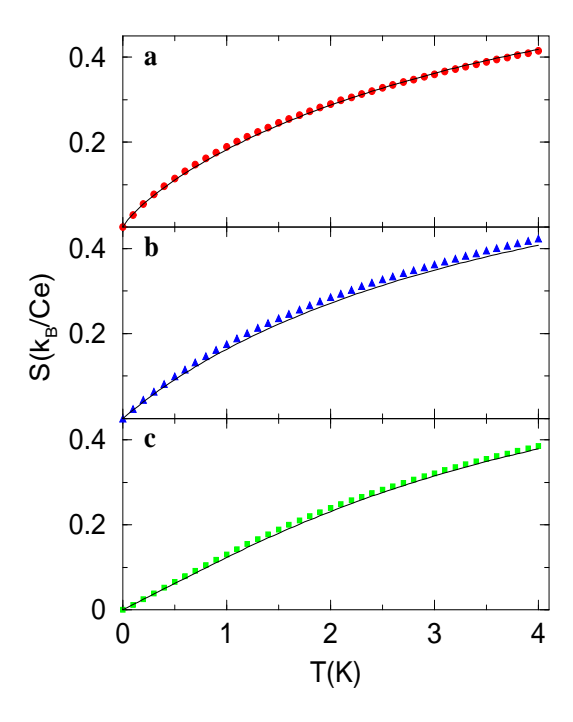


Figure 5.5: Entropy (S) per Ce atom vs temperature (T) at different magnetic fields: a) H=0T, b) H=1.5T and c) H=3T. The discrete points are experimental, obtained by numerically integrating data from specific heat measurement. The solid lines are fits using equation (10).

variation of entropy and magnetization as functions of temperature and magnetic field that one expects from the above free energy matches well with the experiments (see Figs.(5.4), (5.5)). From the fit we estimate T^* to be around 15 K, and $\mu \sim 2.6$. In the absence of magnetic field the specific heat coefficient ($\gamma = C/T$) can be written as $\gamma = a \ln(T_0/T)$. From the fit we estimate a = 0.5 J/mol-K² and $T_0 = 9.4$ K, which have comparable order of magnitudes with the experimentally measured values a = 0.6 J/mol-K² and $T_0 = 5.3$ K [24]. The logarithmic behaviour in specific heat and thermopower in $CeCu_{6-x}Au_x$ is observed around 1 K, which is well below T^* . The experimental fits and the estimates suggest that the spin-fermion model that we have been considering is consistent with the experimental data.

We now discuss the limitations of our calculation. We have completely ignored the interaction between the spin fluctuations (the u_0 term). This is justified since this term is marginally irrelevant. In our calculation we considered only the lowest order diagram

in the perturbation series in terms of the spin-fermion coupling. However, we have examined the lowest order spin-fermion vertex correction, and found that it is well-behaved close to the QCP. So we believe that the qualitative features of our calculation will not be modified by including higher order terms of the series. This is very different from what is found in the two-dimensional spin-two-dimensional fermion model (see appendix), where the spin-fermion vertex is singular indicating a potential breakdown of the approach [66]. So, if the 2d-spin 3d-fermion model breaks down, there is no trace of this breakdown in perturbation theory.

From our calculation we see that irrespective of whether the system is clean or dirty, if there is a large enough hot region in the system, then both specific heat and thermopower should show anomalous logarithmic temperature dependence.

Since the microscopic origin of the quasi two-dimensionality of the spin fluctuations is not known, our model seem to be a fine tuned one rather than one that is expected intuitively. It would be interesting to investigate the origin of the two-dimensional magnetic coupling, and why most of the Fermi surface is hot by means of microscopic first principles calculations. This study should be supplemented by an investigation of the two- to three- dimensional crossover, to estimate the energy scale at which it is expected to occur. We notice that specific heat and resistivity measurements on YbRh₂Si₂ [16] seem to indicate that the model, with most of the Fermi surface hot, is quite valid for it. From this we can conclude that we expect to see the behaviour $S_t/T \propto \ln(1/T)$ from thermopower measurement on YbRh₂Si₂, probably over a wider range of temperatures than the Ce-material.

In very recent times a rather anomalous behaviour of the specific heat coefficient of YbRh₂SI₂ has been reported. Between $0.3K \le T \le 10K \ \gamma(T) \sim \ln(1/T)$ which, as discussed above, can be understood within our model. However at lower temperature $(T_N < T < 0.3K) \ \gamma$ shows an unexpected upturn. In this regime $\gamma \sim T^{-1/3}$. Currently there is no proper understanding of the origin of this behaviour. Neither can it be understood within the framework of the spin fluctuation theory in its current

formulation. In the absence of a satisfying theory we will speculate what this upturn could imply for the thermopower of YbRh₂SI₂ in this same temperature range. We will interpret the upturn of the specific heat as an indication that the self-energy of the electrons is more singular (due to some mechanism which is not yet understood) than what was calculated in Sec.(5.3), and now has the form $\Sigma(\omega) \sim \omega^{2/3}$. This would imply that the quasiparticle residue $Z^{-1} \propto T^{-1/3}$ for fermions close enough to the Fermi surface. Then, following the same line of reasoning as before we will conclude that thermopower should show the same temperature dependence as specific heat, i.e., $S_t/T \propto T^{-1/3}$. This is because in our line of reasoning the non-analytic behaviour of thermopower is entirely thermodynamic in origin. It is possible, though, that in this regime of lower temperature the hot quasiparticles will be short-circuited by the normal carriers. But such a situation would be reflected in the temperature dependence of resistivity. Since in the range $T_N < T < 0.3K$ the resistivity $\rho \sim T$, the possibility of short-circuiting can be ruled out.

Appendix A

DMFT Equations for the Hubbard Model

Here we will discuss a functional integral formulation of DMFT for the Hubbard model defined in Eq.(1.8). We consider $c_{0,\sigma}^{\dagger}$ and $c_{0,\sigma}$ as an impurity degrees of freedom at the site \mathbf{R}_0 interacting with a bath which is made up of the degrees of freedom on the remaining lattice site. In the limit of infinite dimensions one can show that the bath degrees of freedom can be integrated out to get an effective impurity action in imaginary time (τ) of the form

$$S_{\text{eff}} = -\int_0^\beta d\tau \int_0^\beta d\tau' \sum_{\sigma} c_{0,\sigma}^{\dagger}(\tau) \mathcal{G}_0^{-1}(\tau - \tau') c_{0,\sigma}(\tau') + U \int_0^\beta d\tau n_{0\uparrow}(\tau) n_{0\downarrow}(\tau). \quad (A.1)$$

Here $\beta=1/(k_BT)$ is the inverse temperature. $\mathcal{G}_0(\tau-\tau')$ acts as the effective Weiss field for the impurity. It gives the amplitude for an electron to hop on the impurity site from the bath at time τ and to return to the bath at time τ' . We define the Green's function of the effective action as

$$G(\tau) = -\langle T_{\tau}c(\tau)c^{\dagger}(\tau)\rangle_{S_{\text{eff}}},\tag{A.2}$$

and its Fourier transform $G(i\omega_n)$ in terms of fermionic Matsubara frequencies $\omega_n=(2n+1)\pi/\beta$. In the above equation T_τ is the imaginary time ordering operator. From the discussion in Sec.(1.1) it is clear that the Fourier transform of the one-particle Green's function $G_{ij}(\tau)=-\langle T_\tau c_{i,\sigma}(\tau)c_{j,\sigma}^\dagger(\tau)\rangle$ of the lattice theory has the form

$$G(\mathbf{k}, i\omega_n) = \frac{1}{i\omega_n + \mu - \epsilon_{\mathbf{k}} - \Sigma(i\omega_n)}.$$
 (A.3)

Here μ is the chemical potential, $\epsilon_{\mathbf{k}} = -2t \sum_{i} \cos(k_i)$, and $\Sigma(i\omega_n)$ is the self-energy which is momentum independent. One can show that the lattice theory can be mapped

to $S_{\rm eff}$ by the condition

$$\Sigma(i\omega_n) = \mathcal{G}_0^{-1}(i\omega_n) - G^{-1}(i\omega_n). \tag{A.4}$$

The above equation ensures that the local Green's function $G_{ii}(i\omega_n) = \sum_{\mathbf{k}} G(\mathbf{k}, i\omega_n)$ coincides with $G(i\omega_n)$. The above set of equations can now be solved self-consistently. We start with an initial guess for $\Sigma(i\omega_n)$. Then the local Green's function $G(i\omega_n)$ can be calculated by momentum summation of $G(\mathbf{k}, i\omega_n)$ given by Eq.(A.3). In the next step the Weiss field $\mathcal{G}_0(i\omega_n)$ can be calculated using Eq.(A.4). This gives complete information of $S_{\rm eff}$ which will allow us to calculate the local Green's function using Eq.(A.2). Finally, using Eq.(A.4) one gets a new expression for the self-energy. This procedure can be iterated till convergence is achieved.

Appendix B

Mathematical Preliminary

In this appendix we will review some familiar concepts of linear algebra which we will express in the language of a non-orthogonal basis. We will discuss the representation of abstract operators, and the appropriate definition of the trace of an operator in a non-orthogonal basis. We will also discuss unitary and non-unitary transformations from one set of basis to another. Finally we will express a second quantized Hamiltonian in a non-orthogonal basis.

We consider a non-orthogonal set of states $\{|\alpha\rangle\}$ that spans a linear vector space (which means the states are linearly independent). We will regard the states $\{|\alpha\rangle\}$ as defining a non-orthogonal basis for the vector space. The overlap between the basis states is given by the overlap matrix $O_{\alpha\beta} \equiv \langle \alpha|\beta\rangle$. In principle, one can construct an orthonormal basis, say $\{|i\rangle\}$, from the states $\{|\alpha\rangle\}$ by the Gram-Schmidt method. Here we will assume that there exists a transformation S connecting the two bases such that

$$|i\rangle = \sum_{\alpha} S_{\alpha i} |\alpha\rangle$$
 and $\langle i| = \sum_{\alpha} S_{\alpha i}^* \langle \alpha| = \sum_{\alpha} S_{i\alpha}^{\dagger} \langle \alpha|.$ (B.1)

We note that, by definition, the transformation S is non-unitary. Since

$$\delta_{ij} = \langle i|j\rangle = \sum_{\alpha\beta} S_{i\alpha}^{\dagger} \langle \alpha|\beta\rangle S_{\beta j} = \sum_{\alpha\beta} S_{i\alpha}^{\dagger} O_{\alpha\beta} S_{\beta j}, \tag{B.2}$$

we find the overlap matrix is given by

$$O = \left(SS^{\dagger}\right)^{-1}.\tag{B.3}$$

As an example, by using the above equation we find that the representation of the

identity operator in the non-orthogonal basis is given by

$$\hat{I} = \sum_{i} |i\rangle\langle i| = \sum_{i\alpha\beta} S_{\alpha i} |\alpha\rangle S_{i\beta}^{\dagger} \langle\beta| = \sum_{\alpha\beta} O_{\alpha\beta}^{-1} |\alpha\rangle\langle\beta|.$$
 (B.4)

The matrix elements of an abstract operator \hat{A} in the two bases are related by

$$A_{ij} \equiv \langle i|\hat{A}|j\rangle = \sum_{\alpha\beta} S_{i\alpha}^{\dagger} \langle \alpha|\hat{A}|\beta\rangle S_{\beta j} = \sum_{\alpha\beta} S_{i\alpha}^{\dagger} A_{\alpha\beta} S_{\beta j}.$$
 (B.5)

We get back Eq. (B.2) if \hat{A} is the identity operator.

In an orthogonal basis the trace of an operator is given by $\operatorname{Tr}(\hat{A}) = \sum_i A_{ii}$, i.e., the sum of the diagonal terms of the matrix representation of the operator. However, this is not the case in a non-orthogonal basis. In fact, $\sum_i A_{ii} \neq \sum_{\alpha} A_{\alpha\alpha}$. In a non-orthogonal basis the trace is given by,

$$\operatorname{Tr}(\hat{A}) = \sum_{i} \langle i | \hat{A} | i \rangle = \sum_{i \alpha \beta} S_{i \alpha}^{\dagger} \langle \alpha | \hat{A} | \beta \rangle S_{\beta i} = \sum_{\alpha \beta} O_{\alpha \beta}^{-1} A_{\beta \alpha}. \tag{B.6}$$

In particular we have $Tr(\hat{I}) = n$, where n is the dimensionality of the vector space. Using Eqs. (B.4) and (B.6) we recover the familiar result

$$\operatorname{Tr}(\hat{A}\hat{B}) = \sum_{\alpha\beta} O_{\alpha\beta}^{-1} \langle \beta | \hat{A}\hat{B} | \alpha \rangle = \sum_{\alpha\beta\gamma\delta} O_{\alpha\beta}^{-1} A_{\beta\gamma} O_{\gamma\delta}^{-1} B_{\delta\alpha} = \operatorname{Tr}(\hat{B}\hat{A}). \tag{B.7}$$

Next we will consider unitary transformations of an ordered basis $\{|\alpha\rangle\}$ to another ordered basis $\{|\alpha\rangle\rangle\}$ of the form

$$|\alpha\rangle \to U |\alpha\rangle = |\alpha\rangle\rangle = \sum_{\beta} U_{\beta\alpha} |\beta\rangle, \qquad \text{and} \qquad \langle\alpha|U^\dagger = \langle\langle\alpha| = \sum_{\beta} \langle\beta|U_{\alpha\beta}^\dagger, \ \ (\text{B.8})$$

where $U_{\alpha\beta}^{\dagger}=U_{\beta\alpha}^{*}$. The unitarity of the transformation $U^{\dagger}U=\hat{I}$ is expressed in the $\{|\alpha\rangle\}$ basis as,

$$O_{\alpha\beta} = \langle \alpha | U^{\dagger} U | \beta \rangle = \sum_{\gamma\delta} \langle \delta | U_{\alpha\delta}^{\dagger} U_{\gamma\beta} | \gamma \rangle = \sum_{\gamma\delta} U_{\alpha\delta}^{\dagger} O_{\delta\gamma} U_{\gamma\beta}.$$
 (B.9)

The overlap matrix in the new basis $\tilde{O}_{\alpha\beta} \equiv \langle\langle\alpha|\beta\rangle\rangle$ is given by

$$\tilde{O}_{\alpha\beta} = \langle \alpha | U^{\dagger} U | \beta \rangle = \sum_{\gamma\delta} U_{\alpha\gamma}^{\dagger} O_{\gamma\delta} U_{\delta\beta} = O_{\alpha\beta}. \tag{B.10}$$

Thus, the overlap matrix is invariant under unitary transformations, which is a well-known result. As an exercise we note that the identity operator expressed in the $\{|\alpha\rangle\rangle\}$ basis is

$$\hat{I} = \sum_{\alpha\beta} O_{\alpha\beta}^{-1} |\alpha\rangle\rangle\langle\langle\beta| = \sum_{\alpha\beta\gamma\delta} U_{\gamma\alpha} O_{\alpha\beta}^{-1} U_{\beta\delta}^{\dagger} |\gamma\rangle\langle\delta|.$$

Comparing this with Eq. (B.4) we get

$$O_{\gamma\delta}^{-1} = \sum_{\alpha\beta} U_{\gamma\alpha} O_{\alpha\beta}^{-1} U_{\beta\delta}^{\dagger}.$$
 (B.11)

The above relation can also be derived by inverting Eq. (B.9) and therefore has the same content. The matrix element of an abstract operator in the two bases are related by

$$\tilde{A}_{\alpha\beta} \equiv \langle \langle \alpha | \hat{A} | \beta \rangle \rangle = \langle \alpha | U^{\dagger} \hat{A} U | \beta \rangle = \sum_{\gamma\delta} U_{\alpha\gamma}^{\dagger} \langle \gamma | \hat{A} | \delta \rangle U_{\delta\beta} = \sum_{\gamma\delta} U_{\alpha\gamma}^{\dagger} A_{\gamma\delta} U_{\delta\beta}. \quad (B.12)$$

We consider a similarity transformation $\hat{A} \to U^{-1}\hat{A}U$. The representation of the U^{-1} transformation in the $\{|\alpha\rangle\}$ basis is given by $U^{-1}|\alpha\rangle = \sum_{\beta} U_{\beta\alpha}^{-1}|\beta\rangle$ such that $\sum_{\gamma} U_{\alpha\gamma} U_{\gamma\beta}^{-1} = \delta_{\alpha\beta}$. From Eq. (B.9) one can show that $\sum_{\gamma} O_{\alpha\gamma} U_{\gamma\beta}^{-1} = \sum_{\gamma} U_{\alpha\gamma}^{\dagger} O_{\gamma\beta}$. Using this relation we get

$$\langle \alpha | U^{-1} \hat{A} U | \beta \rangle = \sum_{\gamma} \langle \alpha | U^{-1} \hat{A} | \gamma \rangle U_{\gamma\beta} = \sum_{\gamma\delta\rho} \langle \alpha | U^{-1} O_{\delta\rho}^{-1} | \delta \rangle A_{\rho\gamma} U_{\gamma\beta}$$

$$= \sum_{\gamma\delta\rho\eta} O_{\alpha\eta} U_{\eta\delta}^{-1} O_{\delta\rho}^{-1} A_{\rho\gamma} U_{\gamma\beta} = \sum_{\gamma\delta} U_{\alpha\delta}^{\dagger} A_{\delta\gamma} U_{\gamma\beta} = \tilde{A}_{\alpha\beta}.$$
(B.13)

This proves that a unitary transformation of the basis states is equivalent to a similarity transformation of the operators. Also using Eqs. (B.11) and (B.12) we get,

$$\operatorname{Tr}(\hat{A}) = \sum_{\alpha\beta} O_{\alpha\beta}^{-1} \tilde{A}_{\beta\alpha} = \sum_{\alpha\beta\gamma\delta} O_{\alpha b e}^{-1} U_{\beta\gamma}^{\dagger} A_{\gamma\delta} U_{\delta\alpha} = \sum_{\alpha\beta\gamma\delta} A_{\gamma\delta} \left[U_{\delta\alpha} O_{\alpha\beta}^{-1} U_{\beta\gamma}^{\dagger} \right]$$
$$= \sum_{\gamma\delta} O_{\delta\gamma}^{-1} A_{\gamma\delta}. \tag{B.14}$$

This shows that trace of an operator is invariant under unitary transformations of the basis states (or equivalently, under similarity transformations).

Next we consider non-unitary, invertible transformations of the basis $\{|\alpha\rangle\}$ to another basis $\{|\alpha\rangle\rangle\}$ of the form

$$|\alpha\rangle \to T|\alpha\rangle = |\alpha\rangle\rangle = \sum_{\beta} T_{\beta\alpha}|\beta\rangle, \quad \text{and} \quad \langle\alpha|T^{\dagger} = \langle\langle\alpha| = \sum_{\beta} \langle\beta|T_{\alpha\beta}^{\dagger}, \text{ (B.15)}$$

where $T_{\alpha\beta}^{\dagger} = T_{\beta\alpha}^{*}$. Unlike in a unitary transformation, the overlap matrix in the new basis is different from that in the old basis. The two overlap matrices are related by

$$\tilde{O}_{\alpha\beta} \equiv \langle \alpha | T^{\dagger} T | \beta \rangle = \sum_{\gamma\delta} T_{\alpha\gamma}^{\dagger} O_{\gamma\delta} T_{\delta\beta}. \tag{B.16}$$

The matrix elements of an abstract operator in the two bases are related by,

$$\tilde{A}_{\alpha\beta} \equiv \langle \langle \alpha | \hat{A} | \beta \rangle \rangle = \sum_{\gamma\delta} T_{\alpha\gamma}^{\dagger} A_{\gamma\delta} T_{\delta\beta}. \tag{B.17}$$

It is easy to verify that a non-unitary transformation of the basis states is not equivalent to a similarity transformation of the operators, i.e., $\tilde{A}_{\alpha\beta} \neq \langle \alpha | T^{-1} \hat{A} T | \beta \rangle$. In fact, similarity transformations where T is non-unitary do not preserve hermiticity of operators, and as such are not allowed in quantum mechanics. By inverting Eq. (B.16) and using Eq. (B.17) one can show that

$$Tr(\hat{A}) = \sum_{\alpha\beta} \tilde{O}_{\alpha\beta}^{-1} \tilde{A}_{\beta\alpha} = \sum_{\alpha\beta} \left[\sum_{\gamma\delta} T_{\alpha\gamma}^{-1} O_{\gamma\delta}^{-1} (T^{\dagger})_{\delta\beta}^{-1} \right] \left[\sum_{\rho\eta} T_{\beta\rho}^{\dagger} A_{\rho\eta} T_{\eta\alpha} \right]$$
$$= \sum_{\alpha\beta} O_{\alpha\beta}^{-1} A_{\beta\alpha}. \tag{B.18}$$

Thus, the trace of an operator is invariant under non-unitary transformations of the basis states.

Next we will construct a second quantized Hamiltonian in a non-orthogonal basis. We will use Eqs. (B.1), (B.2) and (B.3) to relate a non-orthogonal basis $\{|\alpha\rangle\}$ with an orthogonal basis $\{|i\rangle\}$. The non-interacting part is given by,

$$\hat{H}_{0} = \sum_{ij} \langle i|\hat{H}_{0}|j\rangle c_{i}^{\dagger}c_{j} = \sum_{ij} \sum_{\alpha\beta} S_{i\alpha}^{\dagger} \langle \alpha|\hat{H}_{0}|\beta\rangle S_{\beta j}c_{i}^{\dagger}c_{j} = \sum_{\alpha\beta} \langle \alpha|\hat{H}_{0}|\beta\rangle c_{\alpha}^{\dagger}c_{\beta}, \quad (B.19)$$

where

$$c_{\alpha}^{\dagger} = \sum_{i} S_{i\alpha}^{\dagger} c_{i}^{\dagger}$$
 and $c_{\alpha} = \sum_{i} S_{\alpha i} c_{i}$. (B.20)

We note that $c_{\alpha}^{\dagger}|0\rangle = \sum_{\beta} O_{\beta\alpha}^{-1}|\beta\rangle \neq |\alpha\rangle$, and that $\langle \beta|c_{\alpha}^{\dagger}|0\rangle = \delta_{\beta\alpha}$. Also, the anti-commutation relation of the creation and annihilation operators is given by

$$\left\{c_{\alpha}^{\dagger}, c_{\beta}\right\} = \sum_{ij} S_{i\alpha}^{\dagger} \left\{c_{i}^{\dagger}, c_{j}\right\} S_{\beta j} = O_{\beta \alpha}^{-1}. \tag{B.21}$$

Similarly one can show that the interacting part of the Hamiltonian is given by

$$\hat{V} = \sum_{ijkl} \langle i, j | \hat{V} | l, k \rangle c_i^{\dagger} c_j^{\dagger} c_k c_l = \sum_{\alpha\beta\gamma\delta} \langle \alpha, \beta | \hat{V} | \gamma, \delta \rangle c_{\alpha}^{\dagger} c_{\beta}^{\dagger} c_{\delta} c_{\gamma}.$$
 (B.22)

The two-particle states are constructed from the one-particle states by $|i,j\rangle=|i\rangle\otimes|j\rangle$.

Appendix C

Few Calculations for Non-Unitary Transformation

In this appendix we will give the result of the evaluation of few matrices and traces that are used in Sec. 2.5. The matrices \tilde{X} and \tilde{Y} can be shown to have the form

$$\tilde{X} = \frac{1}{2} \left[1 + \cosh(2(b_0 - d_0)) \left\{ \cosh(2b) \cosh(2d) - \sinh(2b) \sinh(2d) (\hat{u} \cdot \hat{v}) \right\} \right] \mathbf{1}
+ \frac{1}{2} \sinh(2b) \cosh(2d) \sinh(2(b_0 - d_0)) (\hat{u} \cdot \bar{\sigma})
- \frac{1}{2} \sinh(2d) \cosh(2b) \sinh(2(b_0 - d_0)) (\hat{v} \cdot \bar{\sigma})
- \frac{i}{2} \sinh(2b) \sinh(2d) \sinh(2(b_0 - d_0)) (\hat{u} \times \hat{v}) \cdot \bar{\sigma},$$
(C.1)

and

$$\tilde{Y} = \frac{1}{2} \left[\cos(v_0 - u_0) \left\{ \cos(u) \cos(v) + \sin(u) \sin(v) (\hat{u} \cdot \hat{v}) \right\} + \text{c. c.} \right] \mathbf{1}
+ \frac{1}{2} \left[\sin(v_0 - u_0) \sin(u) \cos(v) + \text{c. c.} - e^{i(v_0^* - u_0^*)} \sinh(2d) \sin(u^*) \sin(v) \right]
+ e^{-i(v_0^* - u_0^*)} \sinh(2b) \sin(v^*) \sin(u) (\hat{u} \cdot \hat{v}) \right] (\hat{u} \cdot \bar{\sigma})
- \frac{1}{2} \left[\sin(v_0 - u_0) \sin(v) \cos(u) + \text{c. c.} - e^{i(v_0^* - u_0^*)} \sinh(2d) \sin(u^*) \sin(v) (\hat{u} \cdot \hat{v}) \right]
+ e^{-i(v_0^* - u_0^*)} \sinh(2b) \sin(v^*) \sin(u) \right] (\hat{v} \cdot \bar{\sigma})
+ \frac{1}{2} \left[-\sin(v_0 - u_0) \sin(u) \sin(v) + \text{c. c.} + ie^{i(v_0^* - u_0^*)} \cosh(2d) \sin(u^*) \sin(v) \right]
- ie^{-i(v_0^* - u_0^*)} \cosh(2b) \sin(v^*) \sin(u) \right] (\hat{u} \times \hat{v}) \cdot \bar{\sigma}.$$
(C.2)

Here "c. c." implies complex conjugation of the term in front of it.

The traces used in the evaluation of the local interaction functional given by Eq.

(2.39) have the form

$$Tr(\tilde{X}^2) = \frac{1}{2} [1 + \cosh(2(b_0 - d_0)) \{\cosh(2b) \cosh(2d) - \sinh(2b) \sinh(2d)(\hat{u} \cdot \hat{v})\}]^2 \\ + \frac{1}{2} \sinh^2(2(b_0 - d_0)) [\sinh^2(2b) \cosh^2(2d) + \sinh^2(2d) \cosh^2(2b) \\ - \sinh^2(2b) \sinh^2(2d)(1 - (\hat{u} \cdot \hat{v})^2) \\ - \cosh(2b) \sinh(2b) \cosh(2d) \sinh(2d)(\hat{u} \cdot \hat{v})], \qquad (C.3)$$

$$Tr(\tilde{Y}^2) = \frac{1}{2} [\cos(v_0 - u_0) \{\cos(u) \cos(v) + \sin(u) \sin(v)(\hat{u} \cdot \hat{v})\} + c. \ c.]^2 \\ + \frac{1}{2} [\sin(v_0 - u_0) \sin(u) \cos(v) + c. \ c. - e^{i(v_0^* - u_0^*)} \sinh(2d) \sin(u^*) \sin(v) \\ + e^{-i(v_0^* - u_0^*)} \sinh(2b) \sin(v^*) \sin(u)(\hat{u} \cdot \hat{v})]^2 \\ + \frac{1}{2} [\sin(v_0 - u_0) \sin(v) \cos(u) + c. \ c. + e^{-i(v_0^* - u_0^*)} \sinh(2b) \sin(v^*) \sin(u) \\ - e^{i(v_0^* - u_0^*)} \sinh(2d) \sin(u^*) \sin(v)(\hat{u} \cdot \hat{v})]^2 \\ + \frac{1}{2} [-\sin(v_0 - u_0) \sin(u) \sin(v) + c. \ c. + ie^{i(v_0^* - u_0^*)} \cosh(2d) \sin(u^*) \sin(v) \\ - ie^{-i(v_0^* - u_0^*)} \cosh(2b) \sin(v^*) \sin(u)] (1 - (\hat{u} \cdot \hat{v})^2) \\ - [\sin(v_0 - u_0) \sin(u) \cos(v) + c. \ c. - e^{i(v_0^* - u_0^*)} \sinh(2d) \sin(u^*) \sin(v) \\ + e^{-i(v_0^* - u_0^*)} \sinh(2b) \sin(v^*) \sin(u)(\hat{u} \cdot \hat{v})] \times \\ [\sin(v_0 - u_0) \sin(v) \cos(u) + c. \ c. - e^{-i(v_0^* - u_0^*)} \sinh(2b) \sin(v^*) \sin(u) \\ - e^{i(v_0^* - u_0^*)} \sinh(2d) \sin(u^*) \sin(v)(\hat{u} \cdot \hat{v})] (\hat{u} \cdot \hat{v}), \qquad (C.4)$$

$$Tr(\tilde{X}\tilde{Y}) = \frac{1}{2} [1 + \cosh(2(b_0 - d_0)) \{\cos(2b) \cosh(2d) - \sinh(2b) \sinh(2d)(\hat{u} \cdot \hat{v})\}] \times \\ [\cos(v_0 - u_0) \{\cos(u) \cos(v) + \sin(u) \sin(v)(\hat{u} \cdot \hat{v})\} + c. \ c.] \\ + \frac{1}{2} \sinh(2(b_0 - d_0)) [\sinh(2b) \cosh(2d) - \cosh(2b) \sinh(2d)(\hat{u} \cdot \hat{v})] \times \\ [\sin(v_0 - u_0) \sin(v) \cos(v) + c. \ c.] \\ + \frac{i}{2} \sinh(2(b_0 - d_0)) [\sinh(2d) \cosh(2b) - \sinh(2b) \cosh(2d)(\hat{u} \cdot \hat{v})] \times \\ [\sin(v_0 - u_0) \sin(v) \cos(v) + c. \ c.] \\ + \frac{i}{2} \sinh(2(b_0 - d_0)) [\sinh(2d) \cosh(2d) [\sin(v_0 - u_0) \sin(u) \sin(v) \\ - c. \ c.] (1 - (\hat{u} \cdot \hat{v})^2). \qquad (C.5)$$

Appendix D

Two Dimensional Spin-Fermion Model

In this appendix we will compare the two-dimensional spin-three-dimensional fermion model examined in chapter 5 with the two-dimensional spin-fermion model (where both the spin fluctuations as well as the fermions are two-dimensional). The latter model is interesting from the point of view of high-temperature superconductivity. In these materials the generic presence of an antiferromagnetic phase near the superconducting phase is the motivation for studying fermions interacting with spin fluctuations which are nearly critical.

The Fermi surface of the two-dimensional fermions is shown in Fig.(D.1). Pairs of points on the Fermi surface which are connected by the ordering wave-vector $\mathbf{Q} = (\pi, \pi)$ have low-energy scattering with the nearly critical spin fluctuations. These are

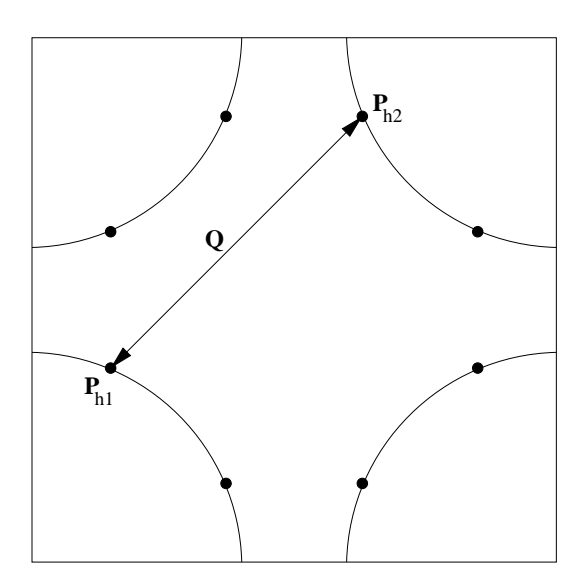


Figure D.1: Two-dimensional Fermi surface with hot spots. Pairs of hot spots are connected by magnetic ordering wave-vector **Q**. The connected hot spots are not nested.

the hot spots. This is to be compared with the case we have discussed before where the entire Fermi surface is hot. The lowest order fermion self-energy and spin-fermion vertex are shown in Fig.(5.3), and their formal expressions are given by Eqs.(5.6), (5.8), (5.10). The difference between the models is in the estimation of the momentum sums in these equations.

To simplify the calculation we will assume that the Fermi velocities at the hot spots \mathbf{P}_{h1} and \mathbf{P}_{h2} are perpendicular (when they are anti-parallel there is nesting). We will rotate the local momentum co-ordinate such that the Fermi velocity at \mathbf{P}_{h1} is along \hat{k}_y and at \mathbf{P}_{h2} it is along $-\hat{k}_x$. The linearized spectrum around these points can be expressed as $\epsilon_{\mathbf{p}_{h1}+\mathbf{k}} = v_F k_y$, and $\epsilon_{\mathbf{p}_{h2}+\mathbf{k}} = -v_F k_x$. In terms of the local co-ordinates (k_x,k_y) one can write $\gamma_{\mathbf{Q}+\mathbf{k}} = \delta + \omega_s(k_x^2 + k_y^2)$. We will now estimate the real part of the self-energy by considering only the first term $1/(\gamma_{\mathbf{k}}^2 + \epsilon_{\mathbf{k}+\mathbf{p}}^2)$ in Eq.(5.10). The momentum integral is well-behaved even when the cut-off is sent to infinity. We get, keeping only the leading term

$$-\lim_{\omega \to 0} \frac{\partial}{\partial \omega} \operatorname{Re}\Sigma \left(\mathbf{p}, \omega\right) = \frac{g_0^2}{\pi} \sum_{\mathbf{k}} \frac{1}{\gamma_{\mathbf{k}}^2 + \epsilon_{\mathbf{k} + \mathbf{p}}^2}$$

$$= \frac{g_0^2}{4\pi^3} \int_{-\infty}^{\infty} dk_y \int_{-\infty}^{\infty} dk_x \frac{1}{(\delta + \omega_s(k_x^2 + k_y^2))^2 + v_F^2(\delta p + k_x)^2}$$

$$\simeq \frac{g_0^2}{4\pi^2 \epsilon_F} \int_{-\infty}^{\infty} dk_y \frac{1}{\delta + \omega_s((\delta p)^2 + k_y^2)}$$

$$= \frac{g_0^2}{4\pi \epsilon_F \omega_s^{1/2}} \left[\frac{1}{(\delta + \omega_s(\delta p)^2)^{1/2}} \right]. \tag{D.1}$$

In the above we have assumed that \mathbf{p} is close to \mathbf{P}_{h1} and δp is the deviation from the hot spot along the Fermi surface.

Next we will estimate the same term for the case where the fermions are three-dimensional. Since the spin fluctuations are quasi two-dimensional, the entire Fermi surface is hot and the momentum dependence of the self-energy is washed out. We linearize the spectrum and write $\epsilon_{\mathbf{k}+\mathbf{p}} = v_F k_\perp$ where \hat{k}_\perp is the direction of the Fermi velocity at the closest hot point. Let k_\parallel be the co-ordinates in the plane of the Fermi

surface. Then $\gamma_{\mathbf{Q}+\mathbf{k}} = \delta + \omega_s(k_\perp^2 + k_\parallel^2).$ We get

$$-\lim_{\omega \to 0} \frac{\partial}{\partial \omega} \operatorname{Re}\Sigma \left(\mathbf{p}, \omega\right) = \frac{g_0^2}{\pi} \frac{1}{(2\pi)^3} \int d^2k_{\parallel} \int_{-\infty}^{\infty} dk_{\perp} \frac{1}{(\delta + \omega_s(k_{\parallel}^2 + k_{\perp}^2))^2 + (v_F k_{\perp})^2}$$

$$\simeq \frac{g_0^2}{\epsilon_F} \frac{1}{(2\pi)^3} \int d^2k_{\parallel} \frac{1}{\delta + \omega_s k_{\parallel}^2}$$

$$= \frac{g_0^2}{8\pi^2 \epsilon_F \omega_s} \left(2\ln(\Lambda) - \ln\left(\frac{\delta}{\omega_s}\right)\right). \tag{D.2}$$

 Λ is a momentum cut-off. The above estimation gives Eq.(5.11).

We estimate the imaginary part of the self energy similarly. In two-dimension we get

$$\operatorname{Im}\Sigma\left(\mathbf{p},\omega\right) = -\frac{g_{0}^{2}}{(2\pi)^{2}} \int_{-\infty}^{\infty} dk_{y} \int_{-\omega/\epsilon_{F}-\delta p}^{-\delta p} dk_{x} \frac{\omega + v_{F}(\delta p + k_{x})}{(\delta + \omega_{s}(k_{x}^{2} + k_{y}^{2}))^{2} + (\omega + v_{F}(\delta p + k_{x}))^{2}}$$

$$\simeq -\frac{g_{0}^{2}}{8\pi^{2}\epsilon_{F}} \int_{-\infty}^{\infty} dk_{y} \ln\left(1 + \frac{\omega^{2}}{(\delta_{p} + \omega_{s}k_{y}^{2})^{2}}\right)$$

$$\simeq -\frac{g_{0}^{2}}{16\pi\epsilon_{F}} \left[\frac{\omega^{2}}{\omega_{s}^{1/2}(\max[\omega, \delta_{p}])^{3/2}}\right], \tag{D.3}$$

where $\delta_p = \delta + \omega_s(\delta p)^2$. In three-dimension we have

$$\operatorname{Im}\Sigma\left(\mathbf{p},\omega\right) = -\frac{g_{0}^{2}}{(2\pi)^{3}} \int d^{2}k_{\parallel} \int_{0}^{\omega/\epsilon_{F}} dk_{\perp} \frac{\omega - v_{F}k_{\perp}}{(\delta + \omega_{s}(k_{\parallel}^{2} + k_{\perp}^{2}))^{2} + (\omega - v_{F}k_{\perp})^{2}}$$

$$\simeq -\frac{g_{0}^{2}}{8\pi^{2}\epsilon_{F}} \int_{0}^{\infty} dk_{\parallel}k_{\parallel} \ln\left(1 + \frac{\omega^{2}}{(\delta + \omega_{s}k_{\parallel}^{2})^{2}}\right)$$

$$\simeq -\frac{g_{0}^{2}}{16\pi^{2}\epsilon_{F}\omega_{s}} \left(\frac{\omega^{2}}{\max[\omega, \delta]}\right). \tag{D.4}$$

Next we will estimate the vertex correction. In two-dimension since $\gamma_{\mathbf{Q}+\mathbf{k}}^2 \sim k^4$ while $\epsilon_{\mathbf{k}} \sim k$, the momentum dependence of the former can be ignored. With this simplification we get

$$\Gamma \simeq \frac{g_0^2}{\pi^3 \epsilon_F^2} \int d\tilde{\omega} \int_0^\infty dk_x \int_0^\infty dk_y \frac{\tilde{\omega}^2}{(k_x + k_y)(\tilde{\omega} + k_x)(\tilde{\omega} + k_y)(\tilde{\delta}^2 + \tilde{\omega}^2)}$$

$$= \frac{g_0^2}{\pi^3 \epsilon_F^2} \int d\tilde{\omega} \int_0^\infty dk_x \frac{\tilde{\omega}^2}{(\tilde{\delta}^2 + \tilde{\omega}^2)(k_x^2 - \tilde{\omega}^2)} \ln\left(\frac{k_x}{\tilde{\omega}}\right)$$

$$= \frac{g_0^2}{4\pi \epsilon_F^2} \int_0^\Omega d\tilde{\omega} \frac{\tilde{\omega}}{(\tilde{\delta}^2 + \tilde{\omega}^2)}$$

$$= \frac{g_0^2}{4\pi \epsilon_F^2} \ln\left(\frac{\Omega}{\tilde{\delta}}\right). \tag{D.5}$$

In the above $\tilde{\omega} = \omega/\epsilon_F$, $\tilde{\delta} = \delta/\epsilon_F$ and Ω is a frequency cut-off. In three-dimension we will assume that the Fermi velocities at \mathbf{P}_{h1} and \mathbf{P}_{h2} are perpendicular (to simplify the calculation) such that $\epsilon_{1\mathbf{k}} = v_F k_x$ and $\epsilon_{2\mathbf{k}} = v_F k_y$. We neglect the k_x , k_y dependence of $\gamma_{\mathbf{Q}+\mathbf{k}}$. Then the k_x , k_y integral are same as in the two-dimensional case. We set δ to zero and get

$$\Gamma \simeq \frac{g_0^2}{\pi^4} \int d\tilde{\omega} \int_0^\infty dk_z \int_0^\infty dk_x \int_0^\infty dk_y \frac{\tilde{\omega}^2}{(\tilde{\omega}_s^2 k_z^4 + \tilde{\omega}^2)(k_x + k_y)(\tilde{\omega} + k_x)(\tilde{\omega} + k_y)}$$

$$= \frac{g_0^2}{4\pi^2 \epsilon_F^2} \int_0^\Omega d\tilde{\omega} \int_0^\infty dk_z \frac{\tilde{\omega}}{\tilde{\omega}_s^2 k_z^4 + \tilde{\omega}^2}$$

$$= \frac{g_0^2 \Omega^{1/2}}{4\sqrt{2}\pi \epsilon_F^2 \omega_s^{1/2}}.$$
(D.6)

Here $\tilde{\omega}_s = \omega_s/\epsilon_F$.

We note that in all the calculations involving three-dimensional fermions we have assumed that the plane formed by the two connected hot points and the centre of the Fermi sphere is not perpendicular to the direction in which the quasi two-dimensional spin fluctuations are incoherent. This is true for generic hot points. However, for a spherical Fermi sea there are four special points where this is not true and as a consequence the self-energy and the vertex at these points are more singular than they are for generic points in the hot region. To elucidate the geometry let us assume that the spin fluctuations are incoherent in the \hat{k}_z direction, and that the magnetic ordering wavevector has the form $\mathbf{Q} = (Q_x, Q_y, a)$, where a is arbitrary. Now there are two pairs of special hot points such that each pair, along with the centre of the Fermi sphere, form a plane which is perpendicular to \hat{k}_z . This implies that the difference in the wave-vectors of the connected hot points must be $(Q_x, Q_y, 0)$ for each of the pairs. For these four special points the linearized fermion spectrum is independent of wave-vector along k_z (since this direction is along the Fermi surface). Thus, dynamics at these special points is entirely two-dimensional (since the fermion and spin-fluctuation propagators are independent of wave-vector along k_z , in the estimation of self-energy and vertex the integrand is independent of k_z and the integral along k_z is cut-off only by the curvature term). The results for the two-dimensional fermions are relevant for these points (the k_x and k_y integrals are the same). However, since $Z^{-1} \sim 1/\sqrt{\delta + \omega_s(\delta p)^2}$, where δp is deviation from these special points along their Fermi surfaces, the contribution of these points to thermodynamics is negligible.

The main difference between the two-dimensional fermion and the three-dimensional fermion models is that the perturbative correction to the spin-fermion vertex is finite in the three-dimensional case (for generic points in the hot region) whereas it diverges logarithmically at the phase transition for the two-dimensional case. The self-energy correction also has square-root singularity at the transition in two-dimension. The perturbative calculation indicate that while in the three-dimensional fermionic model the coupling remains weak close to the phase transition, in two dimension the coupling grows and perturbative calculation will eventually break down. In the language of the renormalization group, this model flows to a strong-coupling fixed point.

References

- [1] P. W. Anderson, *Basic Notions of Condensed Matter Physics*, (Addison-Wesley Publishing Company, 1984).
- [2] For a recent review, see for e.g., G. R. Stewart, Rev. Mod. Phys. 73, 797 (2001).
- [3] A. Auerbach, *Interacting Electrons and Quantum Magnetism*, (Springer-Verlag, New York, 1994).
- [4] S. Sachdev, Quantum Phase Transitions, (Cambridge University Press, 1999).
- [5] S. L. Sondhi, S. M. Girvin, J. P. Carini, and D. Shahar, Rev. Mod. Phys. 69, 315 (1997)
- [6] N. Goldenfeld, Lectures on Phase Transitions and the Renormalization Group, (Perseus Books, 1992).
- [7] G. R. Stewart, Rev. Mod. Phys. **73**, 797 (2001).
- [8] A. C. Hewson, *The Kondo Problem to Heavy Fermions*, (Cambridge University Press, 1993).
- [9] P. Fulde, Electron Correlations in Molecules and Solids, (Springer-Verlag, 1993).
- [10] P. Coleman, Physica B **259-261**, 353 (1999).
- [11] N. D. Mathur, F. M. Grosche, S. R. Julian, I. R. Walker, D. M. Freye, R. K. W. Haselwimmer, and G. G. Lonzarich, Nature (London) **394**, 39 (1998).
- [12] D. Jaccard, H. Wilhelm, K. Alami-Yadri, and E. Vargoz, Physica B **259-261**, 1 (1999).
- [13] F. Steglich, B. Buschinger, P. Gegenwart, M. Lohmann, R. Helfrich, C. Langhammer, P. Hellmann, L. Donnevert, S. Thomas, A. Link, C. Geibel, M. Lang, G. Sparn, and W. Assmus, J. Phys.: Condens. Matter **8**, 9909 (1996).
- [14] P. Estrela, A. deVisser, F. R. deBoer, G. J. Nieuwenhuys, L. C. Pereira, and M. Almeida, Physica B **259-261**, 409 (1999).
- [15] H. von Löhneysen, J. Phys.: Condens. Matter **8**, 9689 (1996).
- [16] O. Trovarelli, C. Geibel, S. Mederle, C. Langhammer, F. M. Grosche, P. Gegenwart, M. Lang, G. Sparn, and F. Steglich, Phys. Rev. Lett **85**, 626 (2000).

- [17] S. Doniach, Physica B **91**, 231 (1977).
- [18] M. A. Ruderman, and C. Kittel, Phys. Rev. **96**, 99 (1954).
- [19] J. Custers, P. Gegenwart, H. Wilhelm, K. Neumaier, Y. Tokiwa, O. Trovarelli, C. Geibel, F. Steglich, C. Pepin, and P. Coleman, Nature **424**, 524 (2003).
- [20] A. Schröder, G. Aeppli, P. Coldea, M. Adams, O. Stockert, H.v. Löhneysen, E. Bucher, R. Ramazashvili, and P. Coleman, Nature **407**, 351 (2000).
- [21] J. A. Hertz, Phys. Rev. B **14**, 1165 (1976).
- [22] A. J. Millis, Phys. Rev. B 48, 7183 (1993).
- [23] R. Shankar, Rev. Mod. Phys. **66**, 129 (1994).
- [24] H.v. Löhneysen, T. Pietrus, G. Portisch, H. G. Schlager, A. Schröder, M. Sieck, and T. Trappmann, Phys. Rev. Lett **72**, 3262 (1994).
- [25] A. Rosch, A. Schröder, O. Stockert, and H.v. Löhneysen, Phys. Rev. Lett **79**, 159 (1997).
- [26] O. Stockert, H.v. Löhneysen, A. Rosch, N. Pyka, and M. Loewenhaupt, Phys. Rev. Lett 80, 5627 (1998).
- [27] S. Pankov, S. Florens, A. Georges, G. Kotliar, and S. Sachdev, cond-mat/0304415.
- [28] Q. Si, S. Rabello, K. Ingersent, and L. Smith, Nature **413**, 804 (2001).
- [29] A. Georges, G. Kotliar, W. Krauth, and M. J. Rozenberg, Rev. Mod. Phys. 68, 13 (1996).
- [30] D. Volhardt in *Correlated Electron Systems* **9**, Ed. V. J. Emery, (World Scientific, 1992).
- [31] N. Marzari, and D. Vanderbilt, Phys. Rev. B 56, 12 847 (1997), and references therein.
- [32] C. Edmiston, and K. Ruedenberg, Rev. Mod. Phys. 35, 457 (1963).
- [33] S. F. Boys, in *Quantum Theory of Atoms, Molecules, and the Solid State*, Ed. P. O. Löwdin, (Academic Press, New York, 1966).
- [34] G. D. Mahan, B. Sales, and J. Sharp, Phys. Today **50**, 42 (March, 1997).
- [35] David J. Singh, and Warren E. Pickett, Phys. Rev. B 50, 11 235 (1994); Lars Nordström, and David J. Singh, Phys. Rev. B 53, 1103 (1996); D. J. Singh, and I. I. Mazin, Phys. Rev. B 56, R1650 (1997).
- [36] G. D. Mahan, and J. O. Sofo, Proc. Natl. Acad. Sci. USA 93, 7436 (1996).

- [37] T. Pruschke, M. Jarrell, and J. K. Freericks, Adv. Phys. 44, 187 (1995).
- [38] G. Palsson, and G. Kotliar, Phys. Rev. Lett. **80**, 4775 (1998).
- [39] V. S. Oudovenko, and G. Kotliar, Phys. Rev. B **65**, 075102 (2002).
- [40] J. K. Freericks, and V. Zlatić, Phys. Rev. B **64**, 245118 (2001).
- [41] V. I. Anisimov, A. I. Poteryaev, M. A. Korotin, A. O. Anokhin, and G. Kotliar, J. Phys.- Condensed Matter **9**, 7359 (1997).
- [42] K. Held, I. A. Nekrasov, N. Blumer, V. I. Anisimov, and D. Vollhardt, Int. J. Mod. Phys. B 15, 2611 (2001).
- [43] G. Kotliar, and S. Y. Savrasov, Model Hamiltonians and First Principles Electronic Structure Calculations in *New Theoretical Approaches to Strongly Correlated Systems*, Ed. A. M. Tsvelik, Kluwer Academic Publishers (2001).
- [44] A. I. Lichtenstein, and M. I. Katsnelson, Phys. Rev. B 57, 6884 (1998).
- [45] G. Palsson, V. S. Oudovenko, S. Y. Savrasov, and G. Kotliar, to be published.
- [46] M. Jonson, and G. D. Mahan, Phys. Rev. B 21, 4223 (1980).
- [47] J. Moreno, and P. Coleman, cond-mat/9603079.
- [48] J. S. Langer, Phys. Rev. **128**, 110 (1962).
- [49] Any book on quantum field theory. See, for e.g., L. H. Ryder, *Quantum Field Theory* (Cambridge University Press, Cambridge, 1996).
- [50] R. Peierls, Z. Phys. 80, 763 (1933).
- [51] For a recent review see, e.g., A. J. Millis, J. Electron Spectroscopy and Related Phenomena **114-116**, 669 (2001).
- [52] H. Schweitzer, and G. Czycholl, Phys. Rev. Lett. **67**, 3724 (1991).
- [53] E. I. Blount, Solid State Physics **13**, 305 (1962).
- [54] J. Bennetto, and D. Vanderbilt, Phys. Rev. B **53**, 15 417 (1996).
- [55] G. D. Mahan, Many-Particle Physics (Plenum, New York, 1990).
- [56] R. D. King-Smith, and D. Vanderbilt, Phys. Rev. B 47, 1651 (1993).
- [57] R. Resta, Rev. Mod. Phys. **66**, 899 (1994).
- [58] W. A. Harrison, Phys. Rev. B **24**, 5835 (1981).
- [59] H. Eskes, A. M. Oleś, M. B. J. Meinders, and W. Stephan, Phys. Rev. B 50, 17 980 (1994).

- [60] We disagree with the claim that the optical matrix elements are completely determined by the tight-binding parameters. See e.g., L. C. Lew Yan Voon, and L. R. Ram-Mohan, Phys. Rev. B **47**, 15 500 (1993).
- [61] N. W. Aschcroft, and N. D. Mermin, Solid State Physics, Holt, Rinehart and Wilson, Philadelphia, 1976.
- [62] A. Khurana, Phys. Rev. Lett. **64**, 1990 (1990).
- [63] Q. Si, S. Rabello, K. Ingersent, and J. L. Smith, cond-mat/0011477.
- [64] A. Schröder, G. Aeppli, E. Bucher, R. Ramazashvili, and P. Coleman, Phys. Rev. Lett **80**, 5623 (1998).
- [65] S. Sachdev, A. V. Chubukov, and A. Sokol, Phys. Rev. B **51**, 14874 (1995).
- [66] Ar. Abanov, and A. V. Chubukov, Phys. Rev. Lett 84, 5608 (2000).
- [67] A. V. Chubukov, Private communications.
- [68] J. Benz, C. Pfleiderer, O. Stockert, and H.v. Löhneysen, Physica B **259-261**, 380 (1999).
- [69] C. Pfleiderer, Private communications.
- [70] R. Hlubina, and T. M. Rice, Phys. Rev. B 14, 9253 (1995).
- [71] A. Rosch, Phys. Rev. Lett **82**, 4280 (1999).
- [72] A. A. Abrikosov, L. P. Gorkov, and I. E. Dzyaloshinski, *Methods of Quantum Field Theory in Statistical Physics*, 171 (Dover Publications, New York, 1963).
- [73] L. B. Ioffe, and A. J. Millis, Phys. Rev. B **51**, 16151 (1995).

Vita

Indranil Paul

1992-1997	Integrated M. Sc. (Physics), Indian Institute of Technology, Kanpur.
1997	General proficiency medal for the best academic performance in the M. Sc. Physics programme, 1997, Indian Institute of Technology, Kanpur.
1997-2003	Graduate study in Physics, Dept. of Physics & Astronomy, Rutgers University.
1997-1999	Excellence Fellowship, Rutgers University.
1999-2000	Teaching Assistantship, Dept. of Physics & Astronomy, Rutgers University.
2000-2003	Graduate Assistantship, Dept. of Physics & Astronomy, Rutgers University.
2001	I. Paul, and G. Kotliar, Thermoelectric behavior near magnetic quantum critical point, Phys. Rev. B 64 , 184414 (2001).
2003	I. Paul, and G. Kotliar, Thermal transport for many-body tight-binding models, Phys. Rev. B 67 , 115131 (2003).
2003	M. Haque, I. Paul, and S. Pankov, Structural transition of a Wigner crystal on a liquid substrate, Phys. Rev. B 68 , 045427 (2003).